G-Safety
SCIENCE FOR GLOBAL SAFETY

The 4th International Symposium on Water Environment Systems ---with Perspective of Global Safety (December 1st-3rd, 2016)

Department of Civil and Environmental Engineering

Graduate School of Engineering

Tohoku University

Sponsors

http://www.g-safety.tohoku.ac.jp/

Tohoku University, Main Administration Office Organization for Leading Graduate School Program of Tohoku University, Sendai, Miyagi 980-8578, Japan

http://www.eng.tohoku.ac.jp/

Tohoku University, Graduate School of Engineering, Sendai, Miyagi 980-8579, Japan

ORGANIZERS

Dr. KAZAMA So (Professor, Tohoku University)

Dr. LI Yu-You (Professor, Tohoku University)
(Chairman of Department of Civil and Environmental Engineering)

Dr. KUBOTA Kengo (Associate Professor, Tohoku University)

Dr. KOMORI Daisuke (Associate Professor, Tohoku University)

SECRETARIES

Assistant Professor, Toshimasa Hojo
toshimasa.hojo.b5@tohoku.ac.jp

Assistant Professor, Yoshiya Touge
yoshiya.touge.a6@tohoku.ac.jp

DC student, Zhe Kong
kong.zhe.t7@dc.tohoku.ac.jp

PARTICIPANTS

Tohoku University	**Japan**
Name	**Identity**
Prem Rangsiwanichpong	Student (D2)
Noriko Uchida	Student (M2)
Yuto Sukegawa	Student (M1)
Kota Nakaguchi	Student (M1)
Yuta Sugawara	Student (M1)
Tanaka Yukako	Student (B4)
Kazuki Tonouchi	Student (M2)
Kazuya Kamiyama	Student (M2)
Lu Li	Student (D1)
Hui Cheng	Student (D1)
Jialing Ni	Student (M2)
Tao Zhang	Graduate Research Student
Yan Guo	Graduate Research Student
Bo Jiang	Graduate Research Student
Yanlong Zhang	JSPS research fellow
Hongyu Jiang	P.D. researcher

National Taiwan University	**Taiwan**
Name	**Identity**
Ke-Sheng Cheng	Professor
Bing-Chen Jhong	P.D.

National University of Laos	**Laos**
Name	**Identity**
Ketsana Xaiyasarn	P.D.

Asian Institute of Technology	**Thailand**
Name	**Identity**
Chanakarn Chanphu	Student（M2)
Pajee Trakanpasakul	Secretary

National Institute of Ecology	**Korea**
Name	**Identity**
JiHyun Kang	Researcher

Tianjing Chengjian University	**China**
Name	**Identity**
Liping Sun	Professor
Chunsheng Qiu	Associate Professor

Chinese Academy of Sciences	**China**
Name	**Identity**
Benyi Xiao	Associate Professor

Xi'an University of Architecture and Technology	**China**
Name	**Identity**
Rong Chen	Associate Professor

Changsha University of Science and Technology	**China**
Name	**Identity**
Hong Chen	Associate Professor

University Teknologi Malaysia	**Malaysia**
Name	**Identity**
Ee Ling Yong	Associate Professor
Khairunnisa Abdul Halim	Student

Venue

Graduate School of Engineering, Aobayama campus, Tohoku University

Lectures and oral presentations

Room 101, Engineering Laboratory Complex building (総合研究棟)

Posters exhibition

Room 201, Engineering Laboratory Complex building (総合研究棟)

Dinner party

(四季彩)

Map of Aobayama Campus

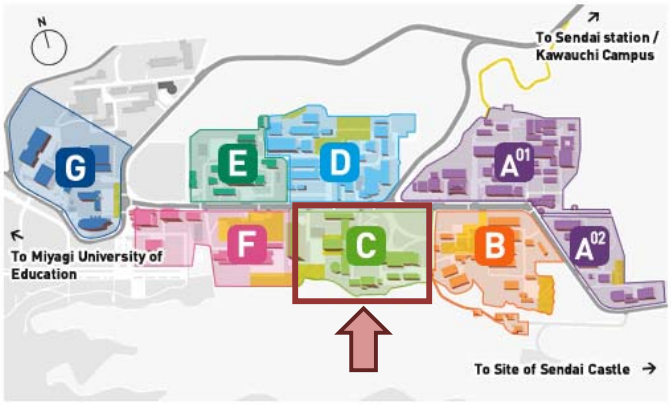

A01 Mechanical and Aerospace Engineering
A02 Quantum Science and Energy Engineering
B Materials Science and Engineering
C Center Square
D Electrical Engineering and Applied Physics
E Applied Chemistry, Chemical Engineering and Biomolecular Engineering
F Civil Engineering and Architecture
G Various Area

Engineering Laboratory Complex building
（総合研究棟）

Dinner Party Restaurant
（四季彩）

Access to Aobayama Campus

(Subway)

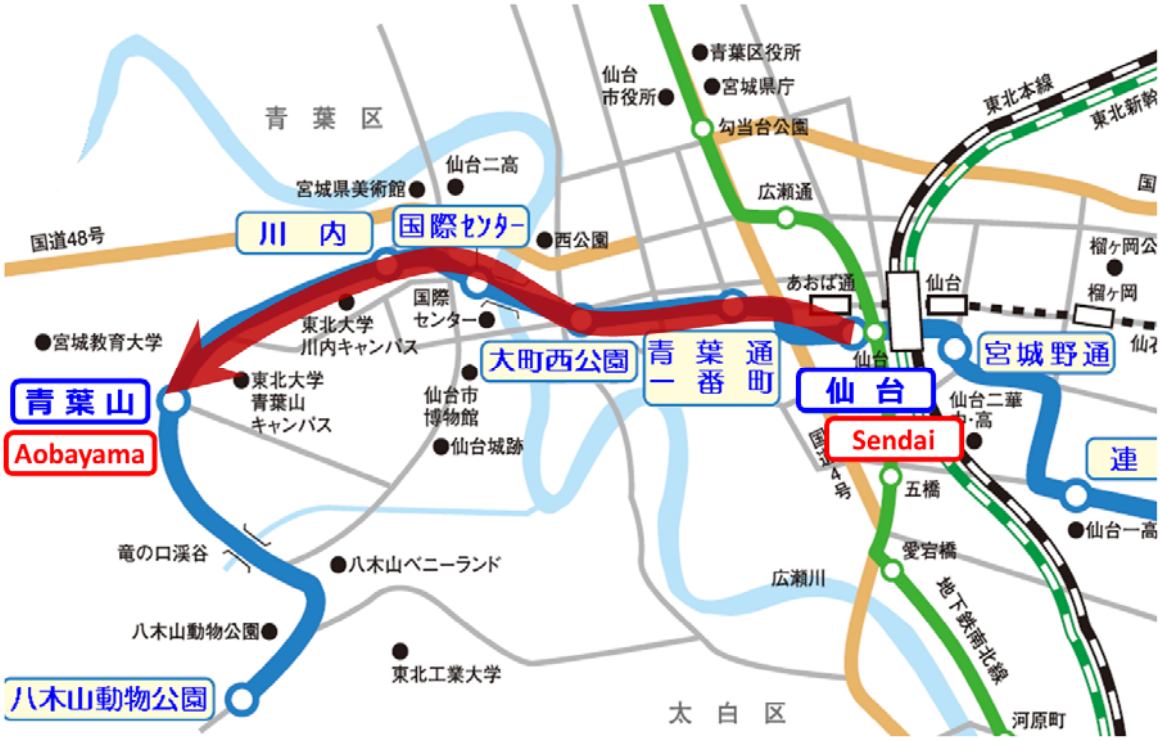

Map of **East-west line subway(地下鉄　東西線)** in Sendai

Please take this subway line and get off on the stop **Aobayama（青葉山）**.

Tips

If you start from Sendai Station, please make sure you are entering **East-west line subway（地下鉄　東西線）** rather than South-north line subway（**地下鉄　南北線**） nor JR station.

Program

Thursday, 01 Dec 2016

Fieldwork

The reconstruction of Minami-gamo sewage treatment plant

・2011/3/11 Tsunami hitting the Sewage Facilities

・Remains of 311-tsunami shocking on the wall of pump station

・Plan view of the sewage facilities

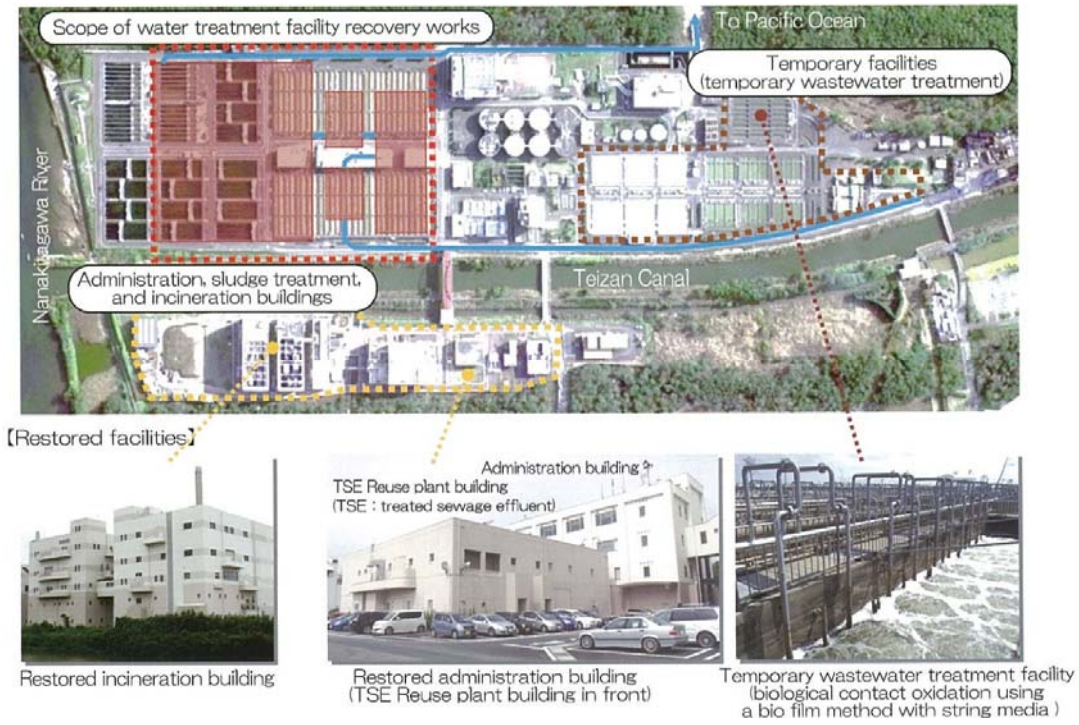

・Location of Minami-gamo sewage treatment plant

Friday, 02 Dec 2016

The 4th International Symposium on Water Environment Systems

Place: Room 101, Engineering Laboratory Complex Building, Tohoku University

9:00 ~ 9:10 **Opening address**

9:10 ~ 9:20 **Memorial photo**

Session I Flood Management

9:20 ~ 9:50 Estimating the return period of multisite rainfall extremes – An example of Taipei City
Ke-Sheng Cheng
National Taiwan University

9:50 ~ 10:20 Effective typhoon characteristics and their effects on hourly inundation forecasting during typhoons
Bing-Chen Jhong
National Taiwan University

10:20 ~ 10:40 Rainfall-runoff hydraulic flow computation at surface of tall building
Chanakarn Chanphu
Asian Institute of Technology

10:40 ~ 11:00 **Coffee break**

Session II Hydrological Environment

11:00 ~ 11:30 Water resources and climate change management in Lao PDR: potential impact of climate change on flow in small river basins
Ketsana Xaiyasarn
National University of Laos
Ministry of Natural Resources and Environment

11:30 ~ 12:00 The environmental characteristics of coastal sand dunes in Korea
JiHyun Kang
National Institute of Ecology

12:00 ~ 13:00 **Lunch break**

13:00 ~ 13:30 Poster exhibition

Place: Room 201, Engineering Laboratory Complex Building, Tohoku University

- Assessment of soil erosion using revised universal soil loss equation (RUSLE) and GIS in Thailand
  Prem Rangsiwanichpong
  Tohoku University

- Environmental assessment in freshwater using eDNA
  Noriko Uchida
  Tohoku University
- Statistical analysis of woody debris volume to specify mechanism of recruitment in dam reservoirs in Japan
  Yuto Sukegawa
  Tohoku University
- The distribution and characteristics on frequent inland inundation areas of metropolitan areas in Japan
  Kota Nakaguchi
  Tohoku University
- Relationship between probabilistic precipitation and flood discharge by DAD analysis
  Yuta Sugawara
  Tohoku University
- Evaluation of flood and storm surge disasters model in Japan
  Yukako Tanaka
  Tohoku University
- Greenhouse-gases emission and mass balances in wastewater treatment plant
  Kazuya Kamiyama
  Tohoku University
- Prokaryotic distribution and diversity of soda lakes and surrounding soil in the desert areas of northern China
  Lu Li
  Tohoku University
- Microbial diversity in a methanol-feeding upflow anaerobic sludge blanket (UASB) reactor operated under different COD and sulfate concentrations
  Jialing Ni
  Tohoku University

Session III Anaerobic biotechnologies

13:50 ~ 14:20	Effect of fermentation temperature on hydrogen production from xylose and microbial community composition Chunsheng Qiu *Tianjin Chengjian University*
14:20 ~ 14:40	Energy production from food wastes by methane fermentation Kazuki Tonouchi *Tohoku University*
14:40 ~ 15:00	Hythane production from Cassava residue by hydrogen and methane fermentation Hongyu Jiang *Tohoku University*
15:00 ~ 15:20	The effects of HRT on the performances of hollow fiber anaerobic membrane bioreactor in treating food waste Hui Cheng *Tohoku University*
15:20 ~ 15:40	Research on the feasibility of dead livestock bodies' anaerobic co-digestion with manure Tao Zhang *Tohoku University*
15:40 ~ 15:50	**Coffee break**

Session IV Wastewater treatment

15:50 ~ 16:20	Quantitation of pharmaceutical and personal care products in Malaysian sewage effluent Ee Ling Yong *University Teknologi Malaysia*
16:20 ~ 16:50	An integrated two-stage anaerobic-aerobic bioreactor for the treatment of raw palm oil mill effluent (POME) Khairunnisa Abdul Halim *University Teknologi Malaysia*
16:50 ~ 17:10	The performance of biotrickling tower for nitrogen removal from wastewater Yan Guo *Tohoku University*

17:10	~ 17:30	The experimental research in water quality control of seawater recirculating aquaculture system (SRAS) using embedded immobilized microorganism pellets Bo Jiang *Tohoku University*
17:30	~ 17:50	Performance of an Anammox attached film expanded bed reactor Yanlong Zhang *Tohoku University*
18:00	~ 20:00	**Closing speech** **Dinner party**

Saturday, 03 Dec 2016

Lab visiting, free communication and discussion

Estimating the return period of multisite rainfall extremes – An example of Taipei City

○Ke-Sheng Cheng[1,2*], Tsong-Hsuin Lien[1]
[1]Department of Bioenvironmental Systems Engineering, National Taiwan University, Taipei, Taiwan
[2]Master Program in Statistics, National Taiwan University, Taipei, Taiwan

*E-mail: rslab@ntu.edu.tw

Abstract
Traditionally, hydrological frequency analyses were independently conducted at individual sites using annual maximum rainfalls. While this approach can provide useful results for site-specific design rainfall depths, it fails to offer insightful information about the return period of the concurrent occurrence of multi-site extreme rainfalls. In this study, we propose an innovative approach of multisite storm rainfalls simulation to tackle the problem of frequency analysis of multi-site extreme rainfalls. The approach is composed of four major components: (1) delineating homogeneous regions within the study area using K-means cluster analysis, (2) standardizing and modeling the same-event rainfall depths at different sites by a Pearson Type III random field, (3) stochastic simulation of multi-site storm rainfalls using a covariance matrix conversion algorithm, and (4) determining the return periods of concurrent occurrences of multi-site extreme rainfalls. Using historical hourly rainfall records available at 15 rainfall stations in northern Taiwan, site-specific rainfall depths of different durations and return periods of this study were found to be very close to results of a previous study of single-site frequency analysis, indicating good applicability of the proposed approach. Additionally, the return period of multi-site extreme storms (for example, storms yielding more than 400 mm 24-hour rainfall at several sites in a watershed) can also be evaluated based on the simulation results of the proposed method.

Keywords: Frequency Analysis, Multi-site Rainfall Extremes, Spatial Correlation, Stochastic Simulation

1. Introduction
Rainfall extremes of certain design durations and return periods are essential elements in hydrological design. Traditionally, such rainfall extremes are required at individual rainfall stations and are determined by single-site frequency analysis. However, there have had many evidences that a major storm (such as Typhoon Morakot of 2009) can result in extreme rainfalls at several neighboring stations and the return period of such concurrent occurrences of multi-site rainfall extremes cannot be determined by single-site frequency analysis. A unique feature of the concurrent occurrences of rainfall extremes is the significant spatial correlations among rainfalls of different stations. Taiwan has experienced increasing intensity, longer duration, and more extensive rainfall extremes of typhoons in recent years. Thus, it is due necessary for hydrological frequency analysis considering concurrent occurrences of multi-site rainfall extremes. In this study, we propose a new stochastic approach for simulation of event-specific multi-site maximum rainfalls with respect to certain design durations. The proposed approach is capable of generating large number of realizations of multi-site typhoon rainfalls which can then be used for multi-site frequency analysis of rainfall extremes.

2. Study area and data
Thirty-three years of hourly rainfall data available at fifteen rainfall stations in northern Taiwan were collected (Figure 1). Since almost all long-duration (longer than 12 hours) rainfall extremes were produced by typhoons, we firstly extracted hourly rainfall series of individual typhoon events at different rainfall stations. From these data, event-maximum rainfalls of 8 design durations (1, 2, 6, 12, 18, 24, 48 and 72 hours) of individual typhoons at all rainfall stations were obtained. Event-maximum rainfalls at individual stations were then standardized with respect to their long term averages and standard deviations. These duration-specific standardized event-max rainfalls have zero expectation and unit variance and their spatial variations were modeled as a Pearson type III random field.

3. Method
Standardized event-maximum rainfall (SEMR) at different stations were modeled by a Pearson type III (PT3) random field with marginal density of zero expectation and unit variance. Parameters of the marginal PT3 density at individual stations were estimated using the method of L-moments. Regional parameters were then calculated as the sample-size weighted average. Spatial covariance structure of SEMR is modeled by variogram analysis. An exponential semi-variogram model was used to fit the experimental variograms of SEMR of various design durations. Spatial covariance (correlation) function is then derived from the semivariogram. Stochastic simulation of the PT3 duration-specific SEMRs were conducted by transforming the PT3 random field (X) to a corresponding standard Gaussian random field (Z). Stochastic simulation of standard Gaussian random field was conducted by sequential Gaussain simulation (Liou et al., 2012; Hsieh, et al., 2014). Finally, the SEMRs were calculated through a frequency factor conversion. The event-maximum rainfalls at individual stations were then obtained by statistical

denormalization of SEMRs using the station-specific means and standard deviations of event-maximum rainfalls.

4. Results and discussion

For each of the eight design durations, a total of 10,000 realizations of multi-site event-maximum rainfalls were generated by the proposed stochastic simulation approach. On average, the study area experiences 3.69 typhoon events every year. A major advantage of the stochastic simulation approach presented in this study is its capability of characterizing the concurrent occurrences of rainfall extremes at different stations. Such capability enables the approach to offer an estimate of the return period for a multi-site extreme event. This is demonstrated using the 24-hour extreme rainfalls observed at several stations within the Taipei City during the typhoon Nari. Four rainfall stations within the Taipei City observed near or higher-than 600 mm rainfall depths in a 24-hour period during typhoon Nari (689, 862, 613, and 604 mm, respectively). Assuming a multi-site extreme event having higher-than 600 mm rainfalls at the four stations, we found 19 out of the 10,000 simulated events met the requirements. It is equivalent to a return period of approximately 142.6 (≈10,000/19/3.69) years.

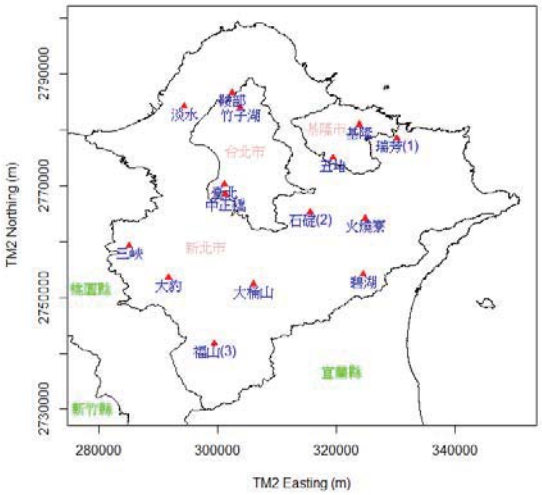

Figure 1. Rainfall stations used in this study.

5. Conclusions

Concurrent occurrences of rainfall extremes at several rainfall stations are commonly observed in Taiwan. The multi-site stochastic simulation approach proposed in this study is capable of generating realizations of multi-site event-maximum rainfalls with respect to given design durations. Such realizations preserve not only the marginal densities but also the spatial correlation structure of the duration-specific event-maximum rainfalls. We also demonstrate that the proposed approach can be applied to estimation of the return period of multisite rainfall extremes.

References

1. Cheng, K.S., Hou, J.C., Liou, J.J., Wu, Y.C., Chiang, J.L., 2011. Stochastic Simulation of Bivariate Gamma Distribution – A Frequency-Factor Based Approach. Stochastic Environmental Research and Risk Assessment, 25(2): 107 – 122, DOI 10.1007/s00477-010-0427-7.
2. Liou, J.J. Su, Y.F., Chiang, J.L., Cheng, K.S., 2011. Gamma random field simulation by a covariance matrix transformation method. Stochastic Environmental Research and Risk Assessment, 25(2): 235 – 251, DOI: 10.1007/s00477-010-0434-8.
3. Hsieh, H.I., Su, M.D., Cheng, K.S., 2014. Multisite Spatiotemporal Streamflow Simulation - With an Application to Irrigation Water Shortage Risk Assessment. Terrestrial, Atmospheric, Oceanic Sciences, 25(2): 255-266.

Effective Typhoon Characteristics and Their Effects on Hourly Inundation Forecasting During Typhoons

Bing-Chen Jhong[1*], Jhih-Huang Wang[1], Gwo-Fong Lin[1]
[1]Department of Civil Engineering, National Taiwan University, No. 1, Sec. 4, Roosevelt Road Taipei, Taiwan

*E-mail: jhongbc@ntu.edu.tw

Abstract
A novel type of inundation forecasting model with the effective typhoon characteristics is proposed by integrating support vector machine (SVM) with multi-objective genetic algorithm (MOGA) in this paper. Firstly, the proposed model and an existing model based on back-propagation network (BPN) are compared to show the forecasting performance. Next, the influence of typhoon characteristics is investigated by comparing the proposed model with the SVM-based model without typhoon characteristics. To demonstrate the superiority of the proposed model, an application to Chiayi City, Taiwan, is conducted. The results clearly show that the proposed model with typhoon characteristics is more appropriate for forecasting inundation depths than the SVM-based model without typhoon characteristics, especially for long lead times. In conclusion, the proposed model with effective typhoon characteristics is expected to provide more accurate hourly forecasts of inundation depths, and to be useful to support other disaster warning systems. Effective typhoon characteristics are also recommended as key inputs for inundation forecasting during typhoons.

Keywords: Inundation forecasting, Long lead-time forecasting, Typhoon characteristics, Multi-objective genetic algorithm, Support vector machine

Introduction

The heavy rainfall caused by typhoons (tropical cyclones occurring in the western Pacific Ocean) frequently lead to serious disasters, such as flood inundation, landslide or debris flow. Taiwan is located in one of the main paths of the northwestern Pacific typhoons. On average, the island is attacked by three to four typhoons in each year.

The flood inundation caused by heavy typhoon rainfall regularly leads to major loss of life and economic impacts. To mitigate flood damage, the development of warning systems has played an important role. For inundation forecasting models, the antecedent rainfall and/or inundation depth are the most frequently used inputs (Chang et al. 2010; Lin et al. 2013b; Pan et al. 2011), and the previous studies show that models with the aforementioned input produce acceptable forecasts for a lead time of 1 to 3 h only. However, the performance of existing models with only the antecedent rainfall and inundation depth often decreases rapidly. Therefore, to allow sufficient time for taking emergency measures, there is justification to add more effective information into models for long lead-time forecasting.

For rainfall, flood and reservoir inflow forecasting during typhoons, typhoon characteristics, which include the position, the intensity, the radius, and the speed of the typhoon, and the distance between the typhoon center and the study area, are important information. The addition of typhoon characteristics to improve long lead-time hourly reservoir inflow forecasting during typhoons has been confirmed (Lin et al. 2009a, 2010a). However, the influence of typhoon characteristics on inundation forecasting has paid little attention on the literature. Hence, it is reasonable to speculate that typhoon characteristics can provide useful information for inundation forecasting.

Associating the information of typhoon characteristics to inundation depth in constructing a physically-based mathematical model is difficult because of the high variability in space and time and the complex physical process, especially for long lead-time forecasting. To provide real-time inundation forecast, techniques with good flexibility in modeling nonlinear processes is necessary. An attractive alternative to the physically-based numerical models is neural networks (NNs), which can effectively extract the complex relationship between input and output of a system. Back-propagation networks (BPNs) and support vector machine (SVM) are used in this paper. In addition, the determination of suitable model input is an important process for establishing NN-based models. The collected information of typhoon characteristics may include noise (irrelative information) than the observed hydrologic data. Hence, to identify effective typhoon characteristics, an optimization approach capable of selecting optimal input combination is desired.

Multi-objective genetic algorithm (MOGA), which is one of optimization methods, has increasingly been applied. Pareto-optimal fronts on multi-objective optimization problems can be explored and discovered by MOGAs, and the capabilities of MOGAs have been well recognized (Liu 2009). The input selection of SVM-based models is regarded as crucial variables for the evolutionary strategy based on MOGAs. A forecasting model integrating SVMs with MOGAs to improve hourly typhoon rainfall forecasting was proposed by Lin et al. (2013a). Lin and Jhong (2015) applied the typhoon rainfall forecasting model to identify the optimal input combinations, and used the forecasted rainfall to present the spatial characteristics of the rainfall process. Therefore, there is justification to develop a real-time forecasting model integrating the

MOGA and SVM to improve the forecasting performance for inundation forecasting.

References

1) Chang LC, Shen HY, Wang YF, Huang JY, Lin YT (2010) Clustering-based hybrid inundation model for forecasting flood inundation depths. J Hydrol 385(1):257–268.
2) Lin GF, Chen GR, Huang PY, Chou YC (2009a) Support vector machine-based models for hourly reservoir inflow forecasting during typhoon-warning periods. J Hydrol 372(1–4):17–29.
3) Lin GF, Chen GR, Huang PY (2010a) Effective typhoon characteristics and their effects on hourly reservoir inflow forecasting. Adv Water Resour 33(8):887–898.
4) Lin GF, Jhong BC, Chang CC (2013a) Development of an effective data-driven model for hourly typhoon rainfall forecasting. J Hydrol 495:52–63.
5) Lin GF, Jhong BC (2015) A real-time forecasting model for the spatial distribution of typhoon rainfall. J Hydrol 521:302–313.
6) Lin GF, Lin HY, Chou YC (2013b) Development of a real-time regional-inundation forecasting model for the inundation warning system. J Hydroinf 15(4):1391–1407.
7) Pan TY, Lai JS, Chang TJ, Chang HK, Chang KC, Tan YC (2011) Hybrid neural networks in rainfall-inundation forecasting based on a synthetic potential inundation database. Nat Hazards Earth Syst 11:771–787.

Rainfall-Runoff Hydraulic Flow Computation at Surface of Tall Building

Chanakarn Chanphu
School of Engineering and Technology, Asian Institute of Technology, Pathumthani 12120, Thailand

*E-mail: st117720@ait.asia

Abstract

Nowadays, increasing urbanization has caused problems with increased flash flooding after sudden rain. Land use and other human activities also influence the peak discharge of floods. Also, the increase in high-rise buildings brings changes to rainfall-runoff characteristics. In highly developed areas, high-rise and tall buildings are constructed in a small area. The vertical area is greater than the drainage (horizontal) area. It seems that increasing area influences runoff and it does not consider conventional method (Rational method, 1889) which includes only the changing of physical conditions which are runoff coefficient (C) and time of concentration (t_c). This study proposes to consider the interaction between wind-driven rainfall and tall buildings. The discharge will combine both flow that is calculated from horizontal area and flow that occurs along the façade of tall building. The developed kinematic wave is used to investigate two components of runoff. Thus, the kinematic-wave model is described by the continuity equation and a uniform flow equation. Nusselt equation for thin film flow will be applied to momentum equation. Single uniform material building in highly urbanized area of Bangkok is selected to measure meteorological data; inputs for the developed model, and flow; for model validation, at the field. Moreover, a model will be developed to analyze not only one building but also a group of buildings. The effects of tall building and wind driven rainfall is expected to promote a higher peak discharge and a longer base time.

Keywords: AIT, Wind driven rainfall, Rainfall-runoff, Tall building

1. Introduction

Nowadays, urbanization is an important issue which especially affects rapidly growing cities. Increasing urbanization has caused problems with increased flash flooding after sudden rain. Land use and other human activities also influence the peak discharge of floods by modifying how rainfall is stored on and run off the land surface into streams. Due to urbanization, vertical, high-rise condominiums, shopping complexes, and business offices began to rise in the inner part of the city. The increase in high-rise buildings brings changes to rainfall-runoff characteristics. In monsoon season, the other component of flow can occur by interaction of wind driven rainfall and façade of building.

In conventional urban drainage design (Rational method, 1889) includes only the changing of physical conditions which are runoff coefficient (C) and time of concentration (t_c) due to urbanization. In highly developed area, high-rise and tall buildings were constructed in a small area. The vertical area is greater than the drainage (horizontal) area. It seems that increasing area has an effect on runoff and it does not take into account in this method. Therefore, the traditional urban drainage design is not appropriate and cannot be used for a particular type of area.

In this study, the influence of high-rise and tall buildings on the response of urban drainage systems to wind-driven rain is considered in proposed urban drainage design including changing of runoff coefficient (C) and time of concentration (t_c) which is same as traditional urban design. The discharge will be combined both of flow that be calculated from horizontal area and flow that occurs along the façade of tall building. There are a few studies related to urban drainage and tall building which is generally found in developing cities. For example, Jorge M.G.P. Isidoro et al., 2012 studied the Influence of wind-driven rain on the rainfall-runoff. Exploratory laboratory simulations were conducted using a scale model of a hypothetical high density urbanized area with high-rise buildings. The laboratory experiments show that building density and the spatial and temporal distribution of rainfall that results from wind and storm movement have a clear influence on the hydrological response to rainstorms.

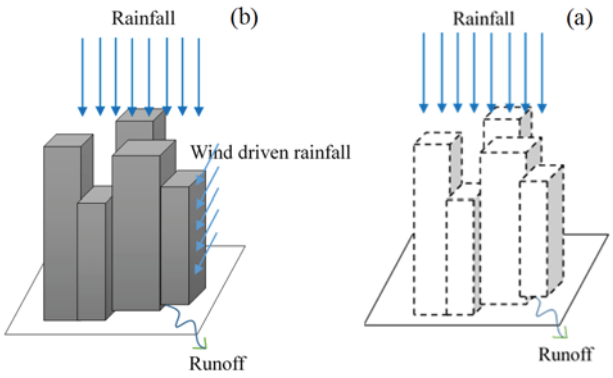

Figure 1 *(a) Feature of conventional design (b) Conceptualization of proposed design*

2. Methodology

The main objectives of this study are to take into account hydraulic flow along the surface of tall buildings which will affect rainfall-runoff. To achieve the objective, modified kinematic wave method will be used. The developed kinematic wave is used to investigate 2 components of runoff. Thus, the kinematic-wave model is described by the continuity equation and a uniform flow equation. In this study, Nusselt equation for thin film flow will be applied to momentum equation. The input data are primary which consists of meteorological data and characteristics of the building. They will be collected in the field. Also, discharge data will be collected there which will be used for validation of model. Single uniform material building in highly urbanized area of Bangkok is selected for data collection.

Also, model will be developed to analyze not only one building but also group of buildings that many variables can be varied. For Single building, variable of building can be varied; height, shape, building to area ratio, material and location of building to drainage system (effect on time of entry). For group of building can vary; number of building, variation of building and location of building to drainage system.

The parameters that have effect on rainfall-runoff for the proposed drainage design are

Wind direction – it affect impinging rainfall amount to vertical surface of building. For monsoon in Thailand, the wind comes from southwest direction. Perpendicular with façade will provide the most value of imping rainfall amount.

Wind velocity – it also affect impinging rainfall amount. The high velocity provides more value of rainfall amount which imping vertical surface than low velocity.

Size of building – it affect the value of driving rain coefficient

Orientation – effect of wind is different in each direction which building orient

Building to area ratio – the tall buildings were constructed in small area. The vertical area will more than horizontal area which increase area. Also, runoff coefficient will increase due to changing to impervious material (c=1)

Wind driven rainfall

According to the wind, WDR intensity is not the same as horizontal rainfall intensity which can be measured at station. Semi-empirical methods can be used to obtain rough estimates of the WDR exposure.

$$R_{wdr} = \alpha \cdot U \cdot R_h \cdot \cos\theta$$

Where U is the wind speed (m/s)
R_{wdr} is the driving rain intensity (mm/h)
R_h is the horizontal rain intensity (mm/h)
θ is the angle between the wind direction and the line normal to the wall (degree)
α is driving rain coefficient (s/m)

The driving rain coefficients vary considerably with the size of the building and variation across the building facade According to intensive review, a constant α is commonly assumed. To simplified, constant α is 0.222s/m be used. The top corner catches as much driving rain as in the free field.

Rainfall-runoff

The rainfall-runoff has two components due to interaction between wind, rainfall and building. The first component of runoff occur at the rooftop of building and flow to floor drain. Then, it flows along the vertical pipe or fall down (in case of no pipe) due to the gravity. For the other component of rainfall-runoff, it passes through façade of the building. In drainage system at ground floor, it collects two components of rainfall-runoff. Rainwater runoff from building facades is a complex process governed by a wide range of urban, building, material and meteorological parameters.

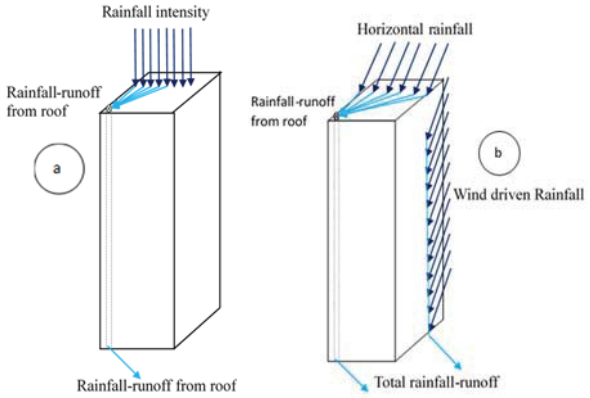

Figure 2 *Definition of rain intensity vector on a building (a) No effect of wind to rainfall (b) Effect of wind to rainfall*

For the first runoff component from rooftop, Rational method will be used to compute discharge. The time of concentration will be divided into two parts to compute time of entry. Firstly, horizontal rainfall interact horizontal area at the rooftop. Runoff will flow to drain floor. From Overtop and Meadows (1976), sheet flow of less than 92 meters (300 feet), use Manning's kinematic solution to compute t_t

$$T_t = \frac{0.007(nL)^{0.8}}{(P_2)^{0.5} s^{0.4}}$$

Where T_t = travel time (h)
n = Manning's roughness coefficient
L = flow length (ft)
P_2 = 2-year, 24-hour rainfall (in)
s = land slope

Second part can be computed due to flow by gravity pass along the pipe. Where h is distance of pipe in case, runoff pass along the pipes or height of the building in case, no pipe system provided for flow from the rooftop. Time of concentration is given by,

$$t_t = \sqrt{\frac{h}{2g}}$$

Where h is height of building or pipe length

Second part of runoff, Ruyer-Quil C and Manneville P (1998) had done the derivation of Nusselt solution from Navier-Stokes equations. Strictly, the Nusselt solution is only valid for the thin film flow of an isothermal Newtonian

liquid with constant density and kinematic viscosity down an inclined plane (with an angle θ to the horizontal) under the action of gravity. The flow is steady and parallel (laminar) and the film thickness is constant in space (no undulatory behavior). It is assumed that the liquid surface is uncontaminated and that the air friction on the liquid surface is negligible. The Nusselt solution is given by:

$$u(y)dy = \frac{gsin\beta(2h_N y - y^2)}{2v}$$

The film flow rate and average velocity are given by

$$q_N = \int_0^h u(y)dy = \frac{gsin\beta {h_N}^3}{3v}$$

From which an average velocity u_N can be defined by $q_N = h_N u_N$,

$$u_N = \frac{gsin\beta {h_N}^2}{3v}$$

Where u is velocity along x-axis
ρ is the density
υ is the viscosity
g is the intensity of the gravitational acceleration.
θ is an angle between inclined plane and the horizontal. In this study, β equal to 90 degrees due to vertical surface of building.

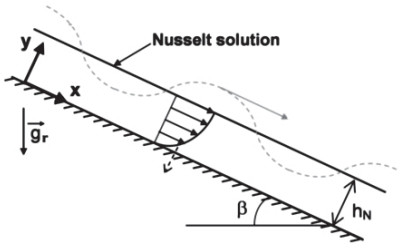

Figure *エラー! 指定したスタイルは使われていません。*

Fluid film flowing down an inclined plane (souce: Blocken and Carmeliet, 2012)

From comparison between numerical and experimental of Blocken and Carmeliet (2012) research, they suggest that the Nusselt solution is a good approximation for representing the time averaged properties of thin film flow, up to film Reynolds numbers of 1000. The relationship Re = q_N/υ implies that the Nusselt solution can thus be used up to runoff rates of q = 4705 L/mh, or horizontal rain intensity = 4-80 mm/h which is a very high threshold unlikely to be exceeded except for very exceptional WDR events.

Fieldwork and Data Collection

1. Select field work by using criteria for selecting building
2. Measure rainfall intensity, wind direction and wind velocity at the top
3. Measure flow (Vpipe+Vsurface) in drainage pipe
4. Location of measurement (the most close to building)

The criteria to select building based on

- Building to area ratio greater than 1; Vertical surface area is more than horizontal area
- The building is made from uniform materials
- The building is located in high urbanization area and high vulnerability to flood
- The building should be geometry shape which starting with simple shape

For installation the equipment, this study has two equipment to install at the field. These are rain gauge and wind measurement to install at the rooftop of building, and Flopro xci that is equipment for measurement flow in the pipe to install in the drainage pipe at ground floor. The criteria to select the place to install based on,

- Safety place for equipment
- Accessibility for installation and collecting data
- Orientation of the building should be perpendicular southwest, which including impact of wind due to monsoon in Thailand.
- Position of building to the drainage system. The good represent is the building covers all of the area which runoff is collected to one point.
- Location for measurement should the most close to building to reduce overland flow.

In this study, the kinematic wave runoff model will be developed to compute runoff for many cases of building. Cases to analyze can be divided for two types of use:

Single building, variable of building can be varied;

- Height
- Shape
- Building to area ratio
- Material
- Location of building to drainage system (effect on time of entry)

Group of building can vary;

- Number of building
- Variation of building
- Location of building to drainage system (has effect on time of entry)

3. Expected Results

According to the objectives of this study, the results should be satisfied and achieved all of objectives as much as possible. By following the objectives of study the expected results should be defined by:

- The developed rainfall-runoff hydraulic flow along the surface of tall building model
- The change of rainfall-runoff due to considered effect of tall building with wind driven rainfall

Therefore, considered effect of tall building and wind driven rainfall is expected to promote a higher peak discharge and a longer base time.

For future study, effect of parameters such as absorption, evaporation, splashing, bouncing, adhesion and spreading should take into account to compute rainfall runoff.

References

1) Abuku, M., Janssen, H., Poesen, J., & Roels, S. (2009). Impact, absorption and evaporation of raindrops on building facades. Build Environ, 44(1), 113-124.

2) Beijer, O. (1977, August 28-31). Concrete walls and weathering. RILEM/ASTM/CIB Symp. on Evaluation of the Performance of External Vertical Surfaces of Buildings, 1, 67-76.

3) Blocken, B., & Cameliet, J. (2004). A review of wind-driven rain research in building science. J Wind Eng Ind Aerodyn, 92(13), 1079-1130.

4) Blocken, B., & Carmeliet, J. (2010). Overview of three state-of-art wind -driven rain assessment models and comparison based on model theory. Buil Environ, 45(3), 691-703.

5) Blocken, B., & Carmeliet, J. (2012). A simplified numerical model for rainwater runoff on building facades:. Build Environ, 53, 59-73.

6) Blocken, B., Abuku, M., Nore, K., Briggen, P., Schellen, H., Thue, J., . . . Carmeliet, J. (2011). Intercomparison of wind-driven rain deposition models based on two case studies with full-scale measurement. J Wind Eng Ind Aerodyn, 99(4), 448-459.

7) Davies, D. B. (2004). Urban Drainage.

8) Hall, C., & Kalimeris, A. N. (1982). Water movement in porous building materials–V. Absorption and. Build Environ, 19, 13-20.

9) Jorge, M., Isidoro, João, L., Lima, d., & Leandro, J. (2012). Influence of wind-driven rain on the rainfall-runoff. Urban Water Journal, 1-12.

10) Ruyer-Quil, C., & Manneville, P. (1998). Modeling film flows down inclined planes. Eur Phys J B, 6, 277-292.

11) Straube, J., & Burnett, E. (1977, March 17). Driving rain and masonry veneer. ASTM Symp. on Water Leakage Through Building Facades, 73-87.

Water Resources and Climate Change Management in Lao PDR: Potential Impact of Climate Change on Flow Small River Basins

○Ketsana XAIYASARN[1*], Bounheng SOUTHICHAK[2]

[1] Lao National Mekong Committee Secretariat, Ministry of Natural Resources and Environment, Lao PDR
[2] Faculty of Engineering, National University of Laos

*E-mail: ketsanalaos@gmail.com

Abstract

Lao PDR is one of many countries that vulnerable to the impacts of climate change. In recent years, the country has witnessed more frequent and severe floods and droughts which are alternately occurring each year. Temperature is continuously increasing and the rainfall is erratic. Management of water resources in Laos PDR is based on the Integrated Water Resources Management (IWRM) Principle that adopted by the Mekong River Commission so called IWRM based Basin Development Strategy. There were two studies on the impact of climate change in Laos with mainly focused on its impact to the water resources: one was done in Namsane river basin in 2015, the study projected that future rainfall will raise little around 1.5% - 5% and temperature will increase around 0.69 °C -2.51 °C, while mean monthly streamflow in Namsane river basin will decrease in January and February but increased from March to December and shift the peak of the streamflow from July to August and slightly decrease in September to December. In addition, the study in Nam Xong river basin in 2013, it was projected that average temperature will increase 0.04°C to 0.47°C. Water flow will decrease due to climate change and land use change for the next 20 years, especially in the middle part of Nam Xong watershed where water transfer to Nam Ngum Reservoir, the water flow will decrease between 11.7%-12.23% in middle part and 0.7%-1.9% for the whole watershed.

***Keywords*:** water, climate change, temperature, rainfall, Namsane, Nam Xong

1. Introduction

Lao PDR is a land locked (linked) country bordering with Myanmar, Cambodia, China, Thailand, and Vietnam with an area of 236,800 km^2. About 6.49 million people live in its 18 provinces (LSB, 2015), GDP growth average 6.8% while most people 63% still living in rural areas. 90% of the total area lay put in Mekong river basin (figure 1) equivalent to 26% of the Mekong River basin and contribute 370 cubic million and 41% of Mekong river from Lao PDR. Mekong river flow 1,898 km through Lao PDR by sharing 11 main tributaries to the Mekong river. The surface water available 332.5 km^3 or 55,000 m^3 per capita, the very high rate compared with many countries in Asia.

Figure 1: Map of Mekong River Basin

2. Water and Climate Change Situation in Laos

Lao PDR is rich in water resources with annual average of rainfall 1,900 mm equivalent to 462 km^3. Surface water serve for rainy season while ground water serves for 20%. Mekong river flow through Lao PDR 1,898 km and 13 tributaries and 41% of the average annual discharge of the whole Mekong Basin. Annual average of the Mekong flow is 8,500 m^3/s. Surface water available 332.5 km^3 or 55,000 m^3 per capita, The very high rate compared with many countries in Asia.

Lao PDR is similar to many leases developed countries that have number of low industries development, therefore the greenhouse gas emission is still low. The study on the greenhouse gas emission conducted in 2011 which is based on the studied in year 1990 and 2000 databases had showed that: annual greenhouse gas emission was in 2011 was 75 million tons/year since 24 MLT in 2000 while forestry sector emitted 66.9 million tons, agriculture emitted 5.7 million tons; energy 1.9 million tons and 0.2 million tons from waste and 0.005 million tons from industries.

South East Asia START Regional Centre SEA START conducted the study in Mekong basin especially in Thailand, Lao and Viet Nam pointed out that average temperature will increase 12 decree Celsius, increasing number of hot day and cold day as well as rainfall (extreme flood and drought) annual average hot day increase up to 23 weeks and cold day that temperature less than 23 degrees' Celsius decline less than 23 weeks in the basin wide.

Impact of climate change in Lao PDR are mainly resulted by flood and drought. Since 1966-2009 the natural disaster has continue occurred almost every year. The main impact area is

the Middle and Southern part of Lao PDR. Since 1995 the flood and drought are increasing and more frequently due to the rising of temperature and irregular warming weather. In 1996 there were flood and drought effected in many parts of Lao PDR in the same year. In addition, there were flash flood and seasonal flood in mountainous areas and the Northern and Southern part of Lao PDR in 1995, 1996, 2000, 2002, 2005 2008 and Typhoon Ketsana (serious case) destroyed Laos in 2009 and wause of big damaged. It was observed that from 1966-2005 the damage of natural disaster was around 32 million USD effect agriculture area 538,845 hectares.

3. Water Resources and Climate Change Management

Management of water resources in Laos PDR is based on the Integrated Water Resources Management (IWRM) Principle that adopted by the Mekong River Commission so called IWRM based Basin Development Strategy in 2011. The Department of water resources (DWR) and Lao National Mekong Committee (LNMC) are the two main direct agencies in management, develop of water resource in the Lao PDR while DWR is taking the task for nationwide river basin management including surface water, ground water, water quality and acting as a focal point for implementation of IWRM principle in Lao PDR and LNMC has direct role to coordinate act as a coordinating agency with the Mekong River Commission and National Mekong Committee of member countries of the Mekong River Commission under the 1995 Mekong Agreement for managing and development the Mekong River Basin.

The Ministry of Natural Resources and Environment of Lao PDR had been assigned to develop the National Mekong Plan to implement the MRC strategy at national level and play a role for focal point for MRC Secretariat by coordinating through the Lao National Mekong Committee Secretariat. The National Mekong Committee coordinates MRC work at the national level and provides links between the MRC Secretariat and the relevant line agencies in implementing MRC core functions and activities.

Implementation of the MRC Core Function is the main task to the Ministry of Natural Resources and Environment to be a leading agency and cooperation with relevant line agencies such as Ministry of Energy and Mines, Ministry of Agriculture and Forestry, Ministry of Public Work and Transport and Ministry of Planning and Investment. All decentralized activities will be transferred to relevant line agencies for implementation. The line agencies has incorporated all decentralized activities into their annual sector development plans and submit to the Ministry of Planning and Investment (MPI) for allocation of national annual development budget. The MPI will then formulate to the National Socio-economic Development Plan (NSEDP) including allocation of national annual development budget to all development projects (including for MRC decentralized activities) and submit to the Government and Parliament for approval.

The two river basin committees such: Nam Teun-Kadin and Nam Ngeum river basin committees were established and continue to expanse to another river basins. In addition, there is one national IWRM demonstration site in Lao PDR for the study and exchange lesson.

To ensure the climate change and disaster management, the government of Lao PDR adopted its National Adaptation Programme of Action to Climate Change (NAPA) which is focus has been placed on, four sectors, namely, agriculture, forestry, water resources and public health. In this regard, 45 priority projects have been identified to implement urgent plans to adapt to climate change and the Strategy on Climate Change of Lao PDR adopted in 2010 defined key strategic priorities and adaptation and mitigation option for key 7 sectors including: (1) agriculture and food security, (2) firstly and land use, (3) water resources, (4) energy and transport (5) industry, (6) urban development and (7) public health and followed by the action plan for climate change adaptation.

The Government of Lao PDR ratified the UNFCCC in 1995 and the Kyoto Protocol in 2003. The National Adaptation Plan of Action (NAPA) was released in May 2009 and contains 45 priority projects totaling US$ 85 million within four identified sectors of priority for climate change adaptation, namely agriculture, forestry, water and water resources and health. Lao PDR's Intended Nationally Determined Contribution for reduction of greenhouse gas emissions and is being implemented with the help of a new project funded by the Global Environment Facility in partnership with UNDP and the Department of Disaster Management and Climate Change. In recently, Lao PDR committed its support to the Climate Change Agenda by submitting its own contribution in time for COP 21. These contributions are seen as a key component informing the ratification of the Paris Climate Agreement.

3.1. Case Study Impact of Climate Change in Namsane River basin

K. Xaiyasarn (2015), projected future situation of climate and assessed the impact of climate change on streamflow in this basin by collecting data from observe stations inside and nearby Namsane river basin then applied hydrological model called Soil and Water Assessment Tool (SWAT) to assess the flow under the present and climate change condition.

Namsane is one of the 14 main Rivers of the Mekong and supply more than 4,271,235,840 m³ annual to the Mekong River with an altitude of 2,620 meters above mean sea level. The River is 157 km long with a catchment area of 2,100 km² lay within 18°33' N - 19°16' N and 103°32' E - 104°03' E. Annual average basin rainfall is 2,710 mm and annual mean Streamflow at Muang Kao station is 135.44 m³/s. (unit discharge in Per litter/Km = 5.6) (figure 2 show location of Namsane river basin in Lao PDR).

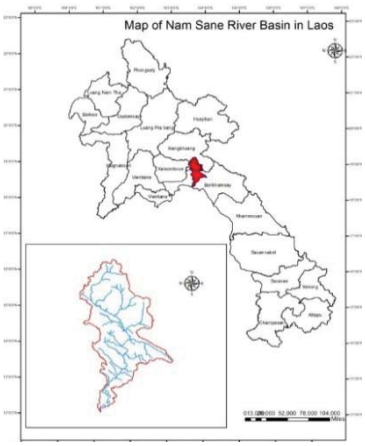

Figure 2: Location of Namsane River Basin

Daily climate data obtain from hydro-meteorological observe stations from 1996-2010 were inputted in the tool and daily model calibration and validation with observe data and applied model before applied adjusted climate change data from Global Climate Change Model (GCM) from 2020-2040 with two climate change conditions called scenarios A2 and B2 were applied for alternative assessment. The result from the study showed that future temperature towards 2040 in Namsane River basin will slightly increase up to 0.62 – 4.34 Degree Celsius (°C) in the whole basin (figure 3).

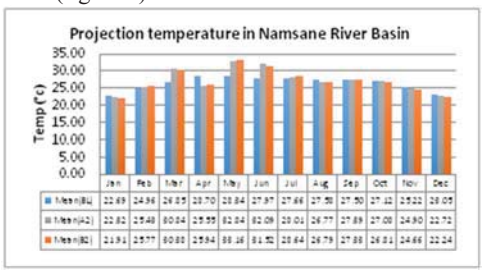

Figure 3: Projection temperature in Namsane River Basin

Rainfall will raise little around 1.5% - 5%. Mean monthly streamflow in Namsane river basin will decrease in January and February but increased from March to December and shift the peak of the streamflow from July to August and slightly decrease in September to December (figure 4).

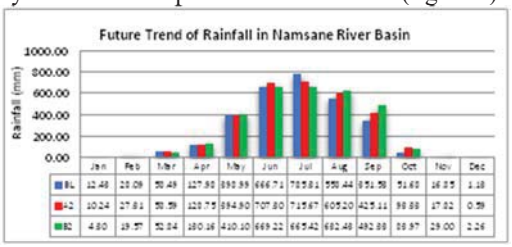

Figure 4: Future Trend od Rainfall in Namsane River Basin

The rising of the rainfall in upper basin of the basin cause of increasing of the streamflow around 8% - 56% in the whole basin. The wet season in Namsane River basin will increase around 50 % of total streamflow and increase around 20% of the streamflow in the dry season (figure 5).

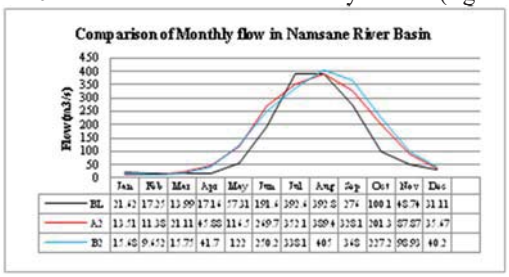

Figure 5: Comparison of Monthly flow in Namsane River Basin

3.2. Case Study Impact of Climate Change in Nam Xong River

R. Sayasane (2013) studied climate change impact on stream flow in Nam Xong river basin and projected climate change and impact of the climate change on flow.

The Nam Xong watershed covers an area of 180,425 ha and is the second largest sub-watersheds out of the 18 sub-watersheds that make up the Nam Ngum Watershed Located in the central part of northern Lao PDR between 18°38‟58”N – 19°17‟10”N and 102°13‟37”E – 102°37‟57”E, the Nam Xong watershed is 83km north of Vientiane and 14 km south of Kasy. Vientiane province makes up 97.3% of the area and 100% of the population. The central and largest city in the basin is Vangvieng, which is well known for its tourist attractions. Nam Xong River supports highly water flow to demand of natures and living of local people. Moreover, it also supports the Nam Ngum 1 reservoir for its electricity generation (figure 6).

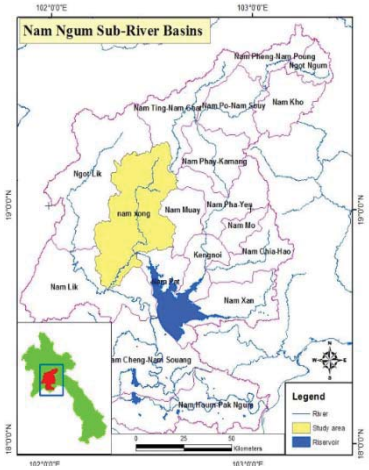

Figure 6: Location of Namxong River Basin

Future climate data of SEA START RC and ArcSWAT was applied as the main tool of water balance assessment, which consists of many components such as physical aspects of watershed (landuse, soil type, slope, and river system), weather data, water use and hydrological process. The study projected that average temperature will increase 0.42°C in wet season and decrease 0.17°C in dry season for A2 scenario and it will increase both wet and dry seasons for 0.47°C and 0.04°C respectively for B2 scenarios (figure 5).

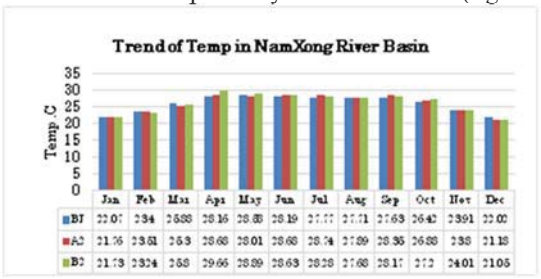

Figure 7:Projection trend temperature in Namxong River Basin

Rainfall will increase in upper part of the basin but decrease in the lower basin around ± 1% (figure 7). Water flow will decrease due to climate change and landuse change for the next 20 years, especially in the middle part of Nam Xong watershed where water transfer to Nam Ngum Reservoir, the water flow will decrease between 11.7%-12.23% in middle part and 0.7%-1.9% for the whole watershed (figure 8).

4. Challenge and Opportunity

Water resources is continuing support the socio-economic development and seem to be double increase since many river in Laos have high potential in generate power, navigation and agriculture and tourism and likely to face with the water shortage and low water quality this will bring to effect to human and environmental health. In addition, natural disaster is frequency happen in Lao PDR such: flood and drought due to the climate change condition.

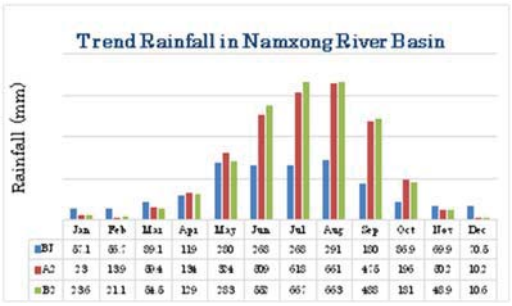

Figure 8: Trend rainfall in Namxong River Basin

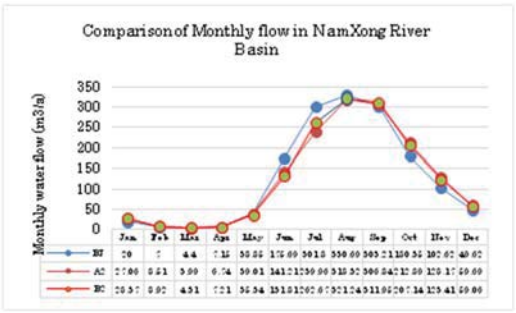

Figure 9: Comparison of Monthly flow in NamXong River Basin

The quantity of water in the Mekong river and its tributary and other water body are getting decrease and shallow cause by sedimentation and impact by climate change especially in the unseasonal dry season effected to the agricultural, industries and recreation sectors result to the low level of people livelihood. In addition, the water quality in some of the tributary decline due to the degradation of the polluted water from development and agricultural project, community and other service sectors; shortage of clean water in some urban and rural area; Water conflict and allocation in some area that mainly for the hydropower, agriculture and irrigation some are and water born disease from water quality.

5. Conclusion and Recommendation

Climate change is continuing impacts Lao PDR not only the physical but also the social and environmental and significant result are the delay of seasonal hot and rainy season in Lao PDR. In addition, the increasing of hot day and raining day is more frequently. The appropriated tools for planning water resources management and the right approach are needed in order to maintain the balance of the water resources development and environmental flow to maintain ecosystem. There are many development projects that require water as a main input, However, water is threat by both development and climate change. Hence, there is a need to improve the capacity of concern orgnasation who deal with water resources and environment in order to improve the water resources system as well as the maintaining water resources in the nation-wide.

There is limited data and information support to the climate change and river basin planning since the data input to the model is more importance to predicted hydrological condition in the basin. Hence, there is a need to strengthening the mandate and responsibility of the concern organization who deal with water resources management and development.

As the projected climate change impact on streamflow varies remarkably between the different climate models, the uncertainty should be taken into account in both river and water management and climate change adaptation. Further, as the study results indicate that variation between climate models is significant, this study also emphasizes the need for a multi-climate model evaluation instead of just one climate model as has so far been mainly the case when estimating the possible climate change impacts to the Mekong hydrological variables (also mentioned by Lauri et al., 2012).

References

1) Mekong River Commission (2016): Integrated Water Resources Management based Basin Development Strategy;
2) Water Environment Partnership in Asia (2004): State of water environmental issues: State of Water: Lao PDR,
3) Strategy on Climate Change on the Lao PDR (2012): Climate Change Situation in Lao PDR (p 4)
4) Tachikawa et al (2004): Catalogue of River for Southeast Asia and the Pacific/Volume 5, The UNESCO-IHP Regional Steering Committee for Southeast Asia and The Pacific/ Unesco –IHP Publication, Kuala Lumpur, Malaysia, 2004
5) Lao Statistics Bureau, (2015) District Population Proportion. 2015
6) IPCC. (International Panel on Climate Change) Contribution of Working Group I to the Fourth Assessment Report of the Intergovernmental Panel on Climate Change. In S. Solomon, D. Qin, M. Manning, Z. Chen, M. Marquis, K. B. Averyt, et al. (Eds.). Climate Change 2007: The Physical Science Basis. Cambridge: Cambridge University Press
7) R. Sayasane et al., (2013) Assessment of Potential Impacts of Climate and Landuse Change on Local Streamflow: A Case Study of the Nam Xong Watershed in Lao PDR
8) Arnold, J.G., J.R.Kiniry, R. Srinivasan, J.R. William, E.B. Haney and S.L. Neitsch: Soil and Water Assessment Tools-Input/Output Document, Texas Water Resources Institute, 2002
9) B. Shrestha M. S. Babel., S. Maskey., A. van Griensven., S. Uhlenbrook., Impact of climate change on sediment yield in the Mekong River basin: a case study of the Nam Ou basin, Lao PDR: Hydrol. Earth Syst. Sci., 17, 1–20, 2013 Hydrol. Earth Syst. Sci., 17, 1–20, 2013
10) Flood Management and Mitigation Programme, Component2: Strutural Measures & Flood Proofing in the Lower Mekong Basin, Mekong River Commission Secretariat, 2009
11) Thanapon Piman, Vanna Nuon, Sasikan Charoensatsiri, Aekkapol Aekakkararungroj and Nguyen Huong Thuy Phan. Climate Change Analysis in the Lower Mekong Basin: Review of Availability of Observed Meteorological Data: he Mekong River Commission, Vientiane, Lao PDR, October 2014

The environmental characteristics of coastal sand dunes in Korea

○JiHyun Kang[1*]
[1]National Institute of ecology

*E-mail: kjhb612@nie.re.kr

Abstract

Coastal sand dunes are eolian landforms which are formed near shore by transported sand. The dunes have functions to storage sand and protect from storm wave. It is buffer zone between terrestrial and marine, and provides important and unique ecosystem. Beautiful landscape makes people take a rest and enjoy leisure activity. Therefore many coastal sand dunes have destroyed by coastal developing. There are a total of 199 sand dunes in all regions including island in South Korea. 150 and 49 sand dunes are formed in west coast include Jeju island and east coast, respectively. Environmental characteristics of dune show difference according to the location. Because of the dunes located in west coast are influenced by northeast monsoon, the sands extend to inland and widths are wide. The sand size is small from 200 to 300 ㎛, the slopes of beach are gentle, generally. On the other hand, the dunes located in east coast are formed above beach ridge formed by ocean currents and waves. The sediment size is coarser than that of dune in west coast. Ocean erosion phenomena have been recognized as a problem. There are several reasons for ocean erosion, the disturbance and disconnection of beach-dune sharing system might be one of them. The sand dunes are recognized as important landscape and ecosystem, many researcher and institutes make effort to conserve. National institute of ecology and Ministry of environment are currently carrying out research for updating the status of 199 sand dunes. The results will used to assess the conservation values for each sand dune, and management guidelines of costal sands will be proposed according the management types.

Keywords: Coastal sand dune, ecosystem, management, conservation

1. Introduction

Sand dunes are eolian landforms and costal sand dunes develop in coastal situations where an ample supply of loose, sand-sized sediment is available to be transported inland by the ambient winds (Martinez and Psuty, 2007). They are in coastal area, and the environment is unique because they are in coastal areas which are between terrestrial and marine environments.

Coastal sand dunes function to supply various benefits for human and ecosystem. First, they provide a reserve supply of sand for use by waves during storms and play a role as natural and soft breakwater. At the same time, we get crucial information on the paleo-environment by buried storm surge. Second, they are important ecosystems, supporting valuable communities of plants and animals. Specially, costal area is buffer zone between terrestrial and marine. There are halophyte species and herbaceous plants which can survive around sea. Furthermore, human generates cultural values, enjoy leisure activities and recharge. Not only the coastal sand dune is a part of ecosystem, the space is social area. Therefore coastal sand dune is recognized as **social-ecological system** (Nordstron, 2008).

Recently sand dunes are destroyed and removed by developing even though the ecological important. Meanwhile some part put a lot of effort into reserve and restoration. Here, I'd like to introduce the efforts to protect coastal sand dunes, as well as the characteristics of sand dunes in South Korea.

2. The status of coastal sand dune in South Korea

Korea is surrounded by sea on three sides, peninsula. That mean we have good condition to form coastal sand dunes. According to the official publication on the Ministry of Environment (MOE, 2001), they reported 133 coastal sand dunes. The report is meaningful first survey to identify the status of coastal dune the whole country except island. The 133 dunes were classified as three classes 'Good[1]', 'Moderated[2]', 'Bad[3]' according to the status of conservation. Recent survey provided a new list in all regions including island areas in South Korea, there is a total of 199 coastal dunes (Choi and Kim, 2015). Over half of them are in southwestern province, Chungnam and Jeonnam (Figure 1). Compared to the research in 2001 and 2015, the conservation status slightly worsened, and the lengths and area of the dune are decreased by 20% and 30%

[1] Good: Beach-dune interaction are active, Natural coast>70%, and Well conserved dune
[2] Moderated: Beach-dune interaction are possible, 20<natural coast<80%
[3] Bad: Natural coast<20%, Disconnected from beach by artificial walls, and Largely destroyed

respectively. Though from the statistics which draw comparison changes of coastal area between 2000 and 2010, the population who live around coastal area has increased by 6% and area for industrial complex has increased by 105%, approximately(Mof, 2011). Landscapes of sand dune have changed by development pressure such as road, building, agriculture and so on. Different use and developing have done each timing by social concern, policy, people's needs. In the '60s and '70s, the sand dunes were recognized as barren sandy ground. At the same time, there was a need for more farmland so that more people do farming. The many sand dunes reclaimed into farm and plant a *Pine* or *Pinus thunbergil* to protect wind in the back of beach, fore-dune. In the '80s-'90s, many houses, buildings and structures have been built for economic and cultural activities around beach. In the 2000s, the important and function of natural sand dunes and coastline have begun to attention partly and several sand dune were designated as conservation area.

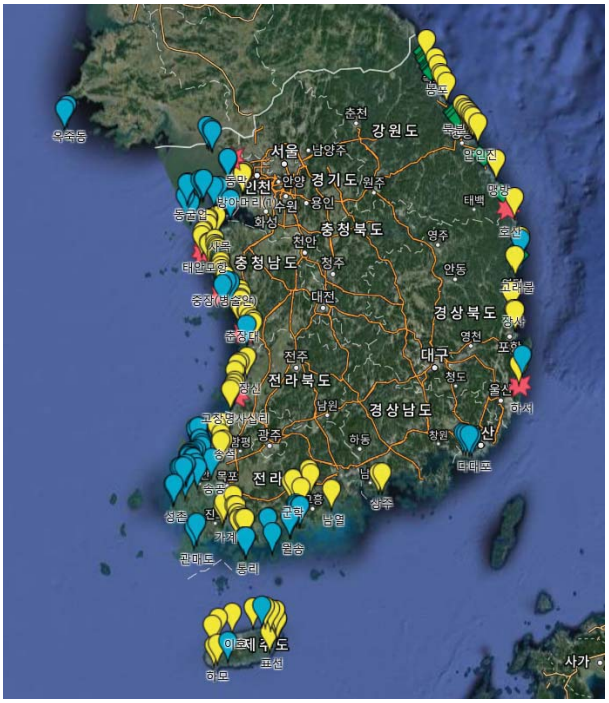

Figure 1. Distribution of coastal sand dune in South Korea

3. The environmental characteristics

Sand dunes are eolian landforms which are formed by wind. Therefore wind direction and speed are important factors to develop sand dunes.

South Korea is located in Northern Hemisphere between 33°N-38°N which is influenced by westerlies. The wind direction has seasonally changed, and northwest monsoon is predominant in winter. Therefore the shapes of sand dunes located western coast reflect the wind direction. Figure 2 shows an example which has been formed by northwest wind. This sand dune where is located island was open in the northwest direction. Sand supply from beach was available to be transported inland by the winds, the maximum width was 600m, approximately. On the other hand, sand dunes where are located east coast are different the shape and formation process.

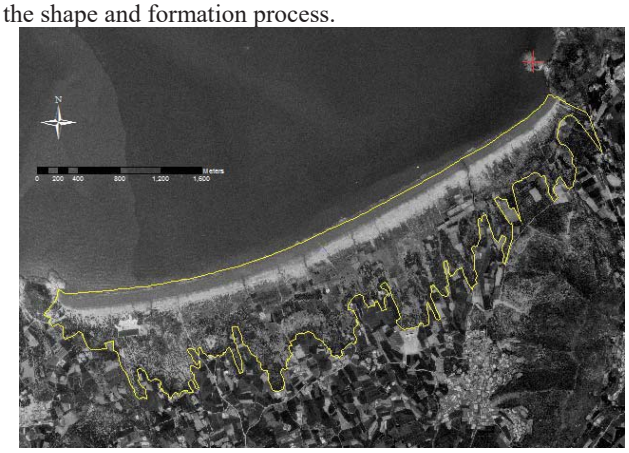

Figure 2. Sand dune in west coast coastline (Geumil Myeongsasimni, 1980). The width from shore line to inland is wide and the direction sand deposit matches up with northwest wind.

One of the important geographical factors affecting the climate in Korea is the Taebaek Mountains. Northwest monsoon is abating by the high mountains. However, sand dunes located east coast are less impacted structurally by Northwest wind. Because beach which supplies sand to dune is located in the east side, therefore sand can be transported to inland by east wind. While northeast wind from the sea of Okhotsk in early spring is blowing, there is a light wind and short time. Therefore the width of dune is relatively short than that of dune in the west coast. Many researches and monitoring explain that the sandy sediment move along ocean current and wave. At first, several beach ridge and coastal barrier have been formed during sea level rise. And then sand was transported to inland by wave (coarser sand) and wind (fine sand), and deposited avobe the coastal barrier (figure 3). Therefore the shape of dune is elongated.

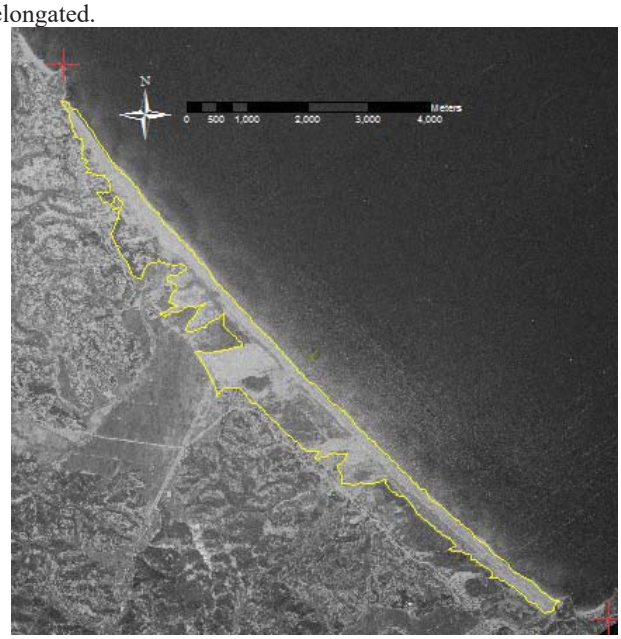

Figure 3. Sand dune in east coast (Dongho, 1972). Beach ridge is formed by ocean currents and wave, and then some part of sand is transported to near shoreline. Therefore the shape is elongate.

Beach sands vary considerably both in size and composition. Grain size especially is an important factor in determining the type of beach that is most commonly observed at any locality. Not only the different shape of dune between west and east coast, but the sand size shows the difference. While the sand size on west coast is small, that of east coast is coarser, relatively. There are many reason to explain the difference, the difference of geomorphological factor is one of them. Coastal sediment can gain from several sources. River is main source to transport sediment from upper to downstream. The sediment size is getting smaller as it goes downstream by weathering process and natural sorting. In other words, river length has relevance to the coast sediment size. The rivers which flow to west coast are long and well developed, while the rivers to flow east coast are short and the size is small, because main mountains are east-sided in South Korea. The sand size of dune is 200-300 ㎛ in west coast, and it is a typical size of aeolian sand dune(Choi *et. Al*., 2011). On the other hand, the size is coarser in sand dune of east coast which formed above beach ridges.

The environment difference of sand dune between west and east coast appears in a beach slope. Figure 4 shows profiles of sand dunes. The (a) is a sand dune in *Guanmedo* and (b) is a sand dune in *Goraebul* where is located west and east coast, respectively. The sand dune (a) has a beach with gentle slope (6˚), while (b) shows very steep slope within 10m from shoreline.

The greater the difference between the ability of swash and backwash to transport sediment, the steeper the beach profile that develops. Swash means that wave run up the beach face, and backwash is that the wave flows back down the beach face. Backwash rapidly drains down into beaches composed of coarse pebbles or cobbles such that little of the material carried up the beach face is transported back down, building a steep beach face. In contrast, fine-grained beaches stay saturated in the short interval between waves due to their low permeability, limiting backwash infiltration into the beach face and resulting in greater seaward transport and flatter beach slopes. Cobble beaches commonly have slopes that exceed 20˚, pebbly beaches have slopes of 10˚ to 15˚, and sandy beaches have slopes of 3˚ or less (Paul, 2014). The slopes of two sites in Figure 4 are steeper than these of general beaches, and the slope of *Gorebul* is nearly similar cliff by coastal erosion. Beach erosion began to occur in the 1990's, and along the shorelines of many beaches, about 400 beaches have reported erosion (Kim *et. Al.*, 2008). The reason occurred ocean erosion is also related with coastal sand dune destruction by developing. Dune and beach is sand-sharing system whose components respond to variations in energy level and to mobilization of sand from one portion to another (Martinez and Psuty, 2007). The sharing system can't work at sand dunes which are destroyed or covered by impermeable layer when the coastal erosion occurs during storm. The road and building constructed between beach and fore-dune is also disturbed to transfer.

The sea level change of the (a) area ranges around about 4 m during the ebb and flow. Therefore the width of beach is wider at low tide. On the other hand, the sea level change of (b) is 0.3m, approximately, there is little difference in the change of coastal line. Furthermore, coastal erosion is proceeding slowly at beach (b). Beach changes within a dynamic system are cyclic. Some part stores and releases sand in exchanges of sediment. Storm waves move sand from the beach and dune to build storm bars. Subsequent calm weather favours onshore movement of the sand to re-establish the beach (Rod, 2001). However the cycle doesn't working in some sand dunes because of breaking of sand-sharing system by artificial structure such as hard walls for shore protection and roads. Therefore the cliff by erosion is maintained without sediment transfer.

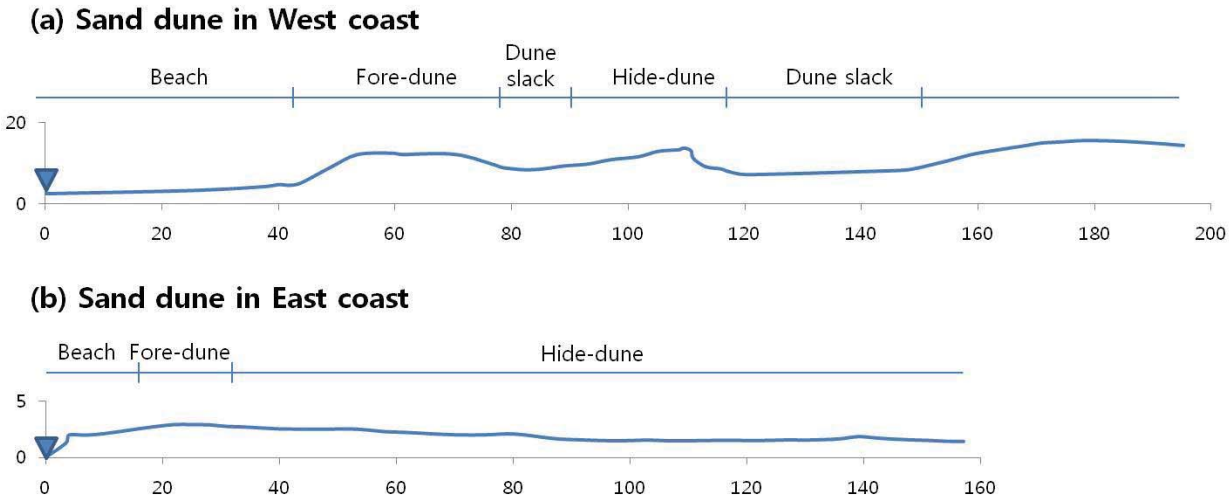

Figure 1. The profiles of sand dune(a: sand dune at *Guanmedo* in West coast, b: sand dune at *Goraebul* in East coast)

4. The management

Despite the systemic and functional significances, many sand dune have been destroyed due to grazing, residential area, mining and recreational activities. However, recently, many person and institutes have come to a new realization about the importance of sand dune as natural coast. For example, the integrated coastal management plan (2011-2021) by ministry of oceans and fisheries is driving strategies to improve ecosystem health and coastalscape. It mentions that the management and restoration for hotspots of marine and coastal ecosystem. And sand dune is one of the protected and restoration areas.

In ministry of environment, survey and research into coastal sand dune ecosystem is under way to investigate and designate protected area since 2001, because the coastal sand dunes serve an important as coastal ecosystem network. It officially reported the list of 133 coastal sand dunes the first time. And researchers in many part was investigating two or three sand dunes each year. The purposes of the ecological survey are to propose conservation area and management plan based on survey and analysis on age of formation, process and ecosystem of the sand dune. As the results of the survey, two sand dunes which are Sowhang and Hasidong-Anin were designated by the government as a preservation zone.

Recently, the concern about the restoration of developed sand dune is on the increase. Ggot-jee beach is a representative place for marine leisure developed in '70s-'80s. However the beautiful sandy landscapes were changed into gravel beach by loss of sand as time passes. It decided plans for restoration into natural sand dune. The coastal road will be removed and used an artificial nourishment method.

National institute of ecology is currently carrying out research for updating the new list and investigation the status of sand dunes. The parameters of geomorphology and vegetation as basic parts for forming ecosystem of sand dune are carried out for 1 year at 199 sand dunes where are reported by reference research. Basically the goal of project is to survey the status and management condition. The results will be used to assess the conservation values for each sand dune. Finally, it will propose management guidelines for costal sand dune according to the management types.

References

1) Choi, K. H., Kin, Y.M., Jung, P. M., and Suh, M. H. : Coastal dunes as a natural barrier, p.142, 2011.
2) Choi K.H., and Kim,Y.M. : Distribution of Coastal dunes and their conservation status in South Korea, Journal of the Korean Geomorphological association, pp123-137, 2015.
3) Kim, K. H., Yoo, H. S., and Joung E. J. : Disaster overall prevention system for beach erosion and its applications, Journal of Korean Society of Coastal and Ocean Engineers, 20(6), pp602-610, 2008.
4) Martinez, M.L. and Psuty,N.P. : Coastal dunes Ecology and Conservation, Springer Verlag, 2007.
5) MOF, the 2nd integrated coastal management plan (2011-2021), The Ministry of Ocean and Fisheries, 2011.
6) MOE, The list of coastal sand dune in South Korea, The Ministry of environment, 2001.
7) Nordstrom,K.F. : Beach and Dune Restoration, Cambridge University Press, 2008.
8) Paul, R. B., David, R. M. : Key concepts in geomorphology, W.H. Freeman and Company Publishers, 2014.
9) Rod K. : Coastal Dune Management: A Manual of Coastal Dune management and Rehabilitation Techniques, Coastal Unit, DLWC, Newcastle, 2001.

	Well preserved sand dune	Sand dune with coastal erosion	Destroyed sand dune
East coast	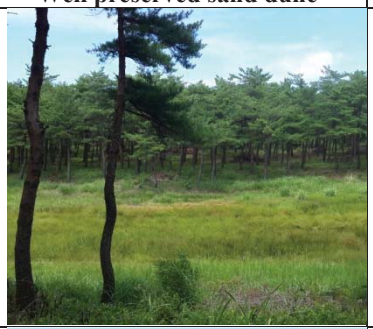		
West coast			

Effect of fermentation temperature on hydrogen production from xylose and microbial community composition

○Chunsheng QIU[1,2*], Liping SUN[1,2], Dandan Zhang[3], Yazhe Zheng[3]

[1]School of Environmental and Municipal Engineering, Tianjin Chengjian University, Tianjin300384, China

[2]Tianjin Key Laboratory of Aqueous Science and Technology, Tianjin300384, China

[3]Tus-Sound Environmental Resources Co., Ltd., Beijing101102, China

*E-mail: qcs254@163.com

Abstract

Batch tests were carried out to investigate the temperature effect on hydrogen production from xylose using mixed culture. Hydrogen production, substrate degradation and metabolite distribution were investigated at wide temperature range from 35 to 65 ºC. The dynamics of microbial communities was investigated by polymerase chain reaction-denaturing gradient gel electrophoresis (PCR-DGGE). Two peaks of fermentation temperatures for hydrogen production were observed at 35 and 55 °C. Butynate and acetate were the major liquid metabolites at 35-60 ºC. While at 65 ºC the main by-product was ethanol. PCR-DGGE analysis indicated that *Clostridium* species were dominant at 35-40 ºC, while at 45-60 ºC the mixed culture was dominated by *Thermoanaerobacterium*. Both species were found at 65 ºC, but with lowest microbial community diversity.

Keywords: Biohydrogen, xylose, dark fermentation, mixed culture, microbial community, temperature

1. Introduction

Biological hydrogen production from renewable biomass, including lignocellulose and organic wastes containing carbohydrates, is recognized as a potential and environmental friendly process for energy production. Lignocellulosic materials are the largest sources of carbohydrates present in the form of cellulose (35-45%) and hemicellulose (25-40%). Xylose, the major monomer of hemicellulose, is the second most abundant carbohydrate after glucose. Hydrogen production through anaerobic dark fermentation by mixed culture is considered to be one of the potential biological processes for xylose utilization. Temperature is one of the most important environmental factors which could affect hydrogen production activity, xylose utilization, liquid metabolites distribution or microbial community. Anaerobic hydrogen production has been reported at a wide temperature range due to the high microbial community in the mixed culture. However, most of the studies were carried out under small temperature range, the shift of xylose metabolic pathway and succession of microflora community under wide temperature range, including mesophilic, thermophilic and extreme thermophilic conditions, has not been reported to our knowledge.

In this study, hydrogen producing mixed culture were enriched in a wide range of temperatures (35-65 ºC), and the effects of cultivation temperature on hydrogen production, xylose degradation, and metabolite distribution were investigated in batch-mode operation. Furthermore, the community structures succession of the mixed culture under various temperatures were analyzed using polymerase chain reaction-denaturing gradient gel electrophoresis (PCR-DGGE).

2. Materials and Methods

2.1 Seed microflora and substrate

T The seed sludge was the mixture of thickened sludge collected from a municipal sewage treatment plant and digested cow manure. Before being seeded into the bioreactor the screened sludge was heat-treated at 100 oC for 75 min to inhibit methane-producing bacteria. The seed sludge used for hydrogen fermentation at 60 and 65 ºC was not heat treated. Based on our previous study, xylose solution of 30.0 g/L was used as carbon source.

2.2 Experimental procedures

Hydrogen producing mixed culture was enriched by repeated batch cultivations. 250 mL serum vials were used for hydrogen production experiments. The vials were seeded with 150 mL seed sludge and fed with 50 mL xylose solution). The initial pH value of the mixture was adjusted to 7.0, and the vial was sealed with rubber stoppers and aluminum crimps. The sealed vial was placed in water bath shakers fixed at 100 rpm. The temperature of the shakers was preset at 35-65 ºC (with 5 ºC step length). The water bath shaker was stopped till no more hydrogen was detected, the supernatants were removed and fresh xylose solution of 50 mL was added, distilled water was also added to the vial to maintain the total volume of 200 mL. Repeated transfer was stopped when no hydrogen yield increase compared to the previous cultivation was observed. Assays with seed sludge alone were used as blank controls. All the experiments were carried out independently in triplicates.

3. Results and Discussion

3.3.1 Effect of culture temperature on hydrogen production and liquid metabolites production

Hydrogen yield peaked with 1.12 mol H_2/mol $xylose_{consumed}$ at 35 ºC of a mesophilic range. However, maximum hydrogen yield of 1.31 mol H_2/mol $xylose_{consumed}$ was obtained at 55 ºC at the thermophilic temperature range. While at extreme thermophilic condition (65 ºC), hydrogen

yield of 0.51 mol H_2/mol $xylose_{consumed}$ was observed. Different hydrogen yield may be attributed to the different xylose metabolic pathways and bacterial community structures.

As shown in Fig.1, for the tested temperatures, the major liquid metabolites were acetate (167.3-1644.9 mg/L), ethanol (184.6-3609.8 mg/L) and butyrate (986.9-3586.1 mg/L). The amount and distribution were affected by the culture temperatures. Acetate and butyrate were the dominant liquid by-products at 35 and 40 ºC (mesophilic range). The hydrogen yield was positively related with acetate concentration. Butyrate-type fermentation may be the dominant hydrogen producing metabolic pathways. While at the transition temperature range (45-50 ºC), besides butyrate, ethanol become the dominant liquid metabolite instead of acetate associated with low hydrogen yield. Hydrogen yield was inversely correlated with acetate concentration at 55-60 ºC. Although nearly equal amount of ethanol was produced at 55 ºC compared with that at 50 ºC. While at 65 ºC, ethanol became the dominant liquid by-product followed by butyrate and acetate. Only minor amounts of propionate (below 61.5 mg/L) were detected in this study, which is positive for optimal hydrogen production.

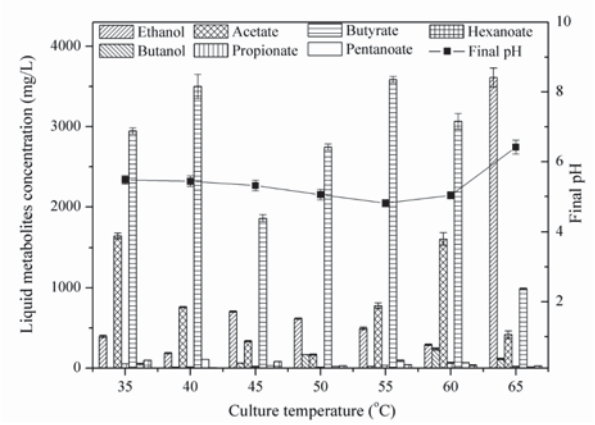

Fig.1. Effects of culture temperature on liquid metabolites distribution

3.3.2 Effect of temperature on the bacteria communities

A As shown in Fig. 2, the DGGE profiles of the microflora from the slurries cultured under different temperatures were apparently different. The change in biohydrogen system temperature has not only altered the hydrogen production activity and liquid by-products distribution, but it also caused the succession of microbial community.

For the bands at 35 and 40 ºC, the predominant bacteria populations were affiliated with *Clostridium butyricum* (bands 3, 5, 7, 12 and 16), *Clostridium acetobutylicum* (bands 18 and 19), and *Clostridium pasteurianum* (band 24). The mixed culture showed similar microbial community structure at 45-60 ºC with bands 10, 14, 20, 21, 23 and 25. *Thermoanaerobacterium sp.* was predominant bacretia (bands 4, 6, 8, 10 and 20) at 45 and 50 ºC. The DGGE profiles at 65 ºC indicated that different microbial community structure was formed at extreme thermophilic condition with fewest bands. Band 15 and 22, present in the DGGE profiles at extreme thermophilic condition, showed 99% identity to *Thermoanaerobacterium thermosaccharolyticum* and *Clostridium butyricum*, respectively.

Although the bacterial species related to *Clostridiales* and *Thermoanaerobacterium* were predominant at most of the tested temperature, microbial communities at mesophilic, thermophilic and extreme thermophilic conditions showed significant differences, being characterized by selective enrichment of specific species. Several microbial community structures were formed at mesophilic conditions, transition conditions, thermophilic conditions and extreme thermophilic condition, resulting in various metabolic pathways of xylose and different hydrogen production performance.

4. Conclusions

(1) Hydrogen production efficiency at certain temperature was mainly affected by the liquid metabolite distributions, which depended mainly upon the culture temperature.

(2) Although the bacterial species related to *Clostridiales* and *Thermoanaerobacterium* were predominant at each temperature, several microbial community structures were formed at mesophilic conditions, transition conditions, thermophilic conditions and extreme thermophilic condition, resulting in various metabolic pathways of xylose and different hydrogen production capacity.

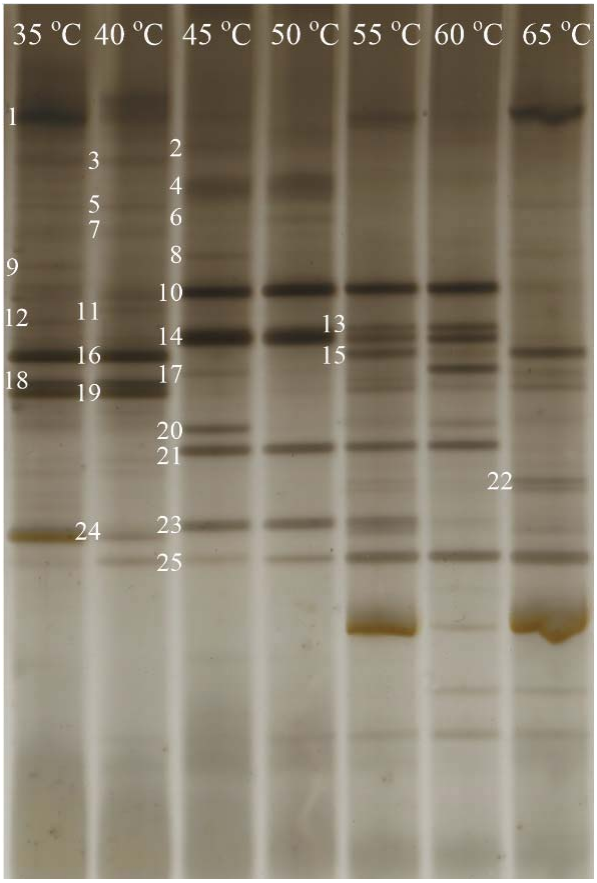

Fig.2. DGGE analyses of the microbial communities in the mixed culture at different temperatures

Energy Production from Food Wastes by Methane Fermentation

○Kazuki TONOUCHI[1*], Toshimasa HOJO[1], Yu-You LI[1]
[1]Department of Civil and Environmental Engineering, Tohoku University, 6-6-06 Aza-Aoba, Aramaki, Aoba-ku, Miyagi 980-8579, Japan
[*]E-mail: kazuki.tonouchi.t4@dc.tohoku.ac.jp

Abstract
Methane Fermentation of food wastes, which were generated by food wholesale section and retail trade section, was conducted in this study. The characteristics of treatment performance, energy recovery and the reduction of greenhouse gases emission through methane fermentation process were investigated. The results showed that stable operation were achieved not only in the single-stage, but also in the two-phase with recirculation methane fermentation system, with the COD and VS degradation efficiencies of 81.7%～86.3%, 72.6%～79.1%, respectively. Amount of energy such as electricity and heat recovered from methane fermentation was likely to be used. Along with the reduction of auxiliary fuel, incineration amount, final disposal amount, and greenhouse gases emission, the feasibility and high efficiency of methane fermentation from food wastes were confirmed. Therefore, the introduction of methane fermentation should be positively promoted in our society.

Keywords: methane fermentation, food wastes, mass balance, energy production, greenhouse gases emission

1. Introduction
The quantity of annual outbreak for food wastes from food industry is over 19 million tons. Until now, food wastes have not been treated and recycled very well. Since, it is hard to be treated by conventional incineration and compost because food wastes are high moisture content and easy to go bad. Nowadays, methane fermentation is considered as the promising method for treating the high moisture content organic wastes and complex components. Simultaneously, methane gases can be generated by biological way with low energy input, and utilized as energy to achieve the self-sufficiency.

In recent years, researches and industrial developments of methane fermentation from biomass focus on long-term stabilization operation and energy-recycle technology. However, there are few researches discussing about energy recovery rate, greenhouse gases emission, the effects involving in resource circulation and so on. So, there are not enough for quantitative evaluation about the role of methane fermentation for the construction of circulating-type and low-carbon society.

In this research, we focused on food wastes from food wholesale section and retail trade section, because the low recycling rate and complex components of food wastes are urgent problems to be solved. Our purposes were to promote recycling energy of food wastes by methane fermentation and to evaluate the effect on the implementation of circulating-type and low-carbon society by the introduction of methane fermentation.

The characteristics of organic matter decomposition, biogas production, the analysis of energy balance, greenhouse gases emission and so on were investigated. In addition, a comparison study of the single-stage system and the two-stage with recirculation as the two typical modes was carried out.

2. Materials and Methods
As illustrates in Fig.1, two methane fermentation systems operated and were investigated over 70days in this study. In the single-stage system, CSTR operated at 35℃with 5L of effective volume and HRT (Hydraulic Retention Time) was maintained at 30days. On the other hand, the first CSTR operated at 55℃ with 3L of effective volume and the second CSTR operated at 35℃ with 12L of effective volume in two-stage with recirculation system. The HRT of the whole system was also maintained at 30days with the recirculation ratio of 1:1.

Substrate was made by 15 kinds of feedstocks mixing (shown in Table 1) and doubling dilution by tap water. The OLR (Organic Loading Rate) was 2.52kg-VS/m^3/day in HRT of 30days.

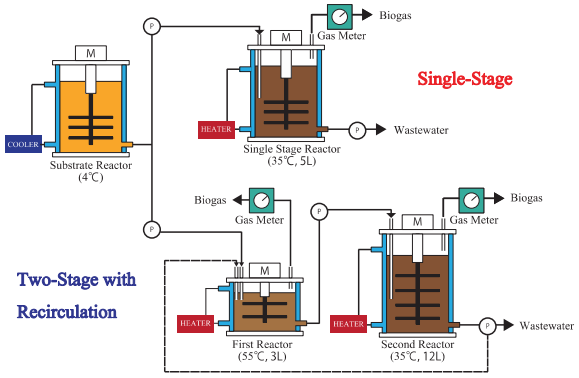

Fig. 1: The outline figure of experiment equipment

Table 1: feedstocks composition of substrate

Large Classification	Small Classification	Weight per 1kg-feedstocks
Dairy Product	Milk	90.0g
	Yoghurt	80.0g
	Cheese	80.0g
Plant Residue	Tofu	20.0g
	Canned Tomatos	40.0g
Animal Residue	Canned Tuna	40.0g
Other Residue	Curry	100g
	Meat Sauce	100g

Large Classification	Small Classification	Weight per 1kg-feedstocks
Alcohol	Beer	10.0g
Crops	Flour	20.0g
Drink	Vegetable Juice	50.0g
	Coffee	50.0g
	Tea	50.0g
Seasoning	Cooking Vinegar	40.0g
Organic sludge	Dewatered Sludge	250g

3. Results and Discussion

3.1. Operation condition of the reactors

The pH values of single-stage reactor and the second reactor of two-stage with recirculation were about 7.60, and VFAs (Volatile Fatty Acids) and NH_4^+-N were no detected in both reactors, which indicated that two systems were under good condition.

In HRT of 30 days, both of systems produced stable biogas. The average of biogas yield for single-stage was 1.08L/g-VS with 66.2% of methane content, and that for first reactor of two-stage with recirculation was 0.78L/g-VS with 19.7%, second reactor was 0.88L/g-VS with 69.7%.

3.2 Organic matters degradation

In HRT of 30days, VS and COD degradation efficiency of single-stage were 72.6% and 81.7%, respectively; and that of two-stage with recirculation were 79.1% and 86.3%, respectively. In Li's research[1], methane fermentation by two-stage with recirculation from kitchen garbage, VS and COD degradation efficiency were 84.8% and 78.8%(HRT of 20days). Compared with our research, substrate can be favorably degraded into the same level as kitchen garbage by methane fermentation.

3.3 The effect on the introduction of methane fermentation of food wastes

To evaluate mass balance of each processing flow and the possibility of the effective utilization of energy recovery by methane fermentation, two cases (Case 1 : the conventional incineration of food wastes, Case 2 : the introduction of two-stage methane fermentation of food wastes with recirculation) under the same substrate condition were supposed. The reduction of volume, energy production and greenhouse gases emission were compared in this study.

Fig. 2 shows that the two cases comparison study based on mass balance. In Case 2, due to the properties of wet methane fermentation, we have to use the flocculent for dewatering and treat filtered water. However, the volume of supplement fuel is about 9% in Case 1. Furthermore, Case 2 can cut down more than 60% of final disposal volume compared with Case 1. And we predicted that we can recover 114 kWh as electricity and 10.7×10^4 kcal as heat by the introduction of methane fermentation. In addition, the usableness of performing methane fermentation of food wastes also lies in the aspect that along with the reduction of auxiliary fuel and food waste capacity, it is also possible to reduce greenhouse gases emission by about 78% (shown in Table 2).

Table 2: Comparison of greenhouse gases emission

unit : kg-CO_2

	Case1	Case2
CO_2 (Fuel Comsumption)	12.9	0.00
CH_4 (Fitrate Processing)	-	0.04
N_2O (Fitrate Processing)	-	3.07
CH_4 (Incineration)	0.02	0.00
N_2O (Incineration)	9.83	1.96
TOTAL	**22.8**	**5.07**

4. Conclusions

(1) The results showed that stable operations were achieved in both of single-stage methane fermentation and two-stage with recirculation, with the COD and VS removal efficiencies of 81.7%～86.3%, 72.6%～79.1%, respectively.

(2) Amount of generated energy such as electricity and heat recovered from methane fermentation was likely to be used. Along with the reduction of auxiliary fuel (91.7%), incineration amount (90.0%), final disposal amount (61.5%), and greenhouse gases emission (77.8%), the feasibility and high efficiency of methane fermentation from food wastes were confirmed. Therefore, the introduction of methane fermentation should be positively promoted in our society.

5. Acknowledgments

1) Yu-You LI, Osamu MIZUNO, Keisuke FUNAISHI, Koji YAMASHITA : High-Rate Methanation of the Food Wastes and Garbage by a Two-Phase Process with Circulation of Digested Sludge, Environmental Engineering Research, Vol.40, pp.321-331, 2003.

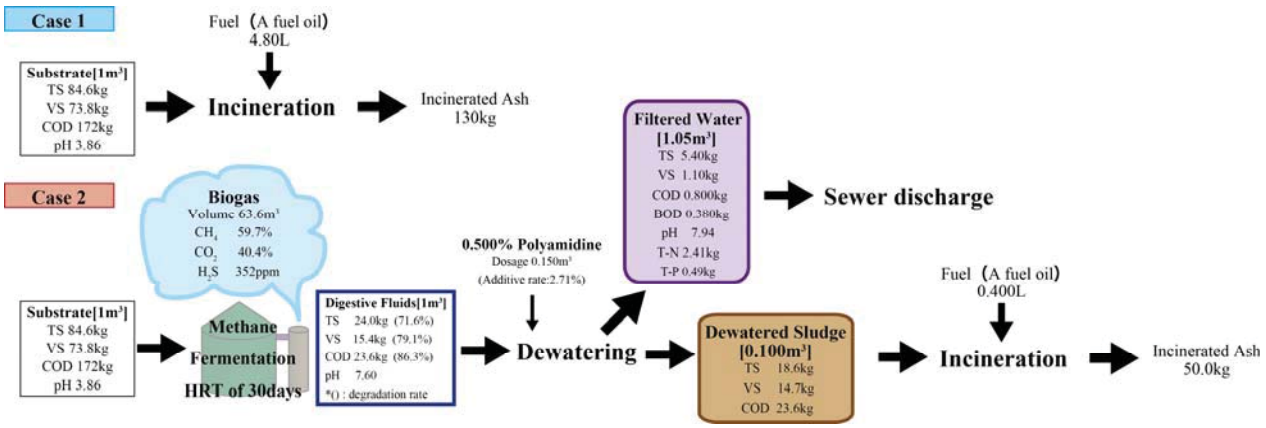

Fig. 2 : the case study based on mass balance

Hythane Production from Cassava Residue by Hydrogen and Methane Fermentation

○Hongyu JIANG[1]*, Yu QIN[1] & Yu-You LI[1]
[1] Department of Civil and Environmental Engineering, Graduate School of Engineering, Tohoku University, 980-8579, Sendai, Japan
*E-mail: jiang1141@hotmail.com

Abstract
The continuous two-stage thermophilic-mesophilic hythane fermentation of cassava residue with recirculation was conducted over 250 days, in order to demonstrate start-up strategy by shorting HRT in methanogenic stage, and to investigate nickel, cobalt and sulfur affection on hythane fermentation. Shorten HRT of methane-stage from 80 days to 12 days with maintaining HRT of hydrogen under 3 days was a quick strategy for hythane start-up process. The hythane fermentation of cassava residue under continuous operation without the addition of nutrients resulted in an unstable performance for long-term operation, which was characterized by a radical decrease in the methane production along with a drop in the methane content. The effects of adding Co_2^+ and Ni_2^+, S^0 and SO_4^{2-} were discussed in this study. The results of nutrients affection demonstrated the sufficient addition of nutrients could recover and enhance hythane fermentation effectively.

Keywords: *Hythane, Two-stage, Recirculation, Cassava residue, Nutrients, HRT*

1. Introduction
Hythane has been viewed as a bridge technology of "de-carbonization" energy transition between natural gas and the final goal of H_2, since it can markedly reduce exhaust emissions of hydrocarbon compounds and drastically improve the efficiency of conventional spark- or compression-ignition engines.

In recent years, the two-stage hythane fermentation of agro-industrial cassava residue such as processing wastewater, cassava stillage and cassava excess sludge has gained prominence along with the rapid development of cassava starch processing manufacture. Moreover, two-stage hythane fermentation may be inevitable developing direction and can readily solve existing problems of single-stage fermentation, for instance, H_2 fermentation bogged down due to low yield of biogas with accompanying smelly odors from volatile fatty acids (VFAs) accumulation; and the hydrolysis of cassava residue is the rate-limitation step for CH_4 production.

It was reported that two-stage hythane fermentation with part of methanogenic sludge recirculated into the first-stage H_2 reactor was able to be successfully operated maintaining appropriate condition for the first-stage without or with less alkaline and NH_4^+ addition, and dilute the concentration of substrate without adding extra water. Therefore, recirculation contributed to the improvement of carbohydrate degradation and an increased biogas production. However, the improper recirculation ratio seems to break the balance in the first-stage, due to many of hydrogenotrophic methanogens and homoacetogens likely results in the settling of H_2 consumers in a H_2 reactor regardless of their growth rates, along with returning hydrolysis bacteria and H_2 producing bacteria back. Therefore, it is necessary to investigate the effect of practical operation mode (HRTs and recirculation) on the efficiency of two-stage hythane fermentation. In addition, cassava residue has low protein content and lack of nutrients, results in the limitation of practical utilization and animal feeding. In this present study, continuous operations of two-stage hythane fermentation with recirculation was carried out, in order to (i) demonstrate the stability of long-term continuous hythane production from cassava residue using recirculation, (ii) clarify the effect of HRTs on H_2 and CH_4 production, and (iii) investigate the effects of nickel, cobalt and sulfur supplement.

2. Materials and Methods
2.1 Inoculum and substrate
The anaerobic mixed microflora was obtained from a mesophilic sewage sludge digester in Japan. The pH in the H_2 reactor was adjusted once in the beginning at 5.5 from original pH 7.3 by feeding 2 mol/L HCl solutions, and the pH in the CH_4 reactor was no adjustment.

Cassava residue was obtained from a starch processing plant in Guangxi, China. The cassava residue were sun dried (16.5% water content), powdered by the electronic blender and screened through a 1 mm size mesh sieve, then stored for use in subsequent experiment. The 10% TS of cassava residue was prepared as substrate by the mixing of cassava residue powder and tap water. Due to lack of nitrogen, 4 g/L NH_4HCO_3 as nitrogen source and pH buffer continuously added in the substrate tank during whole operation. Moreover, 1 mg/L of cobalt, 1 mg/L nickel, and 30 mg/L sulfur were put into CH_4 reactor, respectively.

2.2 Continuous system setup and process operation
The experimental apparatus was consist of two CSTRs and one substrate tank. The first CSTR (R1) as H_2 fermenter was operated at 55℃ with 3L of effective working volume, and the second CSTR (R2) as CH_4 fermenter was operated at 35℃ with 12L of effective working volume. The substrate tank for storing cassava residue was kept by cooling system at 4℃. The HRT of R1 was maintained at 3 days and R2 started from 80 days (Phase 1), 40 days (Phase 2), 20 days (Phase 3), 15 days (Phase 4), to 12 days (Phase 5). In addition, the part of methanogenic sludge in second-stage fed back into first-stage.

2.3 Analytical methods

A routine laboratory analysis was carried out. The gas percentages in the biogas were analyzed by a gas chromatograph [Shimadzu 8A]. The VFAs and ethanol concentrations were determined by a gas chromatograph (Agilent-6890). The pH, volatile solid (VS), volatile suspended solid (VSS), and chemical oxygen demand (COD_{Cr}) were analyzed according to the procedures described in the Standard Methods. The total carbohydrate was analyzed by the phenol-sulfuric acid method and the protein was measured by Lowry method.

3. Results and Discussion

The two-stage hythane fermentation with recirculation system operated over 250 days for confirming the degradation capacity of cassava residue, investigating the stability of fermentation and efficiency of energy recovery. This experiment can be divided into 2 big parts with 9 phases depending on different HRT operation conditions and nutrients addition (see in Fig. 1(a) & (b)).

3.1 The time course of performance under different HRTs

As shown in Fig. 1 (c), the pH of R1 was able to maintain at 5.1±0.1, and the average pH of R2 was 7.5±0.2 during the HRTs variation. The gas production rate in both reactors increased with shorting the HRT of R2, and the highest biogas production rates in R1 and R2 were 5.97 L/L/d with 45.4% of H_2 and 2.17 L/L/d with 63.0% of CH_4, respectively (see in Fig. 1 (d-f)). However, R2 was unable to maintain stability after long-term operation, even NH_4HCO_3 as N-source and pH buffer was added. In HRT of 30 days for whole system, the gas production rate obviously dropped 30% and pH in R2 slightly decreased. These phenomena indicated that system was in an unstable condition and easy to break the fragile equilibrium.

3.2 The effect of trace elements on methane fermentation

Iron, nickel and cobalt are important trace metals in methane fermentative pathway. Qiang et al. revealed that trace elements requirements had a significant effect on mesophilic methane fermentation. In this study, the cassava residue as substrate has some problems to be utilized in dark fermentation, because Ni and Co were not detected and Fe was over-dose. According to theoretical calculation and repeated batch experiment (not mentioned in this abstract), the demand amount were 1mg/L Ni (1.83 mg/L $NiCl_2$) and 1 mg/L Co (1.83 mg/L $CoCl_2$), respectively.

After Ni and Co addition, the gas production rate sharply decreased from 4.60 L/L/d to 2.85 L/L/d in R1. On the other hand, the gas production rate had no significant change in R2, but the pH and CH_4% of R2 continued decreasing. This phenomenon may cause by weakly acidic nickel and cobalt chloride solution reacting with bicarbonate in reactors.

Table 1 the performance of hythane fermentation after nutrients addition

Run	Nutrients addition	1st stage		2nd stage		Hydrogen yield	Methane yield
		GPR	H_2 content	GPR	CH_4 content		
		L/L/d	%	L/L/d	%	mol H_2/kg TVS-added	mol CH_4/kg TVS-added
7	Ni^{2+}+Co^{2+}	2.69	52.0	1.56	55.1	2.08	1.28
8	S^0	3.58	54.8	1.80	57.4	2.91	1.53
9	SO_4^{2-}	3.71	51.1	2.01	61.4	2.81	1.83

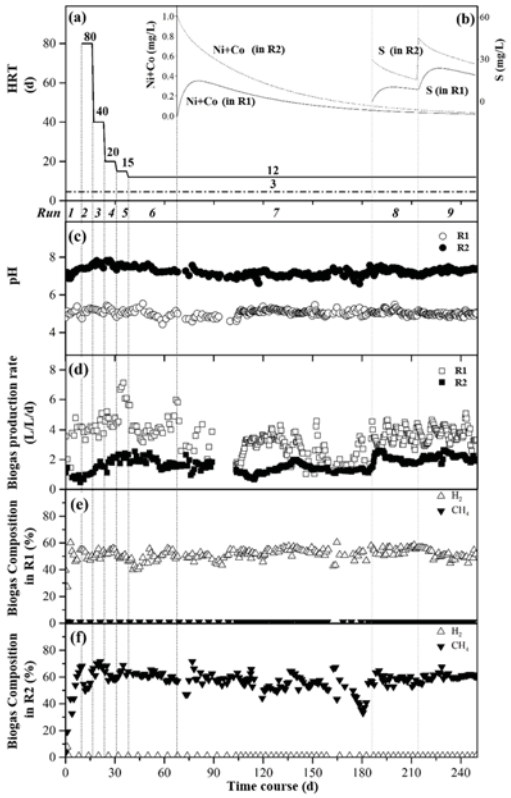

Fig. 1 Time course of HRT variation and the operational performance of pH, gas production rate and composition

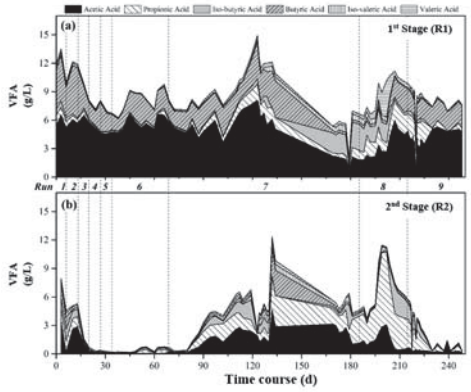

Fig. 2 Time course of VFAs production

However, the total VFA increased after adding Ni and Co, which indicated that Ni and Co may contribute to promote acidogenesis (see in Fig. 2).

On the contrary, when sulfur or sodium sulfate (30 mg-S/L) was added respectively, the performance of both reactors such as the decomposition efficiency, acid generation, and gas production were remarkably promoted (see in Table 1).

4. Conclusions

(1) Shortening HRT of methane-stage from 80 days to 12 days and maintaining HRT of hydrogen-stage at 3 days was a quick strategy for hythane start-up process.

(2) To solve the lack of nutrients in cassava residue itself, Ni, Co and S were respectively added to evaluate the long-term stable hythane fermentation. S may effectively contribute to increase hydrolysis, acidogenesis, and hydrogen/methane production in this system.

The Effects of HRT on the Performances of Hollow Fiber Anaerobic Membrane Bioreactor in Treating Food Waste

○Hui CHENG[1], Yutaka HIRO[1], Yu-You LI[1*]

[1]Department of Civil and Environmental Engineering, Tohoku University, 6-6-06 Aza-Aoba, Aramaki, Aoba-ku, Miyagi 980-8579, Japan

[*]E-mail: cheng.hui.t7@dc.tohoku.ac.jp

Abstract

The characteristics of methane fermentation in a hollow fiber anaerobic membrane bioreactor (HF-AnMBR) fed with food waste were investigated at mesophilic condition. The HF-AnMBR was operated at three different hydraulic retention time (HRT) of 30, 15 and 10 days. The CH_4 rich biogas production was significantly improved by shortening HRT. Biogas production increased from 19.6 L/d to 54.0 L/d with the decrease of HRT. The maximum methane yield was 3.60 L/L-Bioreactor/d at an HRT of 10 days. The total carbohydrate degradation was more than 83.5% throughout the experimental runs. Continuous CH_4 rich biogas production from food waste was successfully sustained. The HF –AnMBR showed CH_4 production capacity at the short HRT due to its higher cell retention.

Keywords: food wastes, hollow fiber anaerobic membrane bioreactor, methane fermentation, mass balance

1. Introduction

In Japan, about 298 million tons of industrial wastes are produced every year, 6.7% of which are food wastes. Most food wastes are generated by food manufacture and restaurants, and unsold food and lunch boxes at supermarkets and convenient stores are also included. Such large amount of food waste has not only caused major economic losses but also wreaked significant harm on climate, water, land and biodiversity. Anaerobic digestion of food waste are the best option for producing CH_4 and reducing environmental pollutants, especially CO_x, C_nH_m and SO_x during gasification. The most recent development in biogas production is the incorporation of anaerobic bioprocesses with membrane separation techniques in a membrane bioreactor. In the fermentation process, the membrane provides for excellent metabolites/suspended solids separation efficiency, reflecting the AnMBR's higher biogas recovery efficiency and cell retention compared with conventional CSTRs. However, continuous methane fermentation HF-AnMBR with different HRT has yet to be reported. Therefore, the objective of this study was to present the performances of HF-AnMBR in treating food waste and mainly illustrate the effects of HRT on this process.

2. Materials and Methods

2.1 Substrate and seed sludge

Seed sludge was obtained from a mesophilic sewage sludge digester at the Sendai municipal sewage treatment plant in Sendai. Substrate (food waste slurry) was artificial organic fraction of municipal solid waste consisting of a great variety of grains, vegetables, meats and fishes. As shown in Fig.1 food waste was loaded into the bioreactor after mechanical pretreatment using a circulation pump. Food waste slurry (45g/L, total solid) was prepared by crushing with a cutting pump and dilution with tap water. The characteristics of substrate was listed in Table 1.

2.2 HF-AnMBR system design and operation

As shown in Fig.1, the system mainly consisted of a substrate tank and an AnMBR. AnMBR was combined by a 15 L CSTR and a 5 L hollow fiber membrane reactor. The effective volumes of two parts were 12L and 3 L, respectively and operational temperature was maintained at 37℃ by heater. The material of membrane was polytetrafluoroethylene (PTFE) with a mean pore 0.2 μm and the effective filtration area was 0.1m^2. Three peristaltic pumps were used to feed substrate to CSTR, to recycle mixed sludge from CSTR to membrane separation unit, and to extract permeate from the membrane. A gas pump was used to recirculate biogas from the head space of CSTR into the biogas diffuser which was located at the bottom of the membrane unit for scouring membranes. A gas meter was used for recording the biogas production.

2.3 Analysis Methods

Biogas production was recorded by a wet gas meter, and the compositions of biogas (CH_4, CO_2 and N_2) were measured by a ShimadzuGC-8A gas chromatograph. The pH, alkalinity, chemical oxygen demand, TS, VS, SS and VSS

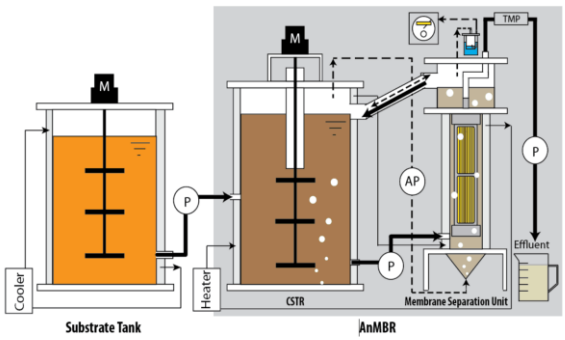

Fig. 1 Schematic diagram of experimental apparatus for HF-AnMBR

were measured according to Japan Standard Testing Method for wastewater.

3 Results and discussion

3.1 The operation performance of HF-AnMBR

As shown in Fig. 2, the pH in the HF-AnMBR kept within the range of 7.1- 7.6 throughout the time course. Under HRT of 30 days, average biogas production rate was 1.31 L/L-bioreactor/d. When HRT decreased to 15 days by doubling the volume of influent, the biogas production increased sharply to 2.42 L/ L-bioreactor/d. After a slight fluctuation at the beginning of HRT of 30 days, the biogas composition maintained at a stable level, which were 61% of CH_4 and 38% of CO_2. When HRT decreased to 10 days, biogas production rate increased to 3.60 L/ L-bioreactor/d.

When HRT was 30 days, TS and SS concentration in bioreactor increased from 12.0 to 18.0 g/L, and 8.25 to14.9 g/L, respectively. The relaxing membrane pressure maintained around 1.54 kPa, and the transmembrane pressure also maintained at a low level about 6.38 kPa. As HRT changed to 15 days, TS and SS concentration increased steadily for the first 10 days, and then increased sharply to 31.7 g/L and 27.6 g/L, whereas, the relaxing membrane pressure increased gradually to 2.30 kPa for the whole stage. Transmembrane pressure kept at 8.25 kPa for the first 10 days, and then it increased sharply to 16.1 kPa, which was mainly caused by the high concentration of TS in the reactor. So after, organic retention time was set to 30 days, in order to keep the appropriate TS in the reactor and stop membrane pollution. Permeate COD almost had no change with the decrease of HRT, which kept at about 0.33 - g COD/L. COD removal efficiency of AnMBR in this study was 99.6 %, which was much high than that reported by He et al., who used anaerobic membrane bioreactor to treat high concentration food wastewater.

The soluble COD in food waste slurry accounted for 43.5%. COD input for 100 %, 91.3 % of COD was recovered as methane, 9.70 % was converted to sludge. However, with the decrease of HRT, CH_4 recovery efficiency decreased to 84.8% a little less than that of 30 days. The reason was that more COD input covered to sludge, which was attributed to lower TS degradation rate in the reactor.

Table 1 Characteristics of the substrate.

Parameters	Unit	Value
Total solids	g/L	45±6.1
Volatile solids	g/L	43±5.4
Total COD	g/L	74±5.6
Soluble COD	g/L	29±5.0
Total carbohydrate	g/L	23±2.6
Soluble carbohydrate	g/L	5.2±0.7
Total protein	g/L	12±3.3
Soluble protein	g/L	2.2±0.3
Total nitrogen	mg/L	22±4.0

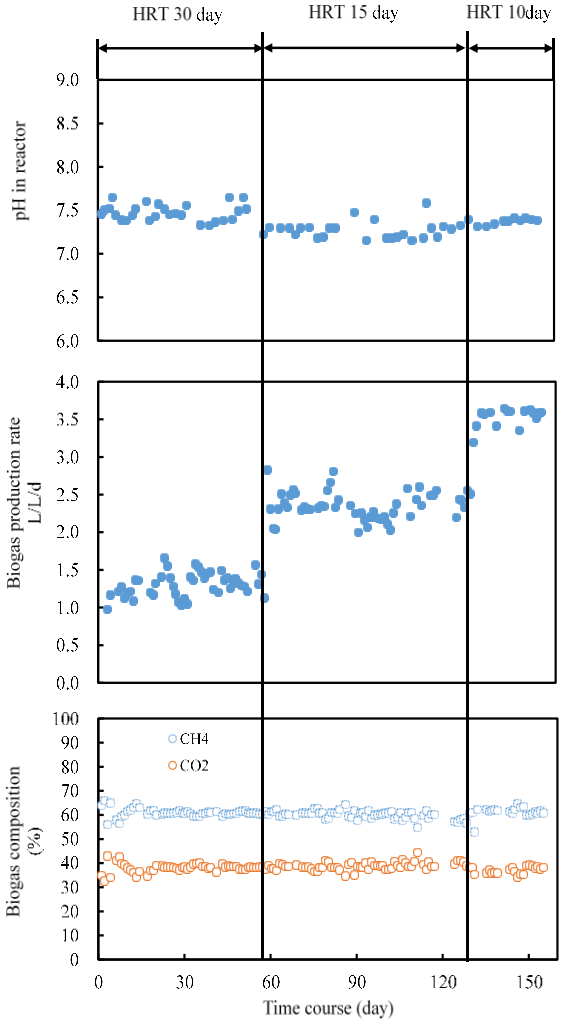

Fig. 2 Time courses of methane fermentation system

4. Conclusion

(1)After HF-AnMBR, the COD concentration was only 0.33 - g COD/L in the effluent and HRT had almost no effects on the quality of effluent.

(2) HF-AnMBR was successfully operated at high concentration of TS and SS, as much as to 31.7 g/L and 27.6 g/L, respectively.

(3) The input COD was converted to 91.3% ,85.1% and 84.8% of methane, at HRT of 30 days, 15 days, and 10 days respectively.

(4) AnMBR operated well for more than 160 days without membrane cleaning, and permeability was recovered by biogas scouring.

5. Acknowledgements

The author would like to thank China Scholarship Council for the fund supporting her study in Japan (File NO.201508370100)

Research on the feasibility of dead livestock bodies' anaerobic co-digestion with manure

○Tao Zhang[1], Xiaowei Cheng[2], Hongguang Zhu[2*] & Yu-You Li[1*]

[1] Dept. of Civil and Environmental Engineering, Graduate School of Engineering, Tohoku University, Aoba-ku, Sendai,980-8579, Japan

[2] Institute of New Rural development, Tongji University, No.4800, Road Cao'an , 201804 Shanghai, China

1*E-mail: yyli@epl1.civil.tohoku.ac.jp

2*E-mail: zhuhg@tongji.edu.cn

Abstract

Livestock industry in China has posed serious threats to environment as far as concern about the dead livestock bodies(DLB) and huge amount of manure. As to the DLB, the contemporary disposal facilities still run under great energy cost, furthermore the sequent effluent remains to be lipid-rich which is hard to deal with. Considering the corresponding source and character of DLB and manure, this study used a co-digestion method to dispose the DLB in an on-site way, exploring a much more economic disposal method to decompose the DLB. Via a series of batch reactors setting different DLB percent, the potential disposal method was optimized. Through the statistical analysis on the data of results in this experiment, it shows that the 6 gratitude of DLB concentration (from 0% to 15%) had not posed a significant impact on the total biogas production, however it had an significant impact on the total methane production, the 5 gratitude groups' methane production was 0.13%, 34%,5.62%,23% and 15% higher against the non-DLB group. As far as the methane production speed, the corresponding time when it reached 80% of total methane production was 732, 756, 850, 924, 1680 and 1620h, it means that addition of DLB to an extent didn't suspend the fermentation speed, but too much addition would suspend fermentation obviously. Thus it is feasible to employ a co-digestion method to dispose DLB according to this work. Furthermore, the experimental data shows that 6% DLB addition would increase methane production by 34% in spite of additional 16% fermentation time against the non-addition group.

Keywords: Dead livestock bodies, manure, co-digestion, feasibility

1. Introduction

Livestock industry in China is a huge industry, in 2014, about 730 million pig were sold all over China. However, as a by-product of livestock industry, dead livestock bodies (DLB) and manure has become a big threat to environment, especially the former one. For the disposal technology of DLB in China, incineration landfill alkaline hydrolysis and fermentation are usually used. In Shanghai's dead animal disposal center, a disposal technology containing high temperature boiling, oil recycling and success anaerobic digestion is in application, which is in operation under high cost. As the only one facility, it is faced with more and more pressure to dispose the DLB collected from thousands of livestock farm all over in Shanghai. In addition, the center's disgusting smell has already fueled local native's protests and forced to relocation once. Thus it is quite necessary to develop an in-place and less-cost disposal method to deal with DLB (except animal plague).

On the one hand, DLB is a protein and lipid-rich raw material for anaerobic digestion, compared to general carbohydrate, much more methane would have been produced based on DLB fermentation. However, it is difficult to employ anaerobic digestion based on DLB only. On the other hand, the other by-product livestock manure is low carbon:nitragen raw material and abundant in the livestock farm.

Thus is it possible to use a co-digestion method to ferment DLB and manure together to solve the problem of DLB? And compared with the manure's digestion, how is the methane production and speed when it comes to the co-digestion?

On the basis of these questions above, this study aims to explore the feasibility and efficiency of co-digestion based on DLB and manure. It would be helpful to develop some new strategies to the decomposition of DLB.

2. Materials and Methods

2.1 Feed stocks and inoculum

The substrate used in this study was streaky pork sold in market and pig manure collected from the local pig farm. The inoculum seed sludge was sampled from mesophilic anaerobic digestion tank of a pig farm's subsidiary water treat plant. The seed sludge and scum's character is shown in Table 1.

Table.1 The character of feed stocks and inoculum

2.2 Analysis methods

A wet gas meter was used to collect the daily data of biogas production. pH, alkalinity, COD,TS,VS,TN and lipid were determined by China Standard Method. The biogas composition was measured by a GC-122 gas chromatograph (Shanghai Jingke).

2.3 Reactors and Experiment design

Glass bottles were used as reactors in this study, and the experiment system was shown in Figure.2. This system was operation in a mesophilic way(35℃). Aluminum foil gas collecting bag was employed to collect biogas.

Table.1 The character of feed stocks and inoculum

Index	Manure	Streaky pork	Inoculum
TS%	19.50	50.03	12.97
VS%	14.71	47.87	11.16
TOC%	6.91	22.50	5.25
TN%	0.76	6.3	1.68
pH	7.8	6.3	7.1
Lipid%	-	53.0	-

3. Results and Discussion

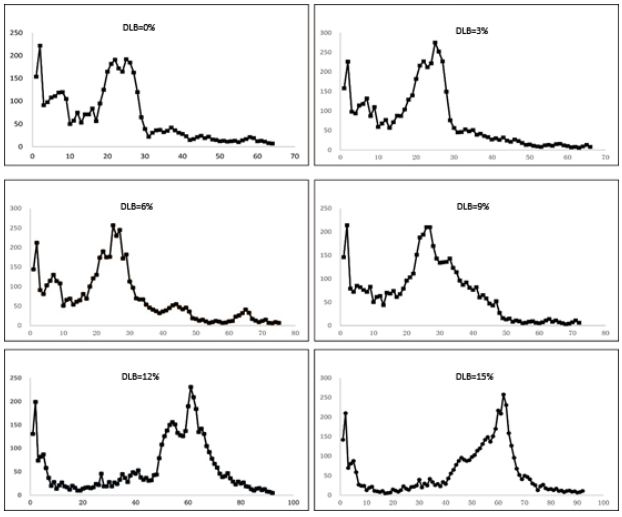

Figure 1 The daily biogas production of Different DLB percent

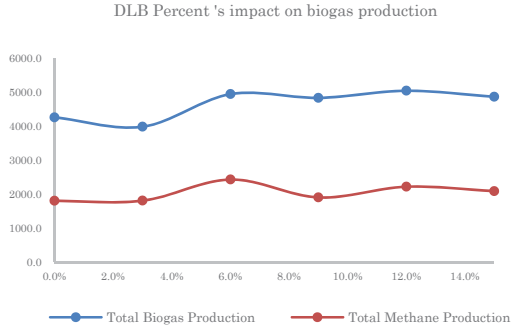

Figure 2 Different DLB percent's impact on Total biogas and methane production

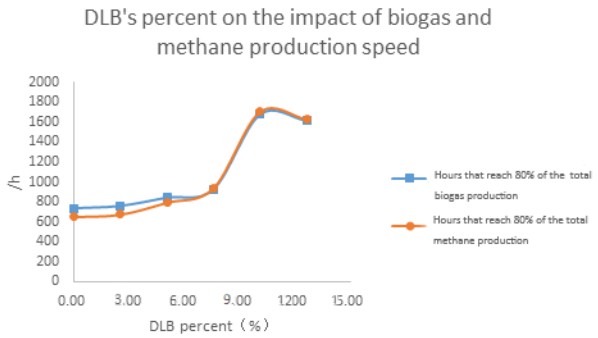

Figure 3 Different DLB percent's impact on biogas and methane production speed

As shown in Figure1, the obvious impact of DLB percent is that the biogas production speed is pushed later, especially for the 2 highest addition percent, it means that too much addition of DLB would have the lag period lengthened.

Different DLB percent's impact on the biogas and methane production was shown as Figure 2. It was shown that the 6% group's biogas production was highest. However after an anova analysis it was found that there were no significant difference between different DLB percent groups($F=0.567 > \alpha = 0.05$). The statistical analysis shows that the DLB percent did not pose a significant impact, ie, there must have been a range in which even more and more DLB was added into the manure, the gas production of co-digestion would not have been impacted. It means that DLB's co-digestion with manure is feasible. On the other hand, the methane production was sort of different from the biogas production, it shows that 6% DLB percent co-digestion would apparently prompt the methane production by 34%.

As to the gas production speed, the Figure 3 shows that 12% and 15% DLB would suspend gas production speed heavily, almost 3 times longer than the group without addition of DLB. But for the less DLB percent groups, production speed did not vary a lot. It indicated that higher DLB percent would suspend the co-digestion's speed, but low addition of DLB would not inhibition the digestion speed.

4. Conclusions

(1) Employing co-digestion with manure to dispose DLB is feasible within a range.

(2) Different DLB percent didn't have a significant effect on total biogas production and when the addition percent was 6% methane production could increase by 34% compared to the non-addition group

(3) The co-digestion speed did not vary a lot when DLB was added at low percent and when the DLB percent reached more than 12%, the production speed would heavily fall down.

5. Acknowledgements The authors would like to thank Shanghai Agricultural Bureau, China for the funding support on Agricultural Technology Research（（2014）5-4）.

Quantitation of Pharmaceutical and Personal Care Products in Malaysian Sewage Effluent

○Halim YACOB[1]*, Hee- Young KIM[2], Jeong-Eun OH[2] & Ee Ling YONG[1,3]
[1]Department of Environmental Engineering, Faculty of Civil Engineering, University Teknologi Malaysia, 81300 Skudai, Johor Darul Ta'zim, Malaysia.
[2]Department of Civil and Environmental Engineering, Pusan National University, 63 Beon-gil 2, Busandaehak-ro, Geumjeong-gu, Busan 609-735, Republic of Korea.
[3]Centre for Environmental Sustainability and Water Security, Research Institute for Sustainable Environment, Resource Sustainability Research Alliance, Universiti Teknologi Malaysia, 81300 Skudai, Johor Darul Ta'zim, Malaysia
*E-mail: eeling@utm.my

Abstract
The presence of pharmaceutical and personal care products in the aquatic environment has brought forth detrimental effects to the aquatic organisms. Sewage effluent was found to be one of the culprits contributing to their presence. Although the determination of pharmaceutical and personal care products was already conducted worldwide, the study on their presence in Malaysian sewage effluent was very little. This study investigated the presence of pharmaceutical drugs in sewage effluent across the different types of conventional biological wastewater treatment systems in Malaysia. The results revealed that only acetaminophen and ibuprofen can be completely removed by the treatment systems while others achieved less than 80% or negative removal. It is, therefore, proposed that advanced physical and/or chemical treatment process needs to be employed as tertiary treatment to avoid the entrance of pharmaceutical and personal care products into the environment.

Keywords: Emerging pollutants, sewage effluent, pharmaceutical and personal care products, ozonation

1. Introduction
Pharmaceutical and personal care products (PPCPs) in aquatic environment first emerged in mid 80's with concentration as low as 10 ng/L. Generally, PPCPs are not monitored frequently as they are not legislated in the environmental legislation. The urgency for PPCPs to be included in the legislation only appeared a decade ago when those of endocrine disruptors such as 17-Beta-estradiol (E2) and 17-Alpha-ethinylestradiol (EE2) have caused "feminization" of male fishes at very low concentration in US and European surface waters. The feminized male fishes was observed to have delayed sperm cell development and able to produce eggs. This was followed by a halt in reproduction and caused the decline in the fish population and eventually disappear. For other PPCPs found in the aquatic environment, their effects towards the aquatic species remain unclear since most of these compounds are specifically designed to induce biological response at very low levels.

Sewage treatment plants were found to be one of the main pathways for PPCPs to enter the environment. Trace level of PPCPs can still be found in the sewage effluent. The by-pass of these compounds from the wastewater treatment processes has raised questions on the competency of biological treatment technologies in removing them. Several alternatives have been suggested to improve the removal efficiencies of PPCPs by increasing the solid or hydraulic retention time. These, however, did not show any significant improvement. At times, bacteria can regenerate the original compounds from the excreted metabolites. Furthermore, waste sludge containing PPCPs was utilized as fertilizers for agricultural plants will contaminate soil with these medications. The contamination in both aquatic and soil environment will ultimately infiltrate human system via our food source.

Malaysia, in general, still employs conventional biological treatment systems including extended aeration, oxidation ditch and sequencing batch reactor. Mainly, these treatment technologies remove organic compounds that are measured in terms of biochemical oxygen demand and chemical oxygen demand, total nitrogenous compounds, sulfurous compounds, phosphorus compounds and suspended solids. To date, only few studies focused on the detection of PPCPs in sewage effluent and none was conducted on their removal.

In this study, the presence of PPCPs at different stages of wastewater treatment plants was determined and the removal efficiencies of the treatment plants were compared.

2. Materials and Methods

2.1 Reagents and Chemicals
All reagents and chemicals were of analytical grade and were used as purchased. Ultrapure water was obtained from Milli-Q Direct 8 system equipped with QPak Polising Cartridge and a 0.22-μm membrane point-of-use cartridge (Merck Millipore, USA). Sulphuric acid, methanol,acetonitrile, ammonium acetate and acetic acid were supplied by QRec (New Zealand). Methyl tert-butyl ether (MTBE) were purchased from Fisher Scientific (USA).

2.2 Sewage sample collection and preservation

Sewage samples were collected from the effluent of three sewage treatment plants located along Sungai Melayu in Johor Bahru. Samples were kept in a 1 L amber glass bottles on ice and transported back to the laboratory within 4 hours of collection. Samples that were not extracted immediately were preserved at pH 2 using concentrated sulphuric acid and stored at 4°C [17]. All samples were filtered through 0.45 µm glass microfiber filter (Whatman, USA) prior to solid phase extraction.

2.3 Solid Phase Extraction

Analytes were extracted according to Vanderford et al. [18] except extractions were performed manually using Thermo Fisher (USA) oil-free vacuum pump. Oasis HLB sorbent (Waters, USA) consisting of 500-mg hydrophilic-lipophilic balance (HLB) cartridges were employed for the extraction of analytes. The cartridges were preconditioned with 5 mL of MTBE followed by 5 mL of methanol and 5 mL of ultrapure water. Conditioned cartridges were dried with a stream of nitrogen for 60 minutes prior to the loading of filtered effluent samples at a flowrate of 15 mL/min. The sorbed analytes were then eluted with 5 mL of 10/90 (v/v) methanol/MTBE followed by 5 mL of methanol into a 20 mL glass bottles. The extract was concentrated to a volume of 1 mL under a gentle stream of nitrogen.

2.4 Instrumentation

Analytes were analyzed with an Agilent 6530 accurate-mass quadrupole time-of-flight (Q-TOF) liquid chromatography mass spectrometry system (Agilent, USA). A Zorbax Eclipse Plus C18 column (2.1×100 mm, 1.8 µm) was used to achieved the desired chromatographic separation. The separation was conducted at 40°C on gradient using water containing 5mM of ammonium acetate with 0.02% of acetate acid and acetonitrile as mobile phases. The flowrate of the mobile phases were set at 0.3 mL/min. In this pre-screening, the Q-TOF mass spectrometry system was operated in positive ion mode and nitrogen gas was employed as a nebulizer and auxiliary gas. Data acquisition and analysis were conducted using MassHunter B.07 software (Agilent, USA).

3. Results and Discussion

Table 1 shows the summary of the total removal efficiencies of PPCPs in sequencing batch reactor, extended aeration (EA) and oxidation ditch (OD).

Table 3 Removal efficiencies of PPCPs in sequencing batch reactor (SBR), extended aeration (EA) and oxidation ditch (OD)

Pharmaceuticals	SBR	EA	OD
Acetaminophen	97.5	99.9	100.0
Lincomycin	11.7	74.2	-827.5
Trimethoprim	74.2	10.6	-3.8
Sulfamethazine	93.4	100.0	-18.1
Sulfamethoxazole	99.1	61.2	-77.4
Clarithromycin	-4161.4	-641.0	-10.9
Carbamazepine	-572.0	-38.5	-240.5
Ibuprofen	100.0	85.2	100.0
Naproxen	96.8	23.2	-12.6

SBR was able to reduce concentration of 7 pharmaceuticals in this treatment plant namely ibuprofen (100.0%), sulfamethoxazole (99.1%), acetaminophen (97.5%), naproxen (96.8%) and sulfamethazine (93.4%). Trimethoprim experienced 74.2% reduction and lincomycin possessed poor removal with only 11.7%. Meanwhile, carbamazepine and clarithromycin showed negative removal of -572.0% and -4161.4%, respectively.

Similar to SBR, EA treatment system enabled high removal for sulfamethazine (100.0%), acetaminophen (99.9%) and ibuprofen (85.2%). Lincomycin reduction was better than SBR with the removal percentage achieving 74.3%. However, sulfamethoxazole was not well removed. The removal rate only achieved 61.2%. Oppose to SBR, naproxen and trimethoprim removal only reached 23.2% and 10.6%, respectively, in EA. Again, negative removal was observed on carbamazepine and clarithromycin, i.e. -38.5% and -641.0%.

Comparing with SBR and EA, OD shows the worst performance as positive removal was only achieved by two pharmaceutical drugs, i.e. acetaminophen and ibuprofen. The rest of the compounds revealed negative removal. The differences in the removal may be due to the retention time of the wastewater treatment. Longer solid or hydraulic retention time might have transformed the metabolites or conjugates into the original form of the pharmaceutical compounds by the bacteria. Meanwhile, carbamazepine and clarithromycin may not be suitable to be treated using biological treatment processes. Therefore, it is proposed that other treatment technologies such as membrane or advanced oxidation processes should be employed as tertiary treatment to avoid the entrance of PPCPs into the aquatic environment.

4. Conclusions

(1) Good removal efficiencies by the biological treatment systems only worked for acetaminophen and ibuprofen.

(2) The biological treatment systems were not capable in removing carbamazepine and clarithromycin.

(3) Tertiary treatment comprises of physical and/or chemical treatment system should be employed to ensure the removal of PPCPs from the sewage effluent.

5. Acknowldegments

The authors would like to thank Ministry of Education, Malaysia for the funding support under the Look East Policy Grant (RJ1300000.7822.4L148).

An Integrated Two-Stage Anaerobic-Aerobic Bioreactor for the Treatment of Raw Palm Oil Mill Effluent (POME)

○Khairunnisa ABDUL HALIM[1], Shawin MAT TAIB[1,2], Mohd Fadhil MOHD DIN[1,2] & Ee Ling YONG[1,2*]

[1]Deparment of Environment, Faculty of Civil Engineering, Universiti Teknologi Malaysia, 81310 UTM Skudai, Johor.

[3]Centre for Environmental Sustainability and Water Security, Research Institute for Sustainable Environment, Resource Sustainability Research Alliance, Universiti Teknologi Malaysia, 81300 Skudai, Johor Darul Ta'zim, Malaysia.*E-mail: eeling@utm.my

Abstract

All three reactors anaerobic digester 1 (AD1), anaerobic digester 2 (AD2) and aerobic were inoculated with sludge separately, before integration. During the start-up phase, insignificant removal of TSS was attained revealing good acclimatization environment was provided for the active bacteria. The COD removal performance was the highest in AD2, i.e. 87.3%, followed by aerobic (41.8%) and AD1(34.3%), respectively. Throughout the 150 days of treatment period, approximately 93% and 55% of reduction were achieved for COD and TSS, respectively, suggesting the integrated system was competent to be employed in high-strength wastewater treatment. Nonetheless, further research need to be made to ensure the stability consistency and feasibility of this integrated system.

Keywords: raw palm oil mill effluent (POME), two-stage anaerobic digestion, aerobic process

1. Introduction

Integrated anaerobic-aerobic bioreactor has been extensively explored recently to overcome the incompetency of the conventional method. However, most if not all studies used diluted POME to examine the treatment efficiencies of the integrated system instead of fresh raw POME owing to the high content of lignocellulosic compounds that affects the operation of the bioreactor. With dilution, all components in fresh raw POME were diluted causing the real application of this integrated system questionable. Therefore, this study proposed an integrated two-stage anaerobic coupled with a single stage aerobic system for the treatment of fresh raw POME. According to theoretical principles, lignocellulosic components can be broken down into simpler organic compounds in the first stage anaerobic bioreactor followed by their reduction in the second stage anaerobic and single stage aerobic bioreactors. This solved the potential mechanical problems, which interfered with the operation of the currently available integrated system. In addition, this study was the first to directly treat fresh raw POME using combined biological treatment processes.

The aim of this study is to investigate the performance of the integrated two-stage anaerobic with aerobic bioreactor for raw POME treatment, which focusing on chemical oxygen demand (COD) and total suspended solid (TSS) reduction.

2. Materials and Methods

2.1 Studied Wastewater

The palm oil mill effluent (POME) wastewater was collected from Felda Bukit Besar Palm Oil Mill in Wilayah Bukit Besar, Johor Malaysia. Upon collection, the samples were preserved at temperature below 4°C to avoid biodegradation of the sample. The following Table 1 shows the characteristics of the studied wastewater. The pH were determined using Orion 4-Star Benchtop pH meter. BOD5 and TSS determination were according to APHA 5210B and 2540B (APHA, 2005), respectively. For COD, inorganic anions and ammoniacal nitrogen, they were measured using DR900 Handheld Colorimeter.

Table 1: Characteristic of Raw POME

Parameter	Concentration
pH	4.6
BOD_5	756 mg/L
COD	239,000 – 431,500 mg/L
TSS	5,500 mg/L
Ammoniacal Nitrogen	30 mg/L
Nitrate	895 mg/L
Nitrite	2,000 mg/L
Sulfate	1,050 mg/L
Sulfide	6.0 mg/L

2.2 Reactor Fabrication

Briefly, this system comprised of two-stage anaerobic digester (AD) and single-stage aerobic processes. In this system, AD1 reactor was designed with 100 mm in diameter and 400 mm in height, where both ends were completely covered. This reactor has approximately about 3.2L of liquid volume; plus a headspace of 0.5L. Meanwhile, AD2 reactor was fabricated with a diameter of 100 mm and height of 300 mm and was packed with polypropylene plastic media. Similar to the AD1, AD2 was completely covered. Aerobic reactor was constructed identical to the AD2 reactor, but with an addition of air diffuser at the bottom of the reactor. Both AD2 and aerobic reactors have an estimated liquid capacity of 2.2L and a headspace of 0.5L. The schematic diagram of the reactors setup was illustrated in Fig.1.

2.3 Experimental Procedure

2.3.1 Acclimatization Phase

All the three reactors were inoculated with sludge obtained from the facultative pond located at aforementioned mill. At day 0, all reactors (AD1, AD2 and aerobic) were filled with POME sludge according to the volume capacity stated before. After 2 days, approximately half volume of the POME was withdrawn from each of the reactor. The AD1 was refilled to the original volume of the reactor with the fresh POME. AD2 reactor was filled to the initial volume with the effluent of AD1 and aerobic with portion ratio 1:1. The purpose for including the sludge from the aerobic reactor was to employ the function of recirculation. The aerobic reactor was loaded with the effluent from the AD2. This feeding process was conducted manually and repeatedly.

The effluents' chemical parameters of each reactor were routinely monitored for every 2 days, especially on the changes of organic matter during the entire inoculation staging. Once the biological stability was achieved, the reactors were integrated.

2.3.2 Reactors Integration

After 90 days of acclimatization period, the AD1, AD2 and aerobic reactors were started to be integrated. During this stage, the AD1 reactor was fed with filtered fresh POME continuously at the flow rate of 1.6 L/day. Unfiltered POME can severely clog the tubing systems of the pumps. The effluent from the AD1 was fed directly into the AD2 reactor, while, the effluent in AD2 reactor was flowed to the aerobic reactor. All the reactors possessed the same flow rate and HRT (2 days) throughout the operation. At the same time, the recirculation process also has been employed from the aerobic reactor to the AD2 reactor, with a flow rate of 0.6 L/day. The performance of this integrated system was evaluated periodically based on COD and TSS.

3. Results and Discussion

3.1. Start-up phase

As presented in Fig.2(a), AD2 shows an efficient performance with 87.3% of COD removal; followed by aerobic (41.8%); and AD1 (34.3%).

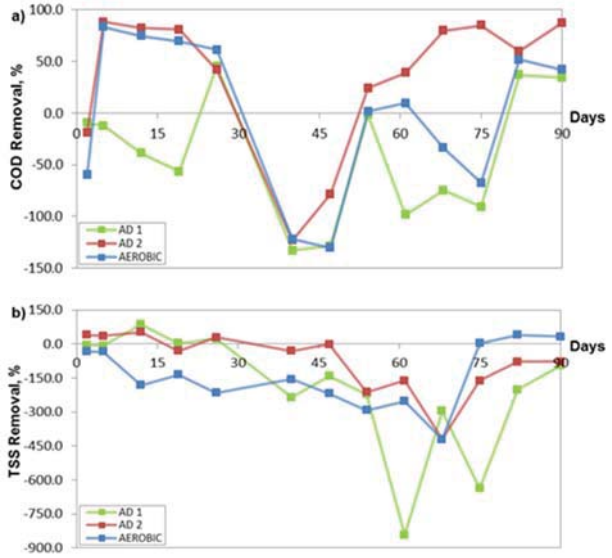

Fig. 2 (a) COD removal; and (b) TSS Removal during acclimatization phase

Based on the comparison illustrated in Fig.2(a), AD2 shows better performance than AD1 in terms of COD removal. This is due to the concentration of the COD in AD2's influent were lower than COD concentration of AD1's influent. In other hand, Fig.2(b) shows negative removal of TSS by all reactors indicated poor achievements of reduction at the early period proves that substrates were acclimatized. However, at the end of the period poor reduction of TSS were spotted.

3.2. Integration Phase

Fig.3 (a) and (b) depicts the COD and TSS removal efficiency for the entire integrated system, respectively. In general, the overall performance of the COD removal achieved satisfactory efficiency, which ranged in between 92%-94.5% of removal. At the end of the 150 operating days, the effluent COD concentration reduced up to 16,450 mg COD/L indicate about 93% of reduction. Despite this study have higher influent COD concentration as undiluted raw POME was used, this study able to performed efficiently.

Meanwhile, by referring the Fig.3(b), the profile trend indicates positive removal fluctuating from 15% to 55%, gives the effluent concentration as 6,700 mg/L at the end of the integrated period. Further study on this principle is vital in order to improve the TSS removal efficiency.

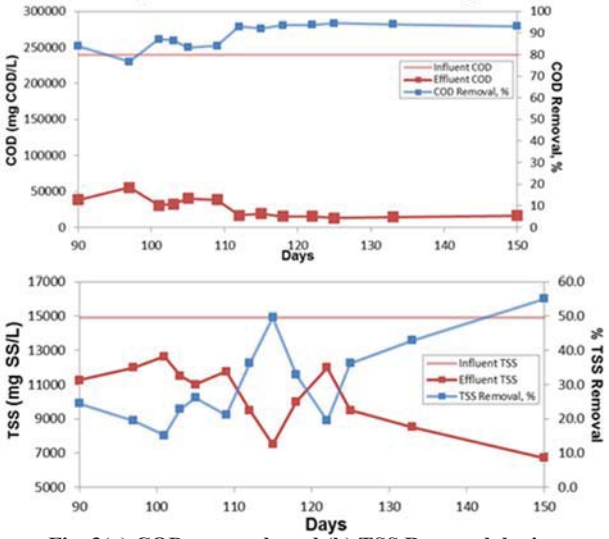

Fig. 3(a) COD removal; and (b) TSS Removal during integration phase

4. Conclusions

1. The principle of the two-stage anaerobic coupled with single stage aerobic process in treating fresh raw POME was successfully implemented.
2. Through the acclimatization stage, insignificant value of the TSS removal accomplished from each of the reactor.
3. At the end of the 150 day of operating period, a satisfactory efficiency of removal for COD and TSS were achieved.

5. Acknowldegments

The researchers would like to thank Universiti Teknologi Malaysia for providing funding via Potential Academic Staff Grant (Q.J1300000.2709.00K85).

The performance of biotrickling tower for nitrogen removal from wastewater

○Yan Guo[1], Yu-You Li[2]*, Qunhui Wang[3]
[1,2]School of Civil and Environmental Engineering, University of Science and Technology Beijing, 30 Xueyuan Road, Haidian District, Beijing 100083, P.R. CHINA
[3]Dept. of Civil and Environmental Engineering, Graduate School of Engineering, Tohoku University, Aoba-ku, Sendai, 980-8579 Japan
*E-mail: gyokuyu.ri.a5@tohoku.ac.jp

Abstract
The nitrogen removal through simultaneous nitrification and denitrification (SND) in one biotrickling tower will bring many advantages such as energy-saving, management-easy. This research investigated the performance of biotrikling tower packing with slow release carbon materials (PLA/starch blends) for nitrogen removal. The results showed that the removal efficiencies of NH_3-N were well achieved by the system, at the inlet concentration of NH_3-N at 800mg/L. Under this condition: the nitrification efficiency was above 98%; the total nitrogen removal efficiency was about 50%; besides, the PLA/starch blends shows a good organic carbon release performance and the main metabolic nitrogen product was nitrate; The goal of SND was achieved. It shows that the BF packing PLA/starch blends having a promising application future.

Key Words： Biotrickling tower, Slow-release carbon, Ammonia, Simultaneous nitrification/denitrification

1. Introduction
Various studies have focused on the treatment of ammonia gas in biotrickling filters (BF). However, in most cases, treatment relied mostly on the absorption of ammonia, which was followed by partial nitrification to nitrite and nitrate, and accumulation of these species in the packing and sometimes partial purging from the system by leaching. However, both free ammonia and free nitrous acid are known inhibitors of nitrification, and when considering the importance of pH effects on both ammonia absorption and on nitrification, it is not surprising to see reactors fail after some time due to the accumulation of metabolites.

When high concentrations of ammonia need to be treated and water consumption should be minimized, nitrification to nitrite or nitrate, followed by denitrification to nitrogen gas is probably the most desirable route, since it will prevent generation of a stream of water contaminated with nitrate and/or nitrite. However, this requires several biotransformation carried out by different microorganisms. Typically, achieving successful simultaneously nitrification and denitrification requires a careful control of pH, substrate and chemical oxygen demand (COD) concentrations, dissolved oxygen, etc. and preventing toxic or inhibitory metabolites such as free ammonia and free nitrous acid to accumulate.

The surface roughness and the interior cavities of PLA/starch blends are conducive to microorganism attachment and the formation of anaerobic environment. Some studies have been carried out for demonstrating the feasibility and efficiency of using solid PLA/starch blends as both solid carbon sources and biofilm carriers for heterotrophy bacteria. Hence, the purpose of this research was to determine technical feasibility and the performance of a biological treatment system mainly comprising of a BF packing with slow release carbon carriers to treat synthesis ammonia-containing wastewater with conversion of ammonia to nitrogen gas.

2. Materials and methods
2.1 BF and packing material
One reactors (BF) was used in this study. The reactor was constructed from clear polyvinyl chloride (PVC) piping and were 1.2 m in length and 10 cm in internal diameter. The button of BF was a tank with a volume of 5 L. The pH automatic adjustment system was added to keep the stability of pH range. Fig. 1 provides a schematic of the setup. Synthetic wastewater with nutrient for the experiments was prepared and adding pure ammonia to reach the desired concentration. The synthetic stream was supplied to the top of the BF (downflow mode). The air was supplied to the button of BF (upflow mode).

PLA/starch blends were used as a packing in this study. PLA/starch blends comprised of PLA and starch were produced by the same procedures as detailed by previous research. In this experiment, the PLA/starch blends (PLA proportions equal to 0.5) were prepared.

2.2 Startup of the bioreactors and operating conditions
The BF was inoculated with activated sludge from a local wastewater treatment plant. Mineral medium (2 L, see composition below), activated sludge (0.3 L) and 3 g $(NH4)_2SO_4$ were circulated through the biotrickling filter and the denitrification beds for 24 h. The suspended solids were not monitored during this phase. The

biotrickling filter was then incubated for a period of 4 months prior to the experiments to establish a dense culture of nitrifying organisms.

2.3 Standard operating conditions

20 mL min^{-1} of recycled liquid continuously trickled through the biotrickling filter. The airflow rate was 100 ml min^{-1}, corresponding to an empty bed residence time of 13.5 s. The exchange of exhausted recycled liquid was batch conduction. Every 24 hours 500 ml of exhausted liquid was replaced with fresh nutrient liquid responding to the HRT of 6 days. The ammonia concentration in the influent liquid stream ranged from 50 to 1500 mg/L, at which the stable statues was achieved then turning to the next stage. All experiments were carried out at a room temperature (22–25 °C).

2.4measurement

During the experiment, the sampled liquid was firstly filtrated through a 0.45μm filter and stored in a 4.0 °C refrigerator before analysis. All the evaluated indexes (e.g., pH, NH_4^+-N, NO_x^--N, TN, COD, etc.) were analyzed according to the standard methods for the examination of water and wastewater.

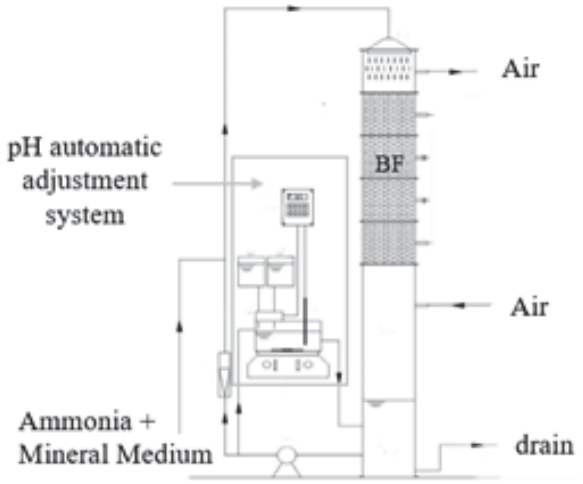

Fig. 1. Schematic diagram of the experimental system (not to scale).

3. Results and Discussion

The results of continuous operation of BF with inlet concentration of NH3-N ranging from 50 to 1500 mg/L are shown in Fig.2. During the initial 90 days with inlet concentration of NH3-N increased from 50 to 800 mg/L after reaching stable stage at each concentration, the NH3-N removal efficiency was above 98%. Besides, the COD concentration gradually increased with the raise of NH3-N loads. When the inlet concentration of NH3-N further raised to 1200 and 1500 mg/L, the NH3-N removal efficiency obviously declined, and the NH3-N accumulated in liquid. However, COD concentration begun decrease at this period.

Besides, the concentration of NH3-N in outlet air almost wasn't been detected during the whole experiment.

COD has close relationship with NH3-N loads.

At influent NH3-N concentration of 800 mg/L, the TN and NO2-N concentration varied during 24 hours after exhausted liquid replaced with fresh nutrient (with proper amount of NH3-N in order to keep the initial concentration of NH3-N stable) was showed in Fig.3. It was obvious that the TN concentration rapidly declined during the first 12 hours and almost keep stable level with the residual time; the concentration of NO2-N also gradually raised and reached the top level at the hour 8, then gradually decreased to the relative low stable as the initial. It indicated that the majority of nitrogen removal was occurred of the initial period; the rapidly increase of NO2-N indicated that the nitrogen content is shortage for nitrification process.

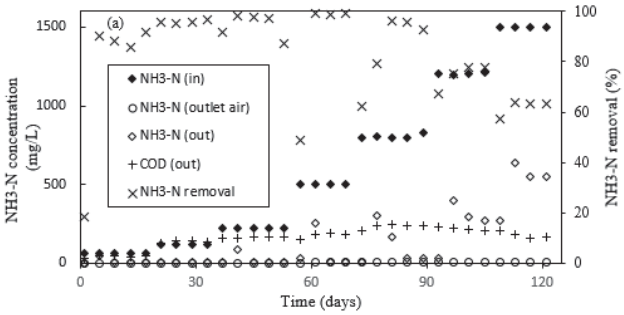

Fig. 2. The nitrification performance of BF at different influent NH3-N concentration.

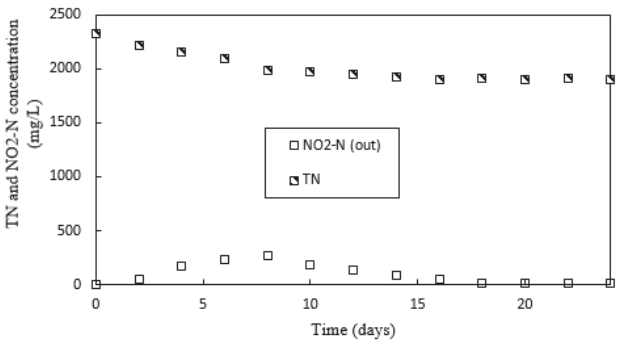

Fig. 3. The nitrogen fate of BF during denitrification at influent NH3-N concentration of 800 mg/L.

4. Conclusions

(1) Good removal efficiencies of NH3-N was achieved by the BF with PLA/starch blends, at the inlet concentration of NH3-N at 800mg/L, the nitrification efficiency was above 98%, besides, the PLA/starch blends shows a good organic carbon release performance.

(2) The nitrogen removal efficiency was about 50% at the inlet concentration of NH3-N was 800 mg/L; and the main metabolic nitrogen product was nitrate. Further investigation about microbial analysis was needed.

(3) In all, the BF with PLA/starch blends shows well performance, having a promising application.

5. Acknowldegments

The authors would like to thank Ministry of Education, Malaysia for the funding support under the Look East Policy Grant (RJ1300000.7822.4L148).

The experimental research in water quality control of seawater recirculating aquaculture system (SRAS) using embedded immobilized microorganism pellets

Bo Jiang[1], Zhenjia Zhang[2], Yu-You LI[1, 3*]

[1]Graduate School of Engineering, Tohoku University, Sendai 980-8579, Japan
[2]School of Environmental Science and Engineering, Shanghai Jiao Tong University, China
[3]Graduate School of Environmental Studies, Tohoku University, Sendai 980-8579, Japan
*E-mail: gyokuyu.ri.a5@tohoku.ac.jp

Abstract

The seawater recirculating aquaculture system (SRAS) was started up with a 300L simulated aquaculture tank, 1.8L untrained embedded immobilized microorganism pellets added in USBR and 8.4L same pellets in UASBR. After 60 days, the domestication of the embedded immobilized microorganism pellets was finished, and the RAS was successfully started. During the domestication period, the removal rate of Ammonia nitrogen higher than 90% and 70% of total nitrogen. When the domestication is finished, the removal rate is approximately 100%. The research results indicated that the use of embedded immobilized microorganism pellets is possible, the whole domestication process took 2 months. And the denitrification process was very sensitive to the change of temperature.

Keywords：seawater recirculating aquaculture system (SRAS)，ammonia nitrogen， pellets

1. Introduction

The seawater recirculating aquaculture system (SRAS), compared with other traditional way of seawater culture, can break the limit of regional restriction, seasonal restriction and greatly improve the unit of production. The SARS has a good social effect, economic returns and ecological benefits, therefore considered to be the main development direction of modern mariculture industry.

The aim of this research focused on the domestication process of the embedded immobilized microorganism pellets inside SRAS and its nitrogen removal rate.

2. Material and Method

2.1 Reactor and experimental design

The seawater recirculating aquaculture system (SRAS) contains a simulated aquaculture tank, an up-flow sludge blanket reactor (USBR) and an up-flow anaerobic sludge blanket reactor (UASBR). The effective working volume is 18L for USBR and 12L for UASBR. The simulated aquaculture tank has an effective working volume of 300L, and the basic composition of simulated seawater is as follows: 3.5% salinity, pH higher than 7.5. Figure 1 is the structure of the SRAS system.

The whole system was initiated on September 8, 2015, with 1.8L untrained embedded immobilized microorganism pellets added in USBR and 8.4L same pellets in UASBR. The pellets added occupied 10% of the working volume of the USBR and 70% of that of the UASBR. The whole system has been continuously run for 60 days, and the detailed operational condition are disposed in Table 1. The HRT maintained 0.05h for USBR and 0.5h for UASBR.

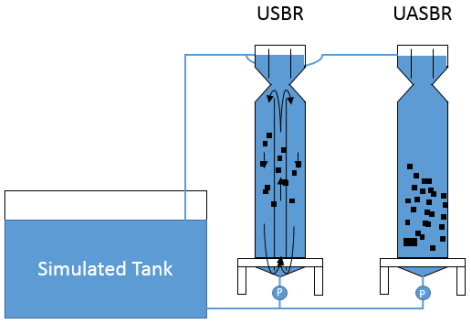

Figure 1 Experiment setup

The stocking density of SRAS was set at 3kg*m^{-3}, thus the increment of the ammonia concentration is 1.5mg*L^{-1}*day^{-1}. Addition time was 9 am, in order to simulate the periodical change caused by the actual breeding process.

Table 1 Operational conditions of the SRAS in this research

Days	1-3	4-25	25-35	35-40	40-45	45-60
Times (h)	0-72	72-600	600-840	840-960	960-1080	1080-1440
Temperature（℃）	26-29	24-26	22-24	18-20	21-23	18-20
pH				7.5-8.8		
Salinity（%）				3.5		
DO（ppm）				7.0-7.5		

3. Results and discussion

3.1 Ammonia nitrogen removal

The ammonia nitrogen concentration of SRAS is shown in figure 2

On day 40, the ammonia nitrogen concentration has dropped below 0.1mg/L, meeting the security requirement of aquaculture. At this point, the domestication process of nitrifying microorganism was finished.

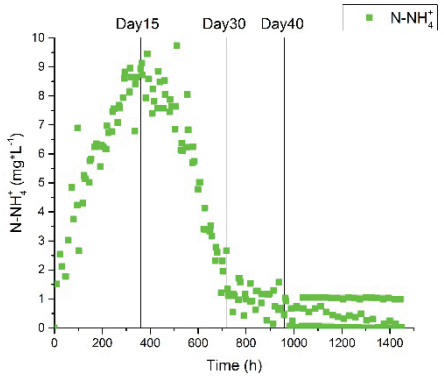

Figure 2 Ammonia nitrogen concentration

3.2 Nitrite nitrogen removal

The nitrite nitrogen concentration of SRAS is shown in figure 3

Nitrite nitrogen concentration had no obvious change in first 10 days. On day 58, the nitrite nitrogen concentration reached safe concentration (0.1mg/L).

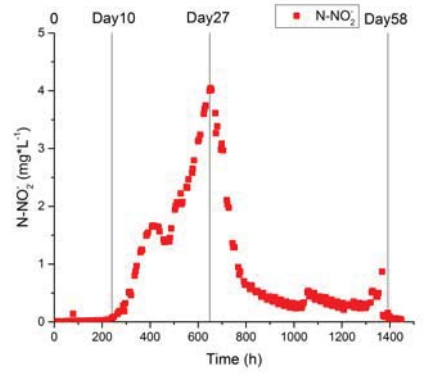

Figure 3 Nitrite nitrogen concentration

3.3 Nitrate nitrogen removal

The nitrate nitrogen concentration of SRAS is shown in figure 4. Nitrate nitrogen concentration had no obvious change in the first 10 days. Nitrate nitrogen concentration rose and achieve three balance statuses during the whole experiment.

3.4 The overall performance

The overall performance of the SRAS is prohibited in figure 5. The total domestication period lasts about 57 days, while the domestication of nitrifying bacteria is relatively short, which lasts about 40 days. The removal of the nitrite nitrogen, in the absence of external carbon source, can be very sensitive to the water temperature. The nitrification suffers little from the temperature change. However the changes indicate that the domestication under seawater condition lasts longer than fresh water condition (usually a week).

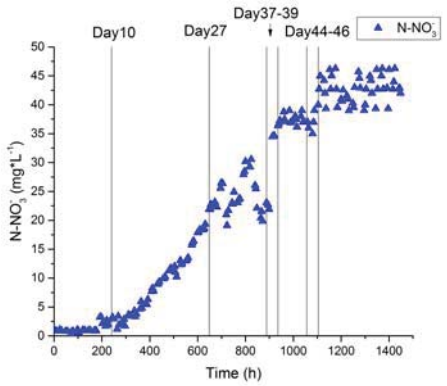

Figure 4 Nitrate nitrogen concentration

The emergence of nitrite nitrogen, which considered as an intermediate, is mainly caused by denitrification. The change trend of nitrate nitrogen concentration lags behind that of ammonia nitrogen and nitrate nitrogen concentration change trend, suggests the possibility of partial nitrification. Seawater condition acts as an inhibitory effect to the removal of nitrite nitrogen, which created a 20-day death period.

Temperature change is the main reason that effects the change of nitrate concentration. In theory, the dissolved ions in SRAS can promote the role of biological galvanic cell, but the low temperature inhibited both biological galvanic cell effect and microbial activity. The experimental results show that only when water temperature is higher than 20 ℃, the embedded immobilized microorganism shows enough removal capacity to nitrate nitrogen.

During the domestication period, the removal rate of Ammonia nitrogen higher than 90% and 70% of total nitrogen. When the domestication is finished, the removal rate is approximately 100%.

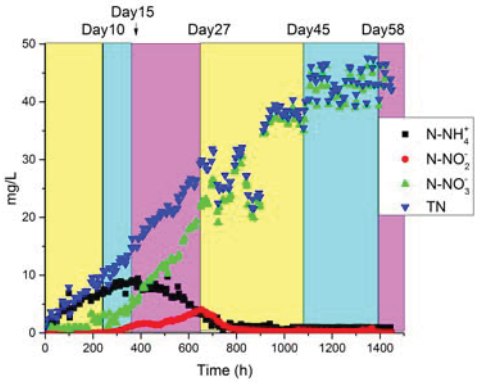

Figure 5 Nitrogen concentration in SRAS

4. Conclusion

In SRAS has a relatively longer domestication period, with death period caused by either ammonia nitrogen or nitrite nitrogen. These factors will restrict its practical application in SRAS. In subsequent experiments, Constant temperature processing should be taken into consideration.

Performance of an anammox attached film expanded bed reactor

○Yanlong Zhang[1*], Haiyuan Ma[1], Qigui Niu[1], Yuyou Li[1]
[1]Graduate School of Engineering, Tohoku University, Sendai 980-8579, Japan

*E-mail: zhang.yan.long.s5@dc.tohoku.ac.jp

Abstract

The possibility of anammox attached film expanded bed (AAFEB) reactor applied for the treatment of high strength ammonium wastewater was investigated in a continuous experiment operated at 35℃. The nitrogen loading rate (NLR) was increased gradually to study the reactor performance and operational stability. The removal efficiency, specific anammox activity (SAA) and granular characteristics were evaluated. As a result, when the NLR increased to a high level of 50 gN/L/d, the TN removal efficiency reached 89.8±0.7%. Furthermore, the maximum specific Anammox activity (MSAA) achieved 0.85±0.05 gN/gVSS/d. The substrate tolerance ability, which was expressed as the lag time and inhibitory concentrations ($IC_{10, 50, 90}$) were increased during the experiment. All the results indicated that the AAFEB reactor is suitable for the treatment of high-strength ammonium wastewater.

Keywords: anammox, AAFEB, granules, high loading, stability

1. Introduction

Since the anaerobic ammonia oxidation (anammox) process was first discovered in Netherland in the early 1990s, it has attracted more attentions for the treatment of ammonium-rich wastewater. The characteristics of low electricity consumption, low greenhouse gas emission and no external organic carbon requirement make the anammox process outstanding in the wastewater treatment processes.

Generally, enhanceing the biomass retention ability and environmental stresses resistence ability are the key pionts for maintaining the stable operation of an anammox-based reactor. Recently, new types anammox reactors, such as up-flow fixed-bed column reactor, three-bio-electrode reactor, and closed sponge-bed trickling filter reactor were developed to enhance the treatment performance and operational stability. However, problems of gas stagnate and substrate short-circuiting caused by sludge blocking in these kinds of fixed-bed reactors increase the difficulty of reactor maintenance. Zhang et al. (2016) reported an new type of anammox attached film expended bed (AAFEB) reactor, which enables high biomass retention ability, high environmental stress resistance ability and flexible operation.

In an AAFEB reactor, biofilm and granular systems are combined so that modify the conventional granules to perform better in settling property as well as in resistance ability to environmental stresses. Furthermore, the effluent recirculation is easily to be controlled to avoid the inhibition from high concentration of substrate. The characteristics of reactor operation and biomass itself enhance the operation stability and maximum treatment ability that extend the application of anammox process. In this study, the long-term performance of a high-load AAFEB reactor with 5L wording volume was evaluated.

2. Materia and methods

As shown in Fig.1, an AAFEB reactor with 5L working volume was used in the experiment. The recirculation ratio was adjusted to dilute the substrate concentration and maintain a certain hydrodynamic shear force to make the biofilm stronger, porous and heterogeneous. The operation temperature was controlled around 35℃ by a water jacket. The anammox granule was enriched from mixed anaerobic digestion sludge and denitrification activated sludge with the conventional anaerobic granule as the functional carrier. The anammox granules were cultured in a lab-scale reactor for over 1000 days and showed high stability and treatment performance. The successfully enriched anammox granule consists of two layers: the anammox biofilm and a nucleus formed from methanogenic granular sludge.

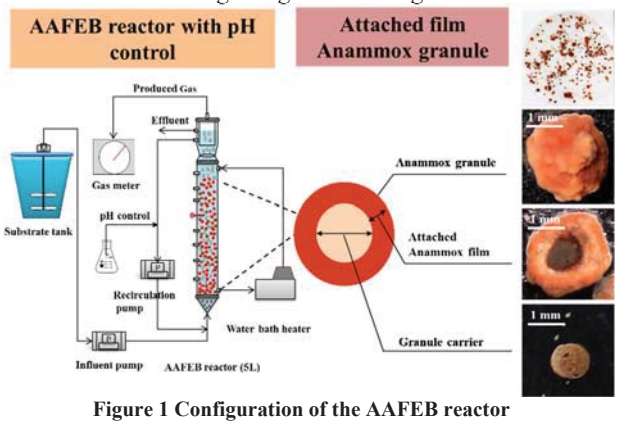

Figure 1 Configuration of the AAFEB reactor

There are 7 stable operation phases during the experiment. The NLR was increased step by step from 5.0 g N/L/d to 50.0 g N/L/d, accrodingly, the substrate TN concentration increased from 313 mg N/L to 1040 mg N/L and the HRT was decreased from 1.5h to 0.5h. When the NLR increased to 60.0 g N/L/d, the reactor was soon be inhibited, then the NLR was decreased and maintained at 50.0 g N/L/d.

3. Results and discussions

3.1 long-term performance

The long-term performance of the high-loading AAFEB reactor was shown in Figure 2. The effluent recirculation ratio was adjusted to dilute substrate concentration lower than the toxic threshold concentration of 320 mg N/L (as the

sum of diluted NO_2^--N and NH_4^+-N), correspondingly, as the true inhibitors, the concentrations of FA and FNA were both in the safety range that reported in the previous research (Zhang et al., 2016). The average reaction ratio of R_S in phase I was 1.13±0.13 that was lower than the influent NO_2^--N/NH_4^+-N ratio of 1.32. The excess NO_2^--N increased the risk of FNA inhibition when the substrate concentration increased. Thus in phase II, when the TN concentration was increased to 625 mg N/L, the influent NO_2^--N/NH_4^+-N ratio was adjusted to 1.0 to avoid the FNA inhibition. However, along with the increase of the average RS to 1.23±0.07 in phase II, the effluent NH_4^+-N increased to 42-63 mg N/L, the NH_4^+-N removal efficiency decreased to 84.51±2.59%. During phase III to phase VII, the influent NO_2^--N/NH_4^+-N ratio was maintained at a constant value of 1.2, the NLR was gradually increased to 50 g N/L/d. The TN removal efficiency was maintained stable at 84-89% that was close to the reported maximum TN removal efficiency. However, when the NLR increased to 60 g N/L/d, the reactor was soon be inhibited. In order to recover the anammox reaction, the NLR was decreased and then gradually recovered to 50 g N/L/d and the reactor was soon be recovered.

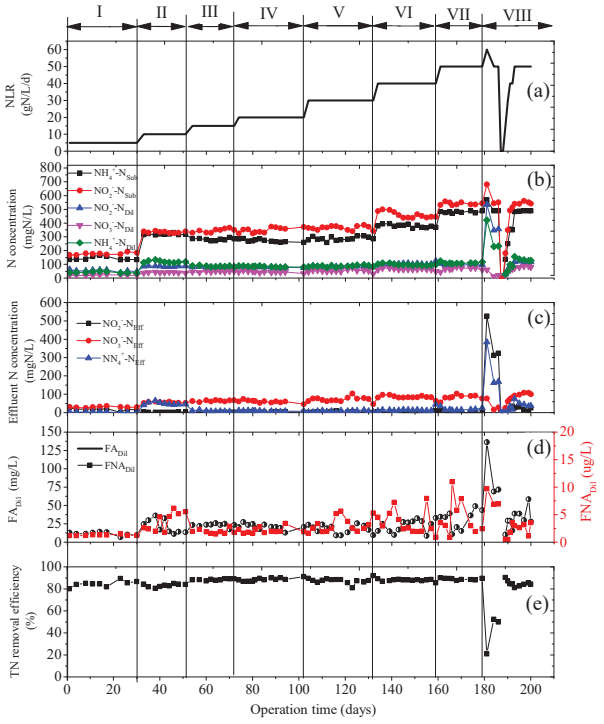

Figure 2 Long-term performance of the AAFEB reactor

3.2 SAA tests

The SAA tests were performed in the end of each phase and the results were simulated with the modified Gompertz equation. The simulation results of the SAA tests were shown in Figure 3. Generally, the value of the SAAs was influenced by the biomass itself and the operation conditions. One the one hand, the abundance of the anammox bacteria directly determines the SAAs. On the other hand, as important enzymes of the anammox pathway, the activity of the hydroxylamine-oxidoreductase (HAO) and hydrazine-oxidoreductase (HZO) also play important roles for determining the SAAs. Furthermore, the substrate concentration was regarded as a key operational parameter that influences the SAAs. In this study, when the substrate concentration was lower than the toxic threshold value, the SAAs increased with the increasing of substrate concentration, but decreased rapidly when the substrate concentration was higher than the toxic threshold value. With the increase of NLR, the average maximum SAA was also increased from 0.37±0.20 g N/gVSS/d to 0.85±0.05 g N/gVSS/d. The decrease of the fluctuating value of the maximum SAA indicated that the anammox biomass distribute more uniformly in the reactor when the NLR was increased.

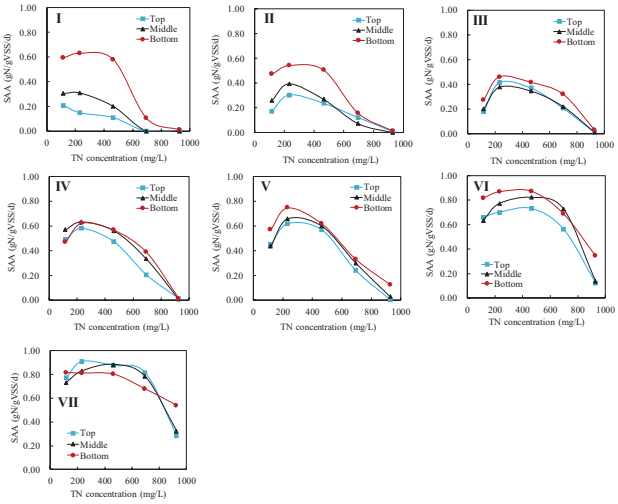

Figure 3 Variation of SAA during the stable operation phases

3.3 Enhancement of the substrate tolerance ability

The inhibitory effects of high concentration substrate were simulated by the modified 2-P logistic model and were shown in Figure 4. The inhibitory concentrations ($IC_{10, 50, 90}$) were all increased during the experiment that indicated the substrate tolerance ability was enhanced along with the increase of the NLR. Furthermore, the lag phase under different substrate shock conditions were significantly shortened with the increase of NLR. In phase I, the SAA was totally inhibited when the substrate concentration was higher than 696 mg N/L thus the lag time was infinite. However, in phase V, the lag time was shorter than 1h when the TN concentration was not higher than 696 mg N/L. The shortening of the lag time indicated that the anammox biomass would recover faster after exposure into the substrate shock conditions.

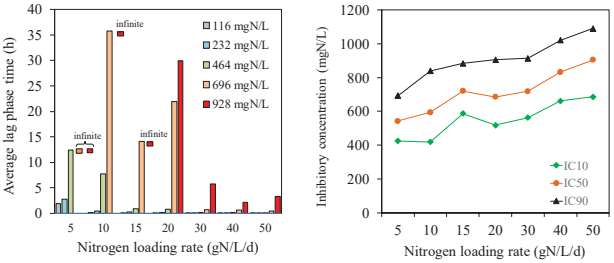

Figure 4 The lag phase time (a) and inhibitory concentrations

4. References

Zhang, Y.L., Niu, Q.G., Ma, H.Y., He, S.L., Kubota, K., Li, Y.-Y. 2016. Long-term operation performance and variation of substrate tolerance ability in an anammox attached film expanded bed (AAFEB) reactor. Bioresource Technology, 211, 31-40.

Assessment of Soil Erosion using Revised Universal Soil Loss Equation (RUSLE) and GIS in Thailand

○Prem Rangsiwanichpong, So Kazama
Graduate School of Environmental Studies, Tohoku University, Sendai 980-8579, Japan
*E-mail: prem.rangsiwanichpong.q8@dc.tohoku.ac.jp

Abstract

Soil erosion susceptibility mapping is one of most important requirement for its planning management and conservation. In this study, soil loss model, The Revised Universal Soil Loss Equation (RUSLE) integrated with GIS has been used to estimate soil erosion in Thailand. GIS data including, rainfall erosivity (R), soil erodability (K), slope length and steepness (LS), cover management (C) and conservation practice (P) factors were computed to determine their effects on average annual soil loss in the area. This study indicated that most of soil erosion occurred in high slope area, especially in the northern and southern part of the country. Furthermore, the results showed that the annual average soil erosion in Thailand estimated using RUSLE model is 130 ton·ha^{-1}·year^{-1}. It is concluded that soil erosion has a significant impact on mountain areas and the estimation of soil loss is an essential input for the adoption of proper land use planning and development strategies.

Keywords: GIS, RUSLE, Soil erosion, Thailand

1 Introduction

Soil erosion represents the amount of soil moved from one particular area to another in the form of sediment yield. This phenomenon depends on relationship between raindrops, runoff and erodibility of each area. For the past decades the experiment on the study of soil erosion were conducted in a number aspects to quantify the amount of soil loss. The accumulation of scientific knowledge in the United States and in the humid tropics has made it possible to do this with the Universal Soil Loss equation (USLE). The Revised Universal Soil Loss Equation (RUSLE) is an empirical model, modified from the USLE model (Renard etal, 1997). It estimates soil erosion as a function of 6 major factors consists of rainfall erosivity (R), soil erodability (K), slope length and steepness (LS), cover management (C) and conservation practice (P) factors. Several researchers in Thailand using the USLE and RUSLE model to study soil erosion (Wijitkosum S., 2012; Shrestha et al., 2014). In 2015, Somprasong K. and Chaiwiwatworakul P. estimated the potential cadmium contamination by RUSLE model in the Mae Tao basin of Thailand.

The objective of this study is to assess a soil erosion for long term in Thailand using the RUSLE model with Geographic Information System (GIS).

2 Study area

Thailand is located at the center of peninsular Southeast Asia. Topography can divided into 5 physical regions consists of central valley, highlands of the north and northwest, northeast, southeast coast, and the peninsular. Roughly 20 percent of Thailand is covered by mountains plateau area (Figure 1.). The average slope of this area exceeds 30%. The study area has a humid tropical climate with a mean annual rainfall of 1100 mm.

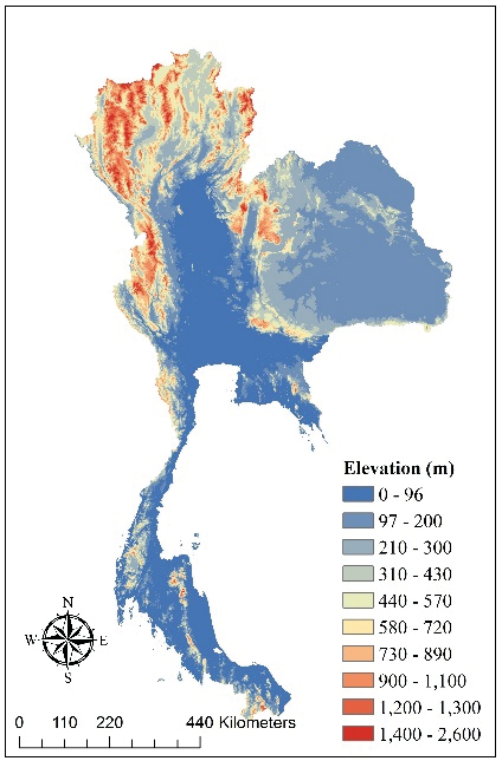

Figure 1. Topography of Thailand

3 Methodology

The Revised Universal Soil Loss Equation (RUSLE) is the method, most widely used around the world for forest mountains and agricultural to predict average annual soil loss. RUSLE is an empirical model, method is expressed as show in equation 1.

$$A = R \times K \times L \times S \times C \times P$$

Where,

A : Annual soil loss per unit area ($TON \cdot ha^{-1} \cdot year^{-1}$)

R : Rainfall erosivity factor ($MJ \cdot mm \cdot ha^{-1} \cdot hr^{-1} \cdot year^{-1}$)

K: Soil erodibility factor ($TON \cdot hr \cdot MJ^{-1} \cdot mm^{-1}$)

LS: Slope length factor (dimensionless)

C: Cover-management factor (dimensionless)

P: Conservation practice factor (dimensionless)

4 Results and discussion

4.1 RUSLE parameter estimation

4.1.1 Rainfall erosivity factor (R)

In Thailand, Development of Methodologies for Land Degradation Assessment Applied to Land Use Planning in Thailand recommended equation for calculate R factor as follows in equation (2) and the map of R factor as shows in Figure 2.

$$R = 0.4669X - 12.141559$$

Where,

R : Rainfall erosivity factor ($MJ \cdot mm \cdot ha^{-1} \cdot hr^{-1} \cdot year^{-1}$)

X : Annual rainfall (mm)

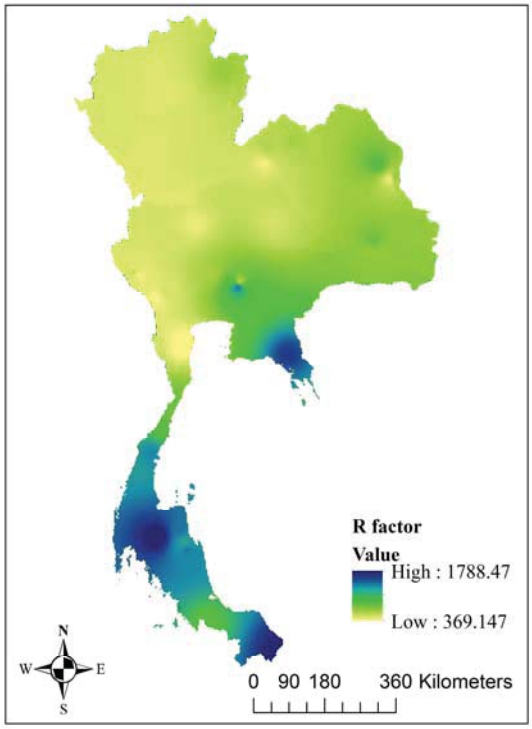

Figure 2. Rainfall erosivity map (R)

4.1.2 Cover-management factor (C)

The C factor expresses the effect of cropping and management practices on the soil erosion rate. We used the normalized difference vegetation index (NDVI) index for calculate C factor. (Farhan Y. et al., 2013). The results of the C factor as shows in Figure 3.

$$C = (-0.7388 \times NDVI + 0.4948)$$

4.1.3 Slope length and steepness factor (LS)

The *LS* factor expresses the effect of local topography on soil erosion rate, combining effect of slope length and slope steepness. (Figure 4.)

$$LS = L_{factor} \times S_{factor}$$

$$L_{factor} = \left(\frac{\lambda}{22.12}\right) \times \left(\frac{\frac{\left(\frac{\sin\theta}{0.0896}\right)}{(3\sin\theta \times 0.8 + 0.56)}}{1 + \frac{\left(\frac{\sin\theta}{0.0896}\right)}{(3\sin\theta \times 0.8 + 0.56)}}\right)$$

$$S_{factor} = 10.8\sin\theta + 0.03$$

(For slope gradient less than 9%)

$$S_{factor} = 16.8\sin\theta + 0.5$$

(For slope gradient equal or above than 9%)

Where

λ = Length of slope

L_{factor} = Slope length factor

S_{factor} = Steepness factor

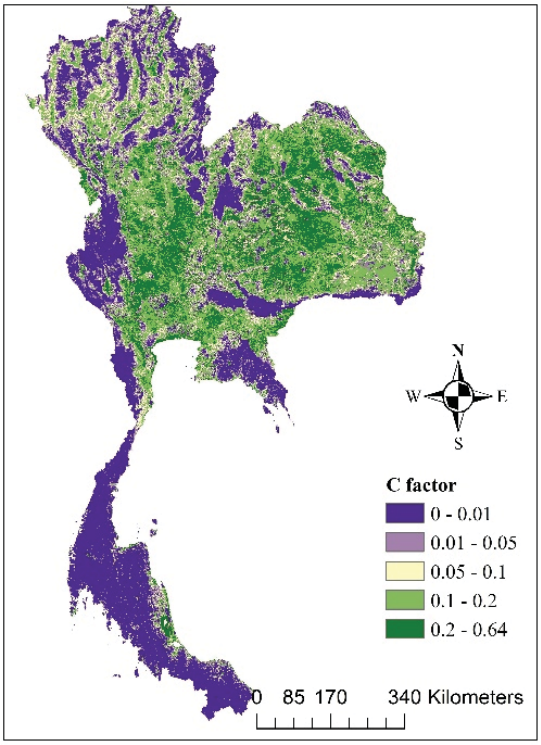

Figure 3. Cover-management factor (*C*)

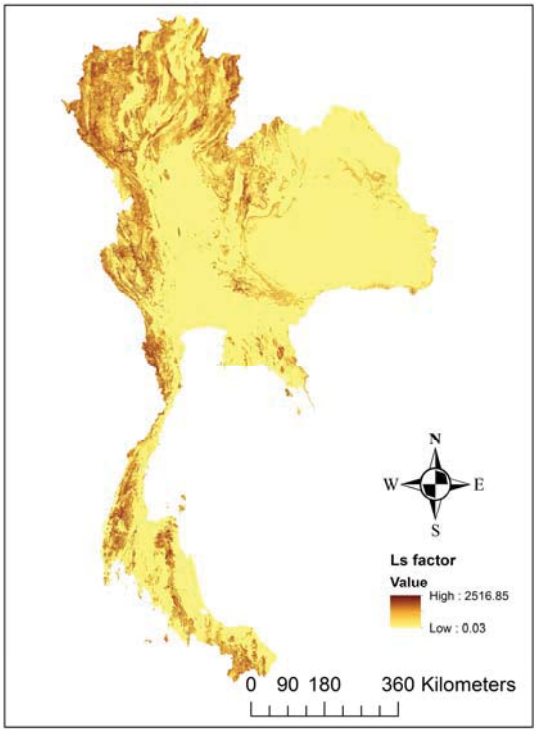

Figure 4. Slope length factor (*LS*)

4.1.4 Conservation practice factor (P) and Soil erodibility factor (K)

The *P* factor expresses the effect of conservation practices that reduce the amount and rate of water runoff, which reduce erosion. The *K* factor integrates the effect of processes that regulate rainfall acceptance and resistance of soil to particle detachment and subsequent transport. These parameters collected data from Land Development Department of Thailand.

4.2 Soil loss assessment

In this research, soil erosion in Thailand was estimated using RUSLE model which the value of some variable was determined from experiment of the Land Development Department of Thailand. The results showed that the GIS software can use for analyzing soil erosion in Thailand by the RUSLE model. After calculating and evaluating the required parameters for RUSLE, annual soil loss per hectare is 130 ton·ha^{-1}·year^{-1}. Most erosion areas occurs in

upstream of basin in Thailand more than downstream area due to the topography of upstream area have high slope area and covered by mountain and plateau. The highest of values of soil erosion were found in the southern part of Thailand. Because in the southern area of country have high slope area and monsoon, which effect of the monsoon can make heavy rainfall and increase the erosion.

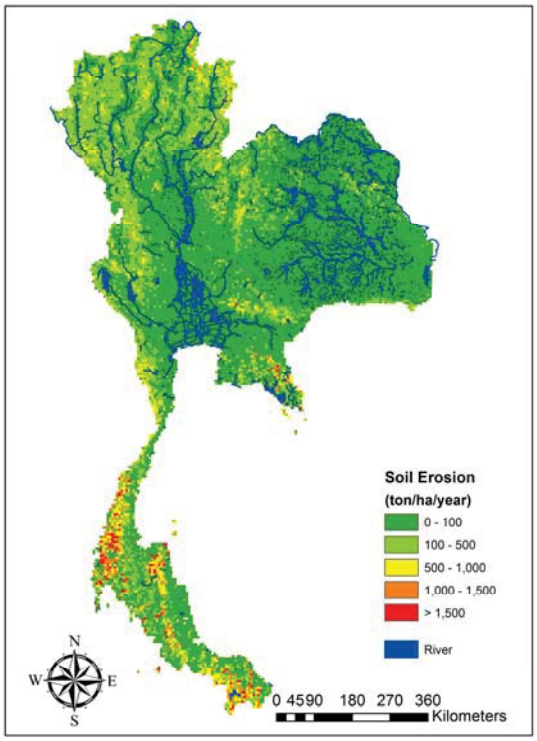

Figure 5. Soil erosion map of Thailand

5 Conclusions

This study determination using RUSLE model for Thailand has revealed the severity of soil erosion. The results showed that high of erosion occurred in the upstream of basin in Thailand more than other area due to the topography. Because in the upstream area have high slope and covered by mountain and plateau area. Furthermore, there is significant evidence that the upstream area of basin in Thailand has the potential to release sediment during erosion to downstream. However, the present investigation has demonstrated that GIS techniques are simple and cheap cost tools for modeling soil loss, with the purpose of assessing erosion potential for Thailand.

6 Acknowledgements

The present research was supported through the Program for Leading Graduate Schools, Tohoku University, "Inter-Graduate School Doctoral Degree Program on Global Safety," by the Ministry of Education, Culture, Sports, Science and Technology.

7 References

Farhan, Y., Zregat, D., and Farhan, I. 2013. Spatial estimation of soil erosion risk using RUSLE approach, RS, and GIS techniques: A case study of Kufranja Watershed, Northern Jordan. Journal of Water Resource and Protection, 5, pp. 1247-1261.

Shrestha, D.P., Suriyaprasit, M., and Prachansri, S., 2014. Assessing soil erosion in inaccessible mountainous area in the tropics: The use of land cover and topographic parameters in a case study in Thailand. Catena, 121, pp. 40-52.

Somprasong, K. and Chaiwiwatworakul, P. 2015. Estimation of potential cadmium contamination using an integrated RUSLE, GIS and remote sensing technique in a remote watershed area: a case study of the Mae Tao Basin, Thailand. Environmental Earth Sciences, 73, pp. 4805-4818.

Renard, K.G., G.R. Foster, G.A. Weesies, D.K. McCool, and D.C. Yoder. 1997. Predicting Soil Erosion by Water: A Guide to Conservation Planning with the Revised Universal Soil Loss Equation (RUSLE). U.S. Department of Agriculture-Agriculture Handbook No. 703.

Wijitkosum S., 2012. Impacts of land use changes on soil erosion in Pa Deng sub-district, adjacent area of Kaeng Krachan National Park, Thailand. Soil and Water Research, 7, pp. 10–17.

Environmental assessment in freshwater using eDNA

○Noriko Uchida[1*], So Kazama[1], Kengo Kubota[1], Kei Nukazawa[2]
[1]Graduate School of Engineering, Tohoku University, Sendai 980-8579, Japan
[2]Department of Civil and Environmental Engineering, University of Miyazaki, Miyazaki 889-2192, Japan
*Email: noriko.uchida.s8@dc.tohoku.ac.jp

Abstract
environmental DNA (eDNA) analysis has been known as novel molecular technique used to detect the presence of species, and it could have considerable advantage to estimate the presence of a species. In this study, we applied this approach to invertebrates and clarified how to detect aquatic invertebrates DNA in our study area: Hirose River, Miyagi Prefecture, Japan. We sampled 2L of stream water from 3 sampling sites, which is located up/ middle/ downstream of the river, once per a month through August to December 2015. For DNA analysis, we used qPCR. From the result which analyzed CO1 gene area and environmental information, we assessed time series and spatial distribution pattern of mitochondrial DNA.

Keywords: aquatic invertebrate, biomass, environmental DNA, mitochondria DNA, qPCR

1. Introduction

Exploitations and climate changes have resulted in habitat deterioration of wild animals. To conserve wild life, it is required to understand distribution of keystone or rare species[1)]. Additionally, in streams, understanding assemblage component (population size or faunal composition) of stream invertebrate is fruitful to assess biological diversity[2)]. Monitoring of aquatic wild life has been practically carried out by visual observation, and fishing in several manners. However, in terms of monitoring in broader scale or longer term, these conventional methods are time- and effort- consuming, require special skills to identify species and involve observer errors or bias.

Environmental DNA (eDNA) is a novel monitoring method to address these problems. eDNA is a small fragment of DNA originated from animal bodies and metabolites such as skin cells, feces, saliva, urine of animals occupying water body and it extracts to water like lake, pond, ocean, river[3)]. By detecting species specific genome sequences in a given water samples using molecular biological methods (e.g. PCR, Next Generation Sequencing) presence / absence of a target species can be determined with high accuracy. Remarkably, it is already verified that using eDNA method is more efficient to know species composition or existence than conventional monitoring methods by Minamoto *et al.* [4)]

Using eDNA method is expected to make optimization of biological monitoring, to improve objectification for monitoring results, and also to help financially cost to be lower. Furthermore, there are some reports which find positive correlation between biomass and amount of observed eDNA collected from closed aquatic habitat such as aquarium, lake and lagoon[5-6)]. On the other hand, there are a few attempts handling these inquiries in river and ocean because these are more complicated environments, which is subject to various chemical degradation factors and physical transportation via water flow.

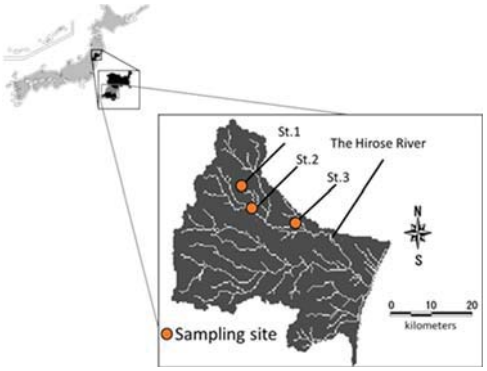

Figure 1: Sampling sites, Hirose River, North part of Japan

In this study, we aim to quantify temporal variation of eDNA collected from 3 sites along Japanese rivers using qPCR (quantitative Polymerase Chain Reaction, one of real-time PCR techniques). To do so, here we mainly describe a methodology to detect the eDNA and quantify the DNA concentration of the target taxa. We currently devote an effort to provide precise condition for the qPCR that enables to determine the eDNA concentration in a given sample as the number of target DNA copies per volume.

2. Materials and Methods

We sampled eDNA at 3 reach sites, which are

longitudinally located along the Hirose River with equivalent intervals as much as possible (Figure 1), in northeast Japan. The samplings were monthly conducted, through August to December 2015 except St.1 on September. We tried to detect eDNA of stream invertebrate species (e.g. larvae of caddisfly) occupying waterbody. We collected 2L of water from water surface to sterilized plastic container by gloved hands. For experimental procedures we mainly followed the earlier reports[7].

The sampled stream water was transported to the laboratory and kept in the cold condition on the same day before subsequent filtering process. The water samples were then filtered by the vacuum filtration with 90mm diameter glass-fiber filters (normal pore size, 0.7µm; Whatman) and GF/D filter (Whatman, diameter 90mm, normal pore size 0.27µm) as a pre-filter. These samples were wrapped in commercial aluminum foil and stored in -20ºC until DNA extraction. DNA was extracted from filters using the DNeasy Blood & Tissue Kit (QIAGEN) and followed the manufactural protocol. Finally, concentration of the extracted DNA was measured using PicoGreen (Thermo Fisher Scientific Inc).

Mitochondrial DNA (mtDNA) was employed as the target genetic marker because copy number of mtDNA in stream water could be larger than that of nuclear DNA per cell so that detection rate is expected to be higher. We used a universal primer targeting mtDNA cytochrome *c* oxidase subunit 1 (CO1), which is divergent among all animal phyla (Folmer *et al*., 1994). We amplified the target DNA fragments of the samples using the PCR primers designed to amplify invertebrate-specific loci from the CO1 region. A 710 bp fragment from CO1 region was amplified with the following primer pair; LCO1490 (5'-GGT CAA CAA ATC ATA AAG ATA TTG G-3') and HCO2198 (5'-TAA ACT TCA GGG TGA CCA AAA AAT CA-3')[8]. We initially validated the primers on tissue samples for a larva of the caddis fly species (*Stenopsyche marmorata*) which was also sampled in the study catchment.

The qPCR was performed using SYBR®Premix Ex Taq (TaKaRa) and LightCycler®2.0 (Roche). The condition of qPCR consists of an initial incubation at 95ºC for 20 seconds followed by 40 cycles of 95ºC for 5 seconds, 53ºC for 30 seconds, 72ºC for 1 minute. Fragment size of amplicons was verified with agarose gels electrophoresis and qPCR products were purified using a MicroSpin S-400 Columns (GE Life Science). Further, we set a template DNA which was extracted from tissue of *S. marmotara* and amplified it using the above mentioned primer pair. Then we created a dilution series from the PCR products of as standard DNA thorough $1.0x10^1$ to $1.0x10^7$ (copies/µl). Further, we processed pre amplification for qPCR (Pre-Amp) using ABI® Pre Amplification Master Mix and Thermal Cycler (TaKaRa) because it was supposed that DNA concentrations extracted from environmental samples could be too small to amplify and detect. PCR conditions

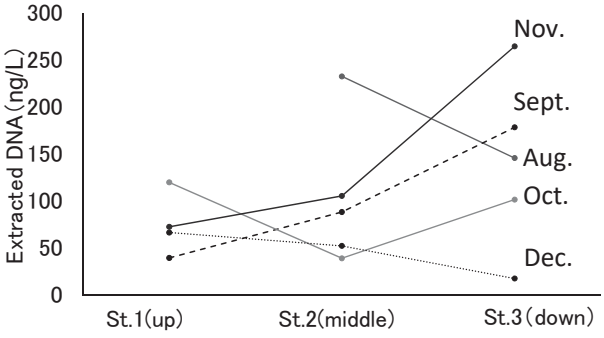

Figure 2: Result of extracted DNA concentration

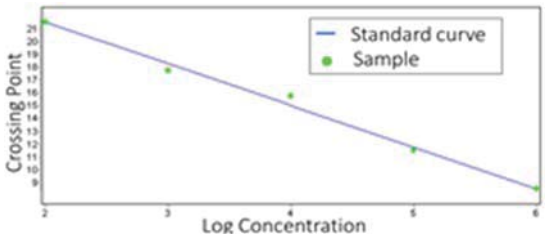

Figure 3: Standard curve of Pre-Amped qPCR.

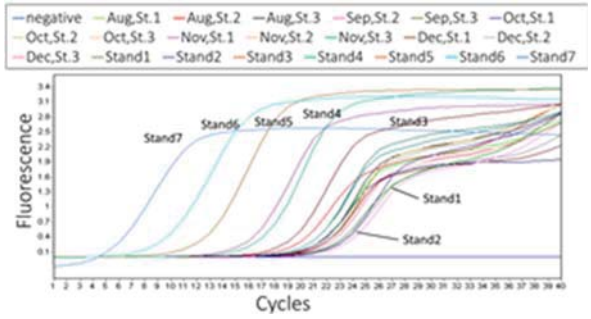

Figure 4: The observed Pre-Amped qPCR process.

for Pre-Amp consisted of an initial incubation at 95ºC for 10 minutes followed by 10 cycles of 95ºC for 15 seconds, 60ºC for 4 minutes. After the Pre-Amp, qPCR was conducted by same process to above simple qPCR.

3. Results

Figure2 describes the extracted DNA concentration of all river samples. These are mostly small and concentrations of total DNA within river water does not show a specific tendency by this survey. It is suggested that eDNA should be observed shorter periods and distance to know the tendency. In qPCR process without Pre-Amp, standard curve showed high efficiency in the range for $1.0x10^7$ to $1.0x10^3$ (copies/µl). Where concentration of the sample DNA is larger than $1.0x10^2$ (copies/µl), it is precise concentration seems to be detectable because they were within the provided standard curve derived through our settings. However, the samples from St.1 to St.3 were amplified lower range than this and the concentrations could

not be detected. This result implies that detecting eDNA from river water requires further accuracy in a range of low concentration, by building an optimized standard curve or using more sophisticated technique such as the digital PCR.

On the other hand, the result of qPCR with Pre-Amp provided wider range than above. The standard curve was expanded from $1.0x10^7$ to $1.0x10^2$ (copies/μl) in better efficiency (see Figure3). Figure4 shows the observed Pre-Amped qPCR process. Using the observed mass of DNA (copies/L) of each samples, except December St.3, we calculated total number of invertebrate's DNA copies per basin area of each sites and it is described as Figure5. By figure5, the number of the DNA copies tends to increase along down-stream even though downstream is generally more artificialized and influenced by human activities than upper stream. Considering each of sites has different land use property, it is possibly able to discuss the influence of land use or human activities to biomass by this method.

4. Conclusion

This study examined the method to measure the DNA concentration from river water eDNA samples focusing mitochondrial DNA region of CO1, targeting invertebrate species. The results show that:

1) It is able to amplify universal region of mitochondrial DNA among invertebrate species from streaming water samples using qPCR.

2) We could determine a suitable annealing temperature and time in qPCR protocol. It enabled to obtain highly reliable standard curve for $1.0x10^7$ to $1.0x10^3$ (copies/μl). However, it could not be detected the concentration of target DNA because of they were out of this range.

3) After pre amplification process, we could describe the precise standard curve with concentrations ranging from $1.0x10^7$ to $1.0x10^2$ (copies/μl). Thus it let all samples except December St.3 be detected the concentration. From the results, we could see the difference of concentration between each sites and seasons. In addition, this results implies that there is quite small number of copies of the target gene sequence in river water and it might make difficult to detect the target samples.

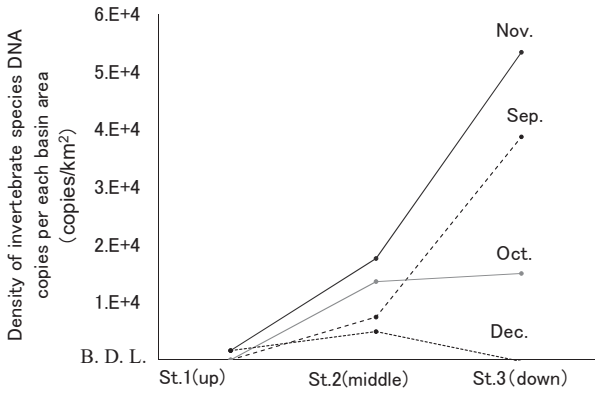

Figure5 Density of invertebrate species DNA copies per an each basin area (i.e. St.1, St.2, St.3)

Using eDNA analysis, we can assess the river environment to discuss river design in the future and to consider the relationship between flood and environment. Furthermore, it is indicated that eDNA also can extend the possibility of continual survey to evaluate wasted water and land use change.

Acknowledgements

This research was partly supported by the Ministry of Education, Science, Sports and Culture through a Grant-in-Aid for Scientific Research (grant nos. 25241024, Yasuhiro Takemon, 26630247, Kozo Watanabe, 26820196, Kei Nukazawa) and Japan society for the Promotion of Science (JSPS) Research Fellowship (grant no. 256493).We express deep appreciating for all of supports.

References

1) Hurlbert, A. H., Jetz W.: Species richness, hotspots, and the scale dependence of range maps in ecology and conservation, PNAS, 104 (33), pp.13384-13389, 2007
2) Heino, J.: Biodiversity of aquatic insects: spatial gradients and environmental correlates of assemblage-level measures at large scales, Freshwater Reviews, 2, pp.1-29, 2008
3) Rees, H. C., Maddison, B. C., Middleditch, D. J., Patmore, J. R. M., Gough K. C.: The detection of aquatic animal species using environmental DNA-a review of eDNA as a survey tool in ecology, Journal of Applied Ecology, vol. 51, pp.1450-1459, 2014
4) Minamoto, T., Yamanaka, H., Takahara, T., Honjo, M. N., Kawabata, Z.: Surveillance of fish species composition using environmental DNA, Limnology, 13 (2), pp.193-197, 2012
5) Pilliod, D. S., Goldberg, C. S., Arkle, R. S. and Waits, L. P.: Estimating occupancy and abundance of stream amphibians using environmental DNA from filtered water samples, Canada Journal of Fisheries and Aquatic Sci., Vol. 70, pp.1123-1130, 2013
6) Takahara, T., Minaoto, T., Yamanaka, H., Doi, H., Kawabata, Z.: Estimation of fish biomass using environmental DNA, PLoS ONE, 7 (4), e35868, 2012
7) Folmer, O., Black, M., Hoeh, W., Lutz, R., Vrijenhoek, R.: DNA primers for amplification of mitochondrial cytochrome c oxidase subunit 1 from diverse metazoan invertebrates, Molecular Marine Biology and Biotechnology, Vol.3, pp.294-299, 1994
8) Ficetola, G. F., Miaud, C., Pompanon, F., Taberlet, P.: Species detection using environmental DNA from water samples, Biology Letters, Vol.4, pp.423-425, 2008

Statistical analysis of woody debris volume to specify mechanism of recruitment in dam reservoirs in Japan

○Yuto Sukegawa[1*], Daisuke Komori[2], So Kazama[1]

[1]Graduate School of Engineering, Tohoku University, Sendai 980-8579, Japan
[2]Graduate School of Environmental Studies, Tohoku University, Sendai 980-8579, Japan

*E-mail: yuto.sukegawa.q3@dc.tohoku.ac.jp

Abstract

The relationship of woody debris volume to their recruitment, transport and export is unrevealed. In previous study, Fremier *et al*. (2010) showed that woody debris were predominately transported during peak flow events and woody debris export increased logarithmically with basin area using 131 dam reservoirs.

To find further relationship between woody debris volume and other parameter, we compiled a data set of woody debris volume deposited annually into 1103 dam reservoirs across Japan. By quality check, we finally used about 550 dam reservoirs data. We compared woody debris volume to basin area, flow discharge, basin characteristics (forest area in basin and forest area ratio of basin) and parameter which related to slope failure (mean relief energy of forest area in basin and mean 5 year daily rainfall). We found that woody debris volume increased logarithmically with flow discharge. Furthermore, the trend of flow discharge and woody debris volume has trend whose is similar to relationship between woody debris volume and flow discharge. By multiple regression analysis, detecting the relationship woody debris volume to forest area and 5 year daily rainfall.

Keywords: watershed area, forested area, slope failure

1. Introduction

Woody debris (WD) were produced by bank erosion, wind-fall, landslides, dying of tree and development of forest area. WD's good point is that altering river environment and floodplain process, such as flood inundation and sediment transport and increases overall biocomplexity. In addition, the presence of WD increases available aquatic habitat for water creatures and can facilitate seeding recruitment on floodplains[1]. In contrast, one of bad points is that process of WD transport cause damage to river structure by collision. In addition, WD accumulated at bridge pier cause inundation of flood water and at outlet of dams cause difficulties to water intake[2]. Current situation of forest Japan is that the number of people involved with forestry is decreasing. And imported timber replaced domestic timber because of cheapness. These are proceeding the devastated forest and the growing stock of forest (**Figure 1**). So, we think that getting knowledge whose WD volume is increasing or decreasing is important.

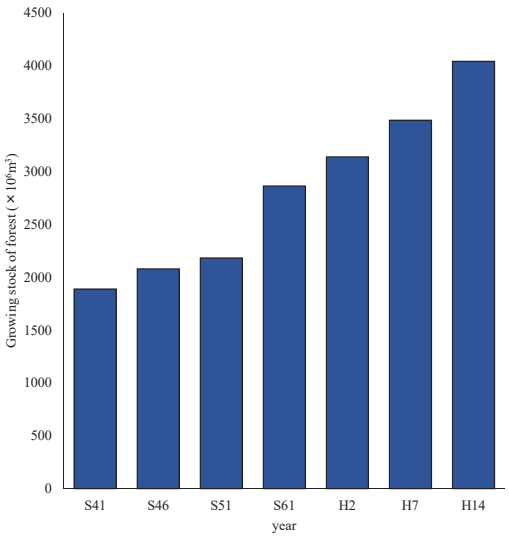

Figure 1 Growing stock of forest in Japan with the change of the times

In previous study, only watershed area was regarded as explanatory variable, strongly related to WD volume[1]. So, our objective is clarifying the factors related to WD volume to get future prediction of WD volume.

2. Data set and Method

This study's targets are 1103 dams in Japan. Used data are WD volume flowing into dam reservoirs and flow discharge, observed for 18 years, presented by Ministry of Land, Infrastructure, Transport and Tourism (MLITT).

The proposed method is into three main steps : (1)Comparing WD volume with watershed area (WA) ; (2)Comparing WD volume with inflow discharge ; and (3)Statistical analysis by using multiple regression analysis.

References

1) Alexander K. Fremier, Jung Il Seo, Futoshi nakamura : Watershed controls on the export of large wood stream corridors, Geomorphology, 117 ,pp.33-43, 2010.
2) Maki takanori, Takahashi masato, Ochi shuichi, Miyake katsuhiro, Ozaki masaaki : Research on the volume of woody debris flowing into dam reservoirs in Japan, Japan Society of Civil Engineers, 63(1), 22-29, 2007.

The distribution and characteristics on frequent inland inundation areas of metropolitan areas in Japan

○Kota Nakaguchi[1*], Daisuke Komori[2], Ryo Inoue[3] and So Kazama[1]

[1]Graduate School of Engineering, Tohoku University, Sendai 980-8579, Japan
[2]Graduate School of Environmental Studies, Tohoku University, Sendai 980-8579, Japan
[3]Graduate School of Information Sciences, Tohoku University, Sendai 980-8579, Japan

*E-mail: kouta.nakaguchi.s1@dc.tohoku.ac.jp

Abstract

In this study, the frequent inland inundation areas in Tokyo's 23 wards, Nagoya city and Osaka city were extracted by using maps of flood damage from 1993 to 2012. The maps were manually drawn at each city as paper-based flood records. Due to the unfixed patterns and ways of drawing the maps, these maps have not been used for the vulnerability analyses of flood damage. These paper-based maps were translated into digitized maps on GIS database, and the frequent inland inundation areas were extracted. The result analysis of the extracted area is as follows: The frequent inland inundation area tends to be distributed in "plain" than "depression", and sewer construction is preferentially carried out in "depression". "plain" and "depression" are extracted by using the flood inundation model. Furthermore, it is also clarified that the frequent inland inundation areas tend to be distributed to the area 1) with small slope or low elevation; 2) around the structure which divides the land surface flow and sewer-by such as road and rail.

Keywords: Flood area map, GIS, flood inundation model

1. Introduction

In recent years, inland inundation is the main reason of flood damage in metropolitan areas. Tokyo's 23 wards, Nagoya city and Osaka city are major metropolitan cities in Japan. The percentage of flood damage occurred by inland inundation occupied the total damage in Japan is estimated at 42%, while Tokyo 63.0%, Aichi Prefecture 85.0%, Osaka 96.5% from 2005 to 2013. Therefore, it is essential to clarify the characteristics on frequent inland inundation area for flood control. The purpose of this study is to clarify the distribution and to analyze the characterization of frequent inland inundation area.

2. Methodology

In this study, the frequent inland inundation areas in Tokyo's 23 wards, Nagoya city and Osaka city were extracted by using maps of flood damage from 1993 to 2012. The maps were manually drawn at each city as paper-based flood records **(Fig.1)**. Due to the unfixed patterns and ways of drawing the maps, these maps have not been used for the vulnerability analyses of flood damage. These paper-based maps were translated into digitized maps on GIS database, and the frequent inland inundation areas were extracted. By the result of extraction, the frequent inland inundation areas were analyzed from various points of view.

3. Distribution of frequent inland inundation area

We defined the area which was flooded more than 2 times in Tokyo 23-wards, more than 4 times in Nagoya City and Osaka City in 20 years from 1993 to 2012 as frequent inland inundation area by 100m×100m mesh. As a result, 99 areas in Tokyo 23-wards, 108 areas in Nagoya City and 70 areas in Osaka City were extracted **(Fig.2)**.

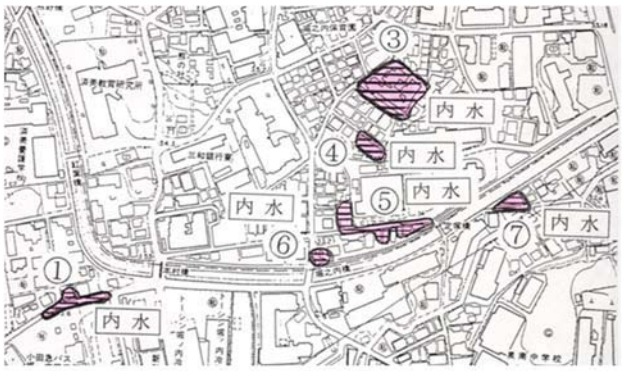

Fig.1 Flood area map

3. Characteristics of frequent inland inundation area

By using the result of extraction, frequent inland inundation areas in Osaka City were analyzed

3.1 Topography

The frequent inland inundation areas were classified by topography using flood inundation model. Flood inundation model is a mathematical model which calculate the inundation depth from altitude, rainfall and landuse. Inundation depth was calculated by fixing rainfall and landuse to the same value at all meshes. The areas which inundation depth is more than 0.45m were defined as depression, and less than 0.45m were defined as plain. As a result, 14% of frequent inland inundation areas locate depression, and 86% of that locate plain.

Furthermore, the drainage capacity in these areas was checked. In this study, drainage capacity is proportional to the density of the drainage well and manhole. As a result, the density both of drainage well and manhole in depression are larger than that in plain **(Table 1)**.

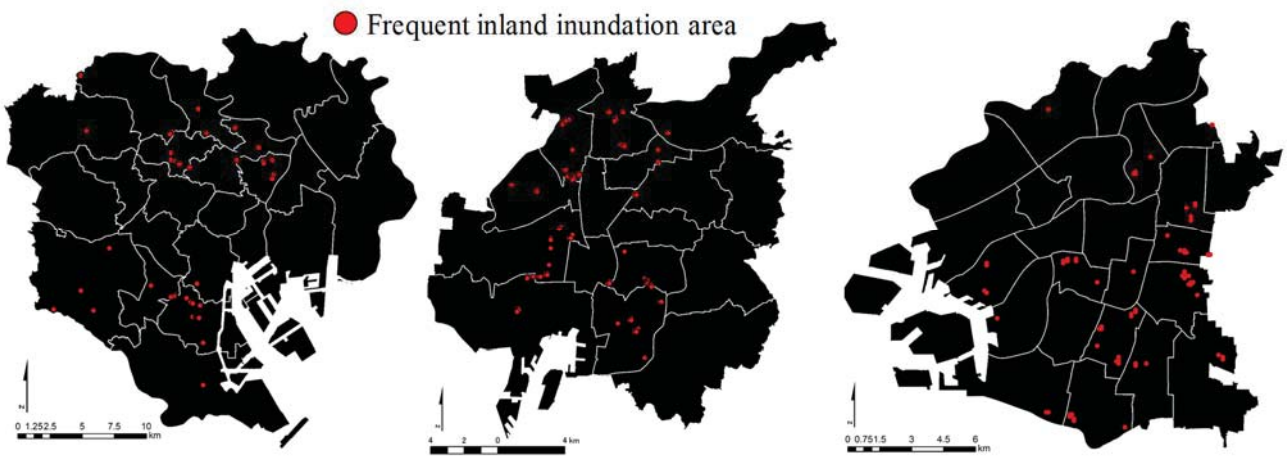

Fig.2 The distribution of frequent inland inundation area

Table 1 Drainage capacity in whole Osaka City and frequent inland inundation areas

	density of drainage well	
	depression	plain
Whole Osaka City	3338	2541
Frequent inland inundation area	6700	5402

	density of manhole	
	depression	plain
Whole Osaka City	977	797
Frequent inland inundation area	1675	1650

3.2 Slope and Height

The value of height and slope at the meshes in Osaka City and frequent inland inundation areas were calculated. The average of slope is 1.56 degree in whole Osaka City, and 1.26 degree in frequent inland inundation area. The average of height is 3.59m in whole Osaka City, and 3.30m in frequent inland inundation area. The number of frequent inland inundation areas of which slope smaller than average slope of whole Osaka City is 58 areas (83%), and larger than average slope of whole Osaka City is 12 areas (17%). The number of frequent inland inundation areas of which height smaller than average height of whole Osaka City is 49 areas (70%), and larger than average height of whole Osaka City is 21 areas (30%). Consequently, frequent inland inundation area tends to be distributed to the area with small slope and height.

3.3 Surrounding structures

The structure which divides the land surface flow and sewer was defined as "surrounding structure disturbed inundation flow" (hereinafter called "surrounding structure"). This is Concretely, road which divides the sewer, railway, levee and building with a side length of more than 100m. We checked whether surrounding structure exist within the surrounding 8 cells from frequent inland inundation area or not. As a result, 90% of frequent inland inundation area has these structures and 10% of frequent inland inundation area doesn't have these structures. Furthermore, frequent inland inundation areas were classified as location of surrounding structure and flow-down direction **(Fig.6)**. As a result, there is a tendency to be located in the flow-down direction (68%).

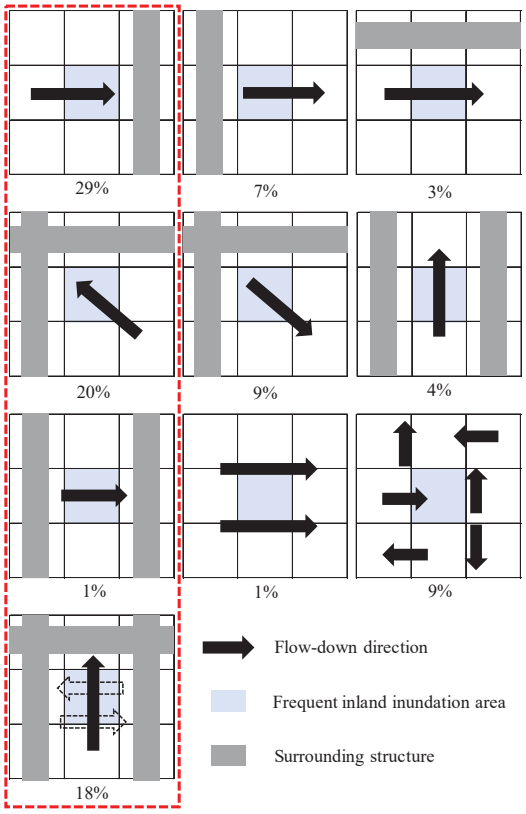

Fig.3 Classification of frequent inland inundation areas

4. Conclusions

The result analysis of the extracted area is as follows.

1) Frequent inland inundation area was existed 99 areas in Tokyo 23-wards, 108 areas in Nagoya City and 70 areas in Osaka City.
2) Frequent inland inundation area tends to be distributed in plain than depression, and sewer construction is preferentially carried out in depression.
3) Frequent inland inundation area tends to be distributed to the area with small slope or low elevation
4) Frequent inland inundation area tends to be distributed around the structure which divides the land surface flow and sewer-by such as road and rail.

Relationship between probabilistic precipitation and flood discharge by DAD analysis

○Yuta Sugawara[1], So Kazama[1], Daisuke Komori[2]

[1]Graduate School of Engineering, Tohoku University, Sendai 980-8579, Japan
[2]Graduate School of Environmental Studies, Tohoku University, Sendai 980-8579, Japan
*E-mail : yuta.sugawara.r3@dc.tohoku.ac.jp

Abstract

Spatial and temporal distribution of rainfall has was made by using DAD analysis at the 3 points (upper stream, middle downstream and downstream) of the Yoneshiro River Basin and contributed the distributed runoff model to calculate flood discharge. The return period for the rainfall and discharge was calculated by frequency analysis. Probabilistic discharge of all discharge observation points became large and small when the heavy rainfall was generated at the upper stream and downstream respectively.

Keywords: Distributed runoff model, Talbot's formula, Horton's formula

1. Introduction

In recent years, the changes of rainfall intensity and rainfall patterns have been occurred in Japan by climate change due to global warming[1] and the frequency of future short time heavy rainfall tends to increase. In addition, there is characteristic of Japanese rivers which is a short length and steep slope in comparison with world rivers. It is concerned that risk of flood is increased with heavy rain, therefore a lot of studies on flood control have been carried out in Japan[2]. It is necessary to understand the probabilistic flood discharge in a basin spatially to carry out for flood control measures in consideration of the increase of risk of flood. It has not yet been known how the probability of the rain influences the probability of flood. Therefore it is intended to estimate the relationship between probabilistic rainfall and flood discharge.

2. Methodology and sources

2.1 Study area

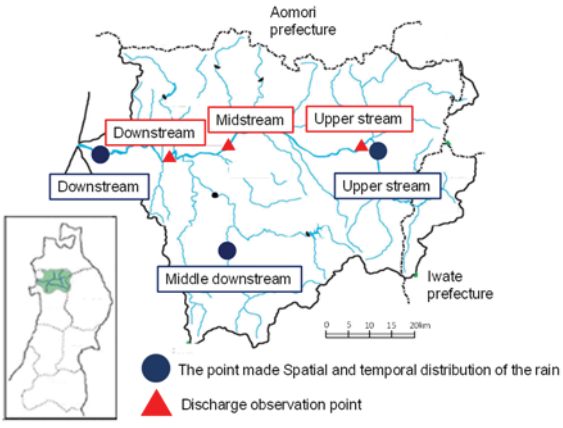

Fig 1. Map of Yoneshiro River Basin

The study area is the Yoneshiro River Basin located in the Akita Prefecture, a northern part of Japan. The Yoneshiro River Basin is the fifth largest river in the Tohoku region and locates in the range of about N39°47′60″ to 40°28′53″, E140°00′45″ to 141°02′04″. The length of mainstream of the Yoneshiro River is 136km long and its catchment area is 4100km^2 (Fig 1). The Yoneshiro River flows into the Sea of Japan through Takanosu valley, Odate valley, Hanawa valley and Noshiro plain which are located on the basin

2.2 Data sources

The hydrological model developed by Tohoku university requires precipitations, temperatures, wind speeds, elevation data. Elevation data is referred Geospatial Information Authority of Japan. Precipitation data and temperature data are referred to the AMeDAS (Automated Meteorological Data Acquisition System) data organized by the Japanese Meteorological Agency. Also, discharge data are referred to the data that Ministry of Land, Infrastructure, Transport and Tourism.

2.3 Making procedure spatial and temporal distribution of rain

The DAD analysis is the method calculating relationship of depth, area and duration and composed of DD (depth and duration) analysis and DA (depth and area) analysis. The DD analysis is the method calculating relationship of duration and depth. Talbot's formula was adopted for the DD analysis[3]. The DA analysis is the method calculating relationship of depth and area. Horton's formula was adopted for the DA analysis[4].There are expressed by the following equations respectively.

2.3.1 Talbot's formula

$$I = \frac{a}{t+b} \quad (1)$$

Where I is depth (mm/h), t is the duration (h), a and b is the constants of each point. calculated by Least square method.

2.3.2 Horton's formula

$$P = 1.06P_0e^{-kA^n} \quad (2)$$

Where P is depth (mm/h), P_0 is the point precipitation maximum (mm/h), A is area (km^2), k and n are calculated by Horton ($k = 0.1$, $n = 0.2$).Wind speeds were set with 5m/s considering the reducing of rain gauge capacity by wind in the case of heavy downpour. Procedure spatial and temporal distribution was showed below. Hyetographs of 50,100,200,300 mm/24hours were made by the DD analysis at each 3 point. The values of P_0 in the hyetograph were input to Horton's formula (2) and spatial rainfall distribution were made every hour at each 3 point. This spatial and temporal distribution is that precipitation observed at the upper stream, midstream and downstream becomes maximum. Fig 2(a) and Fig 2(b) show the minimum rainfall distribution and the maximum rainfall distribution respectively when the heavy rainfall of 300mm/24 hours was generated at the upper stream.

2.4 The hydrological model

We used the distributed runoff model[5] to calculate discharge. In this model, the basin is classified as the portions both slope area and river area. Runoff of the slope area is composed of direct flow and base flow. We applied kinematic wave model and Manning's formula to direct flow and storage function method to base flow.

3. Results

Fig 3 shows the relationship between probabilistic precipitation and flood discharge. When the heavy rain has occurred at the downstream (a), the probabilistic discharge is increased dependent on the order of upper stream, downstream and midstream. When heavy rain also has occurred at the middle downstream (b), Fig 3 showed the increase of discharge in the series of the upper stream, midstream and downstream. When heavy rainfall less than about 50 years return period has occurred at the upper stream (c), it showed the increase of discharge in series of upper stream, midstream and downstream. When the heavy rainfall more than 50 years return period has occurred, probabilistic discharge is increased dependent on the order of midstream, upper stream and downstream. When the heavy rainfall has occurred at the upper stream, the upper stream in the increase rate of probabilistic flood discharge is bigger than 2 points (middle downstream and downstream). When the same distribution of rainfall having maximum rainfall at each 3 point for the upper stream, middle downstream and downstream in spatially and temporally were generated at the upper stream, midstream, middle downstream and downstream, the probabilistic discharge is increased dependent on the order of the upper stream, midstream, middle downstream and downstream. According to the above results, probabilistic discharge was the biggest at the upper stream whenever rainfall distribution generated was set at any point. Adversely probability discharge was the smallest at the downstream wherever generated rainfall distribution was set at any point.

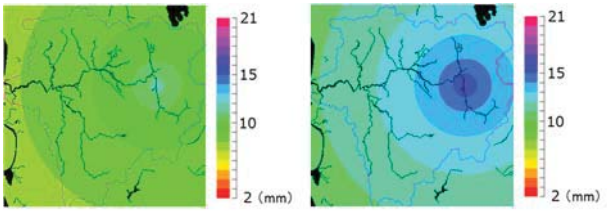

Fig 2(a). Minimum Fig 2(b). Maximum

Fig 2. Rainfall distribution

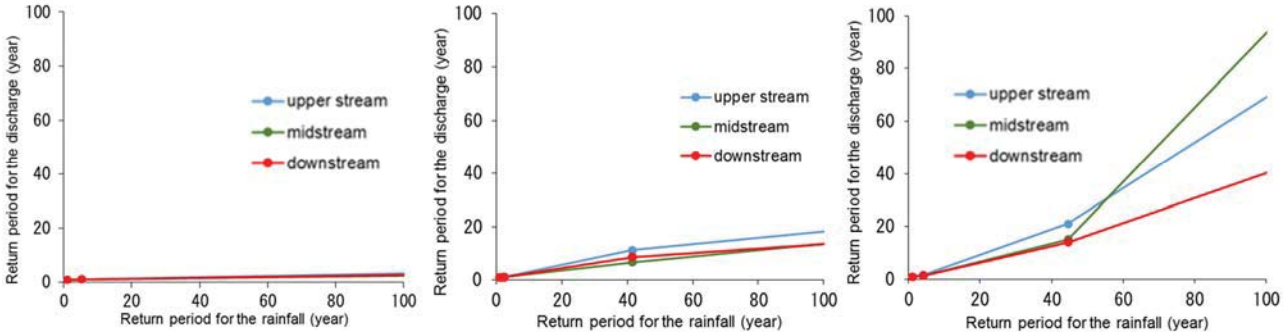

Fig 3(a). Downstream Fig 3(b). Middle downstream Fig 3(c). Upper stream

Fig 3. Relationship between probabilistic precipitation and flood discharge

4. Conclusion

The probabilistic discharge was evaluated when the heavy rain was generated at the upper stream, middle downstream and downstream. Probabilistic discharges of all discharge observation points became large and small when the heavy rain was generated at the upper stream and downstream respectively.

5. Acknowledgements

We wish to thank Tohoku Regional Development Association and Mitsui Consultants Co., Ltd for their generous financial assistance. This research was supported by the Social Implementation Program on Climate Change Adaptation Technology (SI-CAT) of MEXT, Japan

6. Reference

[1]. Global warming prediction information, Vol.8, 2013
[2]. S. Tezuka, H. Takiguchi, S. Kazama, A. Sato, S. Kawagoe, R. Sarukkaliged, Estimation of the effects of climate change on flood-triggered economic losses in Japan, International Journal of Disaster Risk Reduction, Vol.9, pp.58-67, 2014.
[3]. Japan Society of Civil Engineers：The Collection of Hydraulic formulas, pp.133~135, 1949
[4]. R.E.Horton：Discussion on distribution of intense rainfall, Transactions, ASCE,Vol.87,pp.578-585, 1924
[5]. L. Gao, S. Kazama, D. Komori, S. Kikuchi, The evaluation of the peak discharge and the improvement of a distributed rainfall-runoff model in the Yoneshiro river valley, IAHR-APD, 2014.9.24. Hanoi

Evaluation of flood and storm surge disasters model in Japan

○Yukako Tanaka[1]*, Masahiro Akima[2], So Kazama[2], Daisuke Komori[3]

[1]School of Engineering, Tohoku University, Sendai 980-8579, Japan
[2]Graduate School of Engineering, Tohoku University, Sendai 980-8579, Japan
[3]Graduate School of Environmental Studies, Tohoku University, Sendai 980-8579, Japan

*E-mail: yukako.tanaka.s5@dc.tohoku.ac.jp

Abstract

This study run the simulation of a compound disaster involving flood and storm surge and evaluated the damage cost for the disaster in Japan. The tide level and daily rainfall which can cause compound disasters are calculated by means of frequency analysis for annual minimum atmospheric pressure. 2D non-uniform flow model expressing the inundation depth is carried out using the tide level data on coastline in Japan and daily rainfall distribution as input data. Damage cost is estimated using the inundation depth by each land use. The total damage cost in whole Japan for 50-year return period of compound disaster is 52 trillion JPY, and the compound disaster damage costs of Tokyo, Aichi, and Osaka prefecture are higher than any other prefecture.

Keywords: flood, storm surge, inundation, frequency analysis; high-risk area

1. Introduction

Intergovernmental Panel on Climate Change (IPCC/AR5) mentioned that flood and storm surge will be more serious in lower zones caused by sea level. It is anticipated that intense typhoon will be formed stronger and it will bring flood and storm surge on the same time in Japan because of higher sea temperature. Although many studies have done on impacts on each flood and storm surge, few studies have done on a compound disaster involving these two events. To understand the impact of compound disaster, we try to estimate the damage cost in Japan for the compound disaster.

2 Methods

Flood and storm surge coincide as the compound disaster are selected considering damage in lower areas in Japan. We focus on low atmospheric pressure at typhoon because almost compound disasters selected are derived typhoon. The magnitude of the maximum tide level and daily rainfall which can cause compound disasters are calculated from the relationship between annual minimum atmospheric pressure and tide level deviation, and between annual minimum atmospheric pressure and daily rainfall. The tide level data from 59 tide-gauge stations in Japan over 16 years, the daily rainfall data from 143 rain gauges in Japan over 51 years, and the atmospheric pressure data for each observation station are used for analyses on the maximum tide level and daily rainfall. We consider the fluctuations of the tide level by using the maximum tide level of each stations and distribute spatially the tide level and daily rainfall by means of Inverse Distance Weight (IDW) method. 2D non-uniform flow model expressing the inundation depth is calculated using the tide level data on coastline in Japan and daily rainfall distribution as input data. Damage cost is estimated using inundation depth calculated by the above method and prices per unit of area calculated by each land use developed by the flood control economy investigation manual. Inundation depth and damage cost are calculated with one square kilometer mesh, with a land use inventory having 11 classifications including rice field, farmland, building site, golf course, main road site, forest, wasteland, other site, river and lakes, beach and sea area is used for the damage cost estimation.

3 Results and discussion

The total damage cost in whole Japan for 50-year return period of compound disaster is 52 trillion JPY. As shown in **Fig. 1**, the compound disaster damage costs of Tokyo, Aichi, and Osaka prefecture are higher than any other prefecture and the amount of damage cost in the three prefectures accounts for 25% of the total cost in Japan. Asset values of these prefectures are higher and most of their areas located on low altitude areas compared with the others. The damage cost by the Ise Bay Typhoon in 1959 which actually bought a compound disaster in Japan is compared and shows good agreement with this estimation.

4 Conclusions

Results show where government should invest intensively in disaster prevention by infrastructure in high-risk area to raise resistance to water disasters in Japan. This can support considering city planning based on the regional characteristics. Our result can contribute to flood control design and the efficient adaptation method against water disasters.

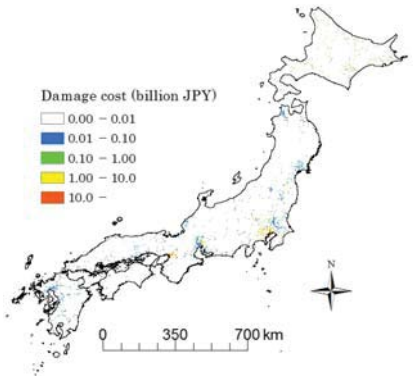

Fig. 1 The damage cost distribution

Greenhouse-Gases Emission and Mass Balances in Wastewater Treatment Plant

○Kazuya KAMIYAMA[1], Nobuyuki TANAKA[1], Toshimasa HOJO[1], Yu-You LI[1]*

[1] Graduate School of Engineering, Tohoku University, Sendai 980-8579, Japan
*E-mail: gyokuyu.ri.a5@dc.tohoku.ac.jp

Abstract

In wastewater treatment plant treating same influent by pseudo Anaerobic Oxic process (p-AO process) and Anaerobic Anoxic Oxic process (A_2O process), survey of C and N mass balances including Greenhouse Gases (GHGs) emission were carried out, and comprehensive environmental loads in wastewater treatment plant were evaluated. The results indicated integrated environmental loads with effluent, water quality, GHGs emission and sludge production in A_2O process were lower than p-AO process. Enough nitrification and denitrification may contribute to not only improvement of effluent quality but also reduction of CH_4, N_2O emissions and excess sludge amount.

Keywords: Greenhouse gases, Wastewater treatment plant, Life cycle CO_2, CH_4, N_2O, mass balance

1. Introduction

Building of wastewater treatment system with little total environmental loads are required. Recently, pseudo Anaerobic Oxic process (p-AO process) is becoming popular. Even though p-AO process requires small reconstruction expenses, it's capable of securing effluent quality following advanced treatment process. But, it has been reported that p-AO process discharges more nitrous oxide (N_2O) being one kind of Greenhouse Gases (GHGs) than advanced treatment system removing nitrogen such as Anaerobic Anoxic Oxic process (A_2O process). Therefore, it is necessary to assess integrated environmental loads such as GHGs emission, effluent water quality and sludge amount.

In this study, survey of C and N mass balances including Greenhouse Gases (GHGs) emission were carried out, and comprehensive environmental loads in wastewater treatment plant that treats same wastewater with p-AO process and A_2O process were evaluated. Elucidation of C and N flow for each treatment process becomes valuable knowledge in developing reduction of environment load.

2. Materials and Methods

In this study, on site survey were carried out 5 times in plant S (figure.1) in Miyagi prefecture. CO_2 produced with usage electric power and methane (CH_4) and N_2O discharged from water surface in treatment plant were measured. CH_4 and N_2O Emission Factor (EF; emission per water quantity of treatment plant) were combined with CO_2 EF and p-AO process was compared with A_2O process. And TOC, T-N, D-CH_4 and D-N_2O in liquid phase in treatment plant were analyzed, C and N mass balances of each processes were calculated. At calculating, TOC and T-N amount in influent were taken as 100% C and N.

3. Results and Discussion

As a result of survey in wastewater treatment plant treating same wastewater with p-AO process and A_2O process, GHGs EF of p-AO process was about twice as high as A_2O process. (figure.2). To evaluate GHGs emission characteristic through elucidating GHGs flow from production to emission (figure.3), it was discovered that enough nitrification and denitrification in A_2O process

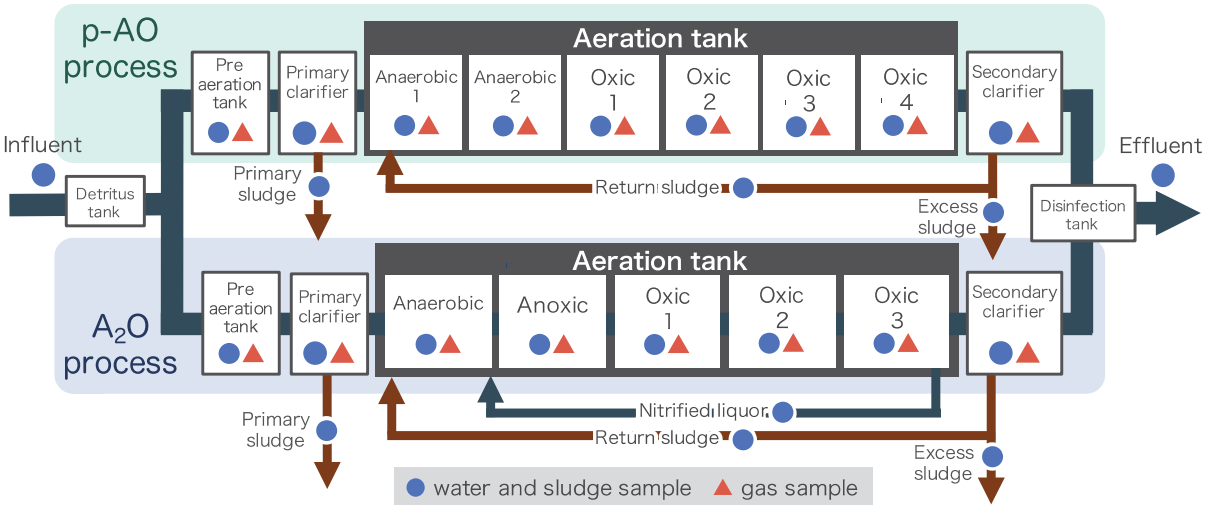

Figure.1 Sampling points in plant S

might contribute to reduction of CH_4 and N_2O emission.

As shown in figure.4, about 0.7% and 0.8% of C, N converted to CH_4 and N_2O as GHGs emission in p-AO process, but about 0.3% and 0.04% of C, N converted to CH_4 and N_2O in A_2O process. In addition, both of C and N discharged as effluent in p-AO process were higher than A_2O process. And in p-AO process, 2.4% and 11% of C, N are discharged as excess sludge, but in A_2O process, only 1.4% and 4.6% C, N are discharged. To evaluate solid contents of excess sludge per 10,000m^3 influent in each process, amount of A_2O process and p-AO process were 1.02m^3 and 1.20m^3 respectively. The amount of excess sludge in A_2O process was smaller than that of p-AO process. According to past research, when both of C and N removal rates are high, amount of excess sludge is decreased. In this study, high C and N removal rates in A_2O process contribute to reduction of excess sludge amount too. So it was revealed that enough nitrification and denitrification contribute to improvement of effluent quality, reduction of GHGs emission and excess sludge amount, as a result enough nitrification and denitrification are effective in reduction of environmental loads.

4. Conclusion

C and N mass balances including GHGs emission were examined, and comprehensive environmental loads in wastewater treatment plant that treats same wastewater with p-AO process and A_2O process were evaluated. The results indicated environmental loads with effluent, GHGs and sludge in A_2O process were lower than p-AO process. Enough nitrification and denitrification may contribute to not only improvement of effluent quality but also reduction of CH_4, N_2O emissions and excess sludge amount.

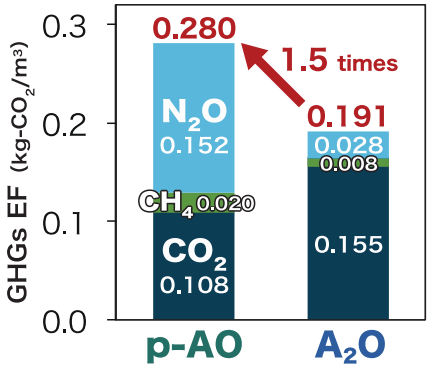

Figure.2 GHGs EF in this study

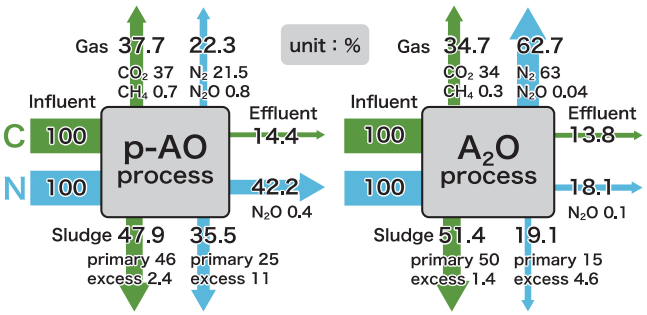

Figure.4 C, N mass balances

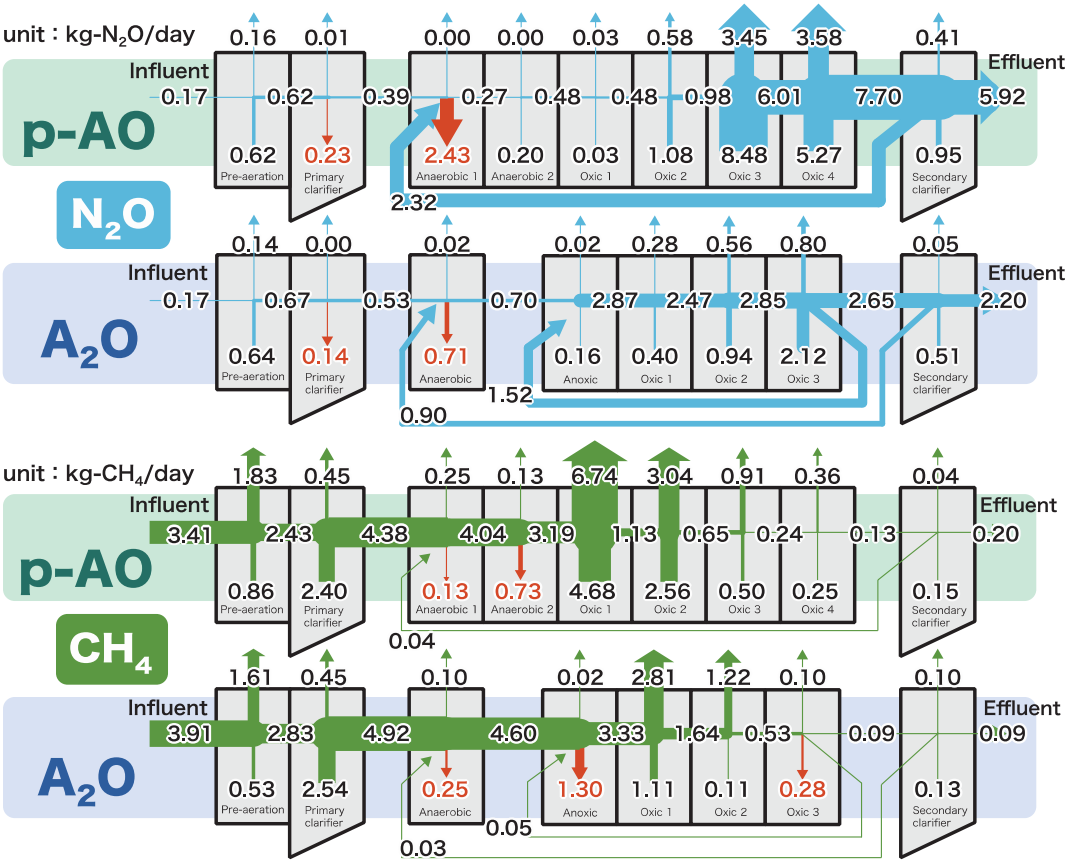

Figure.3 GHGs flow from production to emission

Prokaryotic distribution and diversity of soda lakes and surrounding soil in the desert areas of northern China

○Lu Li[1], Zhe Kong[1], Chunbo Hao[2], Yu-You Li[1]*

[1]Department of Civil and Environmental Engineering, Tohoku University, Sendai, Miyagi 980-8579, Japan
[2]N School of Water Resources and Environment, China University of Geosciences (Beijing), No. 29 Xueyuan Road, Haidian District, Beijing 100083, China
*E-mail: gyokuyu.ri.a5@tohoku.ac.jp

Abstract

In Badain Jaran desert, numerous lakes existed with both high salinity and high alkalinity whose pH usually above 10 and named soda lakes. Due to the unique groundwater system, even though the water is high salinity, the surrounding soil maybe opposite, which have low salinity. Here, we aim at investigating the difference of microbial distributions and diversities between water and soil media and clarify the influence of salinity on the relative distribution ratio of bacteria to archaea. By analyzing 16S rDNA through Illmina sequencing platform, we found that communities of prokaryotes varied greatly between water and soil media. Soil usually have greater microbial diversity. Diversity of bacteria was always higher than archaea in whichever medium samples of this study. Bacteria-archaea ration of soil samples presented high correlation with salinity while which was inconspicuous in water samples. Salinity influenced the microbial distribution regularities greatly, as highly saline samples clustered together as well as the mesosaline ones. In this study, 7 water samples and 7 soil samples with different salinity were collected, it was the first investigation on prokaryotic distributions of soda lakes in Badain Jaran desert and proposing a research basis for the further study.

Keywords: Soda lakes, soil, 16S rDNA, Microbial diversity

1. Introduction

Most of previous studies on ecological distribution of halophiles and correlation to environmental factors simply focused on sea areas where salinities were below 30 g/L. Although microbial community structures under hypersaline environments were well reported and documented, those studies were majorly concentrated on artificial environments such as solar salterns, and whose single environmental factor usually resulted in simplified diversity, therefore which could hardly reveal a detailed variation regularity of indigenous microbial communities in these high salinity soda lakes. Water samples as well as soil samples in this study were collected from soda lakes in Badain Jaran desert, the fourth largest desert in the world, whose unique groundwater system formed a great amount of salt lakes with high salinity but the surrounding soil may have a low salinity because of the covered vegetation. Moreover, Badain Jaran desert had not been influenced by human activity because of few inhabitant, hence, this wild area was considered to be a proper place for conducting a systematical investigation of influence from environmental factors on microbial community structures.

Our study aims to: (1) identify predominant strains of microorganisms in salt lakes and surrounding soil; (2) analyze the difference of microbial distributions and diversities between water and soil media; (3) clarify the influence of salinity on the relative distribution ratio of bacteria to archaea.

2. Materials and Methods

2.1 Sampling

4 lakes with different salinities and features were selected as sampling sites, namely Xiaoshaozao (Lake1), South Sangenjilin (Lake2), Zhongnaoertu (Lake3) and West Badan (Lake4), from whose surface water and surrounding soil, 7 water samples and 7 soil samples were separately collected in September, 2013. Temperatures, pH, DO, Salinity, concentrations of carbonate, bicarbonate, ammonium, nitrate, ion concentrations etc. were determined.

2.2 Genome DNA extracting, PCR and sequencing

Genome DNA was extracted by MPbio FastDNA® extraction kit. Extractive was amplified by using primers F515 (5'-GTGCCAGCMGCCGCGGTAA-3') and primers R806 (5'-GGACTACVSGGGTATCTAAT-3') targeting the V4 region of 16S rDNA for 14 samples respectively. PCR cycling conditions: an initial denaturation step at 94 ℃ for 3 min; 35 cycles of PCR (94 ℃ for 30 s, 50 ℃ for 60 s, 72 ℃ for 90 s), and a final elongation step at 72 ℃ for 10 min. PCR products were detected by 1% agarose electrophoresis, then cut out for the target band in UV system, and purified with Agarose Gel DNA purification Kit Ver.2.0 (TaKaRa, Japan). The purified DNA were quantified by NanoDrop2000 (Thermo, USA) and then pooled with equal quantity and sequenced by using 2nd generation Illumina sequencing platform (Illumina, USA).

2.3 Sequence processing

Chimeras and sequences with low quality were denoised by Mothur to ensure length of sequences>300 bp, and regulated into 12,000 sequences. Targeted sequences were then aligned against Sliva.bacteria-archaea database. Sequence data were binned into species-approximating OTUs using definitions of ≥97% sequence similarity.

2.4 Statistical analyses and phylogenetic analyses

Shannon α-diversity index, Simpson α-diversity index were calculated with the program Mothur with summary.single command. Heatmap was drown based on the top 50 OTUs in OTU table using the heatmap.2 ( ) function in R 3.0.3 package gplots, value of clones were transformed into ln (x+1) type. Phylogenetic tree were generated by using MEGA6.0.

2.5 Accession number

Representative sequences were submitted to GenBank under accession numbers KR297067 ~ KR297086 for water samples and KR297087 ~ KR297110 for soil samples.

3. Results and discussion

3.1 Analysis of physicochemical properties

Lake 1 was observed with transparent water with a few artemia and surrounded by sandy soil. Lake 2 appeared red with large amount of artemia and salt crystallization soil. Lake 3 was almost transparent with a little amount of green algae, whose surrounding soil was yellowish-brown and covered by vegetation. Lake 4 appeared dark green with black soil surrounded (as shown in Fig. 1). Analysis results indicated that all samples were highly alkaline with pH above 9. Besides, mineralization degrees of all water samples were relatively high, all above 165 g/L. However, soil samples of Lake 3 and 4 presented low salinities.

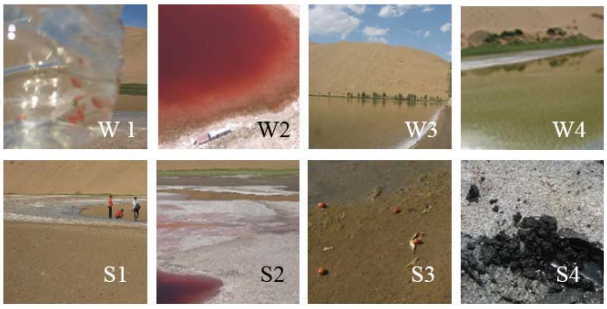

Fig. 1 Samples of water and soil in salt lakes.

3.2 Proportion analysis

Bacteria of water samples were divided into 13 phyla, mainly represented by Gammaproteobacteria and Bacteroidetes, while archaea were sorted as 3 phyla, mainly Euryarchaeota. For soil samples, phylum of Firmicutes, Bacteroidetes, Deltaproteobacteria, Epsilonproteobacteria and Gammaproteobacteria mainly represented 34 phyla of bacteria, archaea was the same situation with water samples (Fig. 2). As shown in the figure, microbial diversities of soil were higher than water samples, which was also demonstrated by Shannon and Simpson diversity indexes.

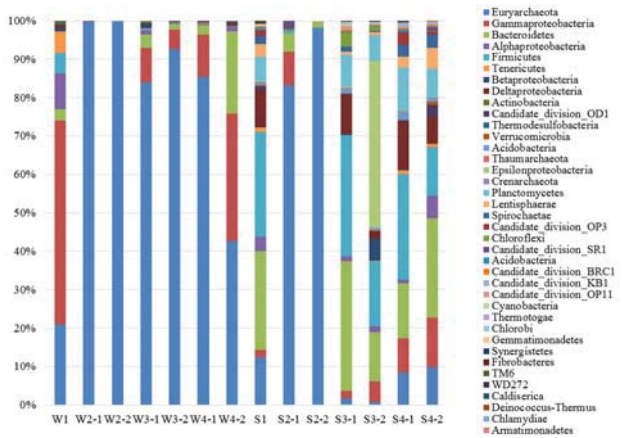

Fig. 2 Proportion of phyla in the samples.

A taxon unit was defined as difference of 0. 03 to calculate Shannon and Simpson diversity indexes. Results demonstrated that the microbial diversities of soil samples were apparently higher than water, especially for sample 4-2 (Fig. 3), which was because that S4-2 appeared black and contained so much humus that highly diversified microorganisms.

Relative distribution regulations of bacteria and archaea were shown in Fig.4, the ration of soil samples presented high correlation with salinity while which was inconspicuous in water samples.

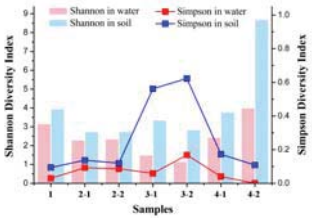

Fig. 3 Shannon diversity index and Simpson diversity index in the samples of water and soil.

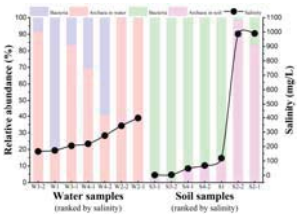

Fig. 4 Distribution of bacteria and archaea in the samples.

3.3 Cluster analysis

In total 105 thousand sequences were obtained from water samples and separated to 2487 OTUs, a heat map was illustrated as Fig. 5 (A) by using the top 50 OTUs. 88 thousand sequences were obtained from soil samples with 7816 OTUs, Fig.5 (B) was drawn with the top 200 OTUs. The clustering of samples accorded with the variation of salinities well for the samples with similar salinity almost gathered together.

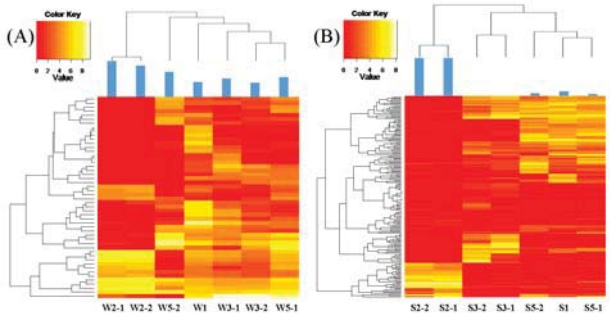

Fig. 5 Heat map of water samples (A) and soil samples (B).

4. Conclusions

(1) Microbial diversity and population dominance of soil microorganisms were generally higher than water samples. In other words, microorganisms is much more predominant in soil than in water.

(2) Diversity of bacteria was always higher than archaea in whichever medium samples of this study. Bacteria in water samples were divided into 13 phyla while archaea were only 3 phyla. Similarly in soil samples, bacteria were divided into 34 phyla while archaea were only 3 phyla.

(3) Salinity influenced the microbial distribution regularities greatly, as highly saline samples clustered together as well as the mesosaline ones.

5. Acknowledgements

The authors would like to thank their advisors and workmates in the lab of China University of Geosciences (Beijing) and Tohoku University, this article was supported by the Fundamental Research Funds for the Central Universities (2652012028, 2652013100).

Microbial diversity in a methanol-feeding upflow anaerobic sludge blanket (UASB) reactor operated under different COD and sulfate concentrations

○Jialing Ni[1]*, Yusuke Shimada[1], Kengo Kubota [1], Xueqin Lu[1], Jiayuan Ji, Yu-You Li[1]

[1]Department of Civil and Environmental Engineering, Tohoku University, Sendai, Miyagi 980-8579, Japan
*E-mail: jialing@dc.tohoku.ac.jp

Abstract

The aim of this study was to investigate the succession of the microbial community structure in a methanol feeding upflow anaerobic sludge blanket reactor, which was operated under different COD and sulfate concentrations. In phase I, during which the COD/SO_4^{2-} ratio was kept at 20, high COD removal efficiency was achieved, but when COD concentration was increased to 15,000 mg/L, the treatment efficiency dropped (about 80% total COD removal). In the phase II, COD concentration was kept and sulfate concentration was gradually increased. Pyrosequencing of 16S rRNA gene amplicon revealed that the dominant *Archaea* was *Methanomethylovorans*, known as methanol-utilizing methylotrophic methanogen, regardless of the COD and sulfate concentrations. During phase I, the fraction of *Archaea* increased with the elevation of COD concentration, but it decreased when the removal efficiency was dropped. In phase II, predominant phyla were *Firmicutes* and the fraction of *Archaea* was about 20% even high concentration of sulphate was added. Bacterial community analysis at operational taxonomic unit level is needed for more understanding of microbial community succession in the reactor.

Keywords: 16S rRNA gene pyrosequencing, methanogens, methanol-containing wastewater, sulfate-reducing bacteria

1. Introduction

Among all the wastewater treatments biological treatment has been wildly used through the whole world. In order to improve the efficiency of the treatment, many researches focus on the process by changing different conditions such as hydraulic retention times (HRT), COD concentration, temperate and so on. However direct evidence cannot be supplied just using these methods, because the most important point is the role that activated sludge played during the whole process. Activated sludge contains many kinds of microorganisms, but 99% of them cannot be cultured so far. So a major research measurement is to analyze the structure of the microbial communities through gene sequencing.

Therefore, in this study, 16S rRNA gene pyrosequencing was used to analyze the anaerobic sludge in an upflow anaerobic sludge blanket (UASB) reactor fed with methanol under different COD and SO_4^{2-} concentrations.

2. Materials and Methods

2.1 UASB reactor, sampling and DNA extraction

The schematic flow of the UASB reactor treating methanol-containing wastewater is shown in **Fig. 1**. A total of 10 anaerobic sludge samples were taken after 153, 178, 231, 296, 326, 339, 395, 426, 454, 488, and 537 days since the start-up. A seed sludge was also sampled. Operational conditions (HRT, COD concentration, and COD-to-SO_4^{2-} ratio) of the reactor are shown in **Table. 1**.

Table. 1, Operational conditions of the UASB reactor at respective sampling days

Sample	seed	153	178	231	296	326	339	395	426	454	488	537
HRT (h)	6											
COD (mg/L)		3000	6000	15000	15000	3000						
COD/SO_4^{2-}		20				20	10	5	3	2	1	0.5

The anaerobic sludge samples (about 10 mL each) were washed with phosphate-buffered saline for three times and pelleted by centrifugation for DNA extraction. For each sample, the extraction was conducted in duplicate using the ISOIL for Beads Beating (Nippongene). The extracted DNA concentration and purity were determined by microspectrophotometry (NanoDropND-2000, NanoDrop Technologies, and Wilmington, DE).

2.2 Pyrosequencing

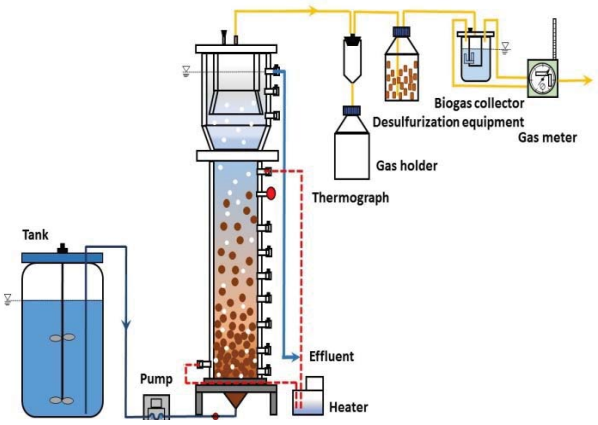

Fig. 1, Schematic flow of the UASB reactor

The prokaryotic 16S rRNA gene was amplified with a 341f-806r primer pair targeting the V3-V4 regions (about 460 bp). Pyrosequencing was carried out according to the manufacture's instruction using Roche GS Jr. The sequence data was analyzed by using QIIME software.

3. Results and discussion

3.1 Pyrosequencing

The number of sequence read for each sample ranges from 2,486 to 6,230, and sufficient numbers of sequence reads were obtained to monitor the succession of dominant microorganisms in the reactor.

3.2 Prokaryotic community changes under different COD concentrations

The whole experiment can be departed for two phases according to the different COD/SO_4^{2-} ratio conditions. During the phase I, the COD/SO_4^{2-} ratio was kept at 20, and COD concentration was increased from 3,000 to 15,000 mg/L. The removal rate of total COD (TCOD) around the153rd day (fed with 3,000 mgCOD/L) was higher than 90%, and was still the same level around the 179th day (fed with 6,000 mgCOD/L). However, the removal efficiency dropped to around 80% of the TCOD around the 231st day (fed with 15,000 mgCOD/L). The biogas production also showed the same trend. The biogas production rate achieved more than 12 L/L/d when 3,000 or 6,000 mgCOD/L was fed to the reactor, but it showed only 5 L/L/d when 15,000 mgCOD/L was supplied.

The **Fig. 2** shows the prokaryotic community compositions at different COD and sulfate concentrations. The figure is based on pie chart data, and rare phyla refer to the taxa with maximum abundance below 0.5% in any sample are grouped into 'other'. Pyrosequencing of 16S rRNA gene amplicons revealed the fractions of archaeal community changed drastically, 4.5% in the sample taken in 153rd day, 46.0% in 179th day sample, and 15.2% in 231st day. It shows a link among COD loading, COD removal efficiency, methane production and archaeal community. When high COD removal efficiency was achieved (i.e., 3,000 and 6,000 mgCOD/L), the relative abundance of *Archaea* increased as elevated COD loading. When high concentration of COD (15,000 mgCOD/L) was fed and the removal efficiency was dropped, the archaeal fraction decreased. Therefore, archaeal fraction in sludge has strong correlation with process performance. The most predominant *Archaea* in these samples was *Methanomethylovorans*, known as a methylotrophic methanogen utilizing methanol as substrate. Thus the most of methanol fed to the reactor was most likely converted to methane by this member.

3.3 The influence of COD/SO_4^{2-} ratio on prokaryotic community

After decreasing COD concentration to 3,000 mg/L to see the effect of sulfate concentration, the composition and the population of microbial community of the 326th day sample looked similar to the samples taken in 153rd day. Even after elevating sulfate concentration, *Firmicutes* was the dominant phylum.

Desulfovibrionales and *Syntrophobacterales* are the largest group of sulfate-reducing bacteria belonging to *Proteobacteria. Proteobacteria* is about 5% of all the prokaryotic community. In *Proteobacteria,* the percentage of *Desulfovibrionales* shifted 0%, 10%, 41%, 36%, 27%, 45%, and 54% after 326, 339, 395, 426, 454, 488, and 537 days. It clearly showed a link between the sulfate concentration and the proportion of sulfate-reducing bacteria.

Besides, *Euryachaeota* maintains lower fraction with slightly undulating (10-20%). It can be considered as this was due to the increasing sulfate concentration, so that sulfate reducing bacteria and methanogenic archaea were in competition for methanol utilization. According to the **Fig. 3,** the result shows that the effects on microbial community structure caused by COD concentration are larger than the COD/SO_4^{2-} ratio conditions.

4. Conclusions

(1) During phase I, *Archaea* increased with the elevation of COD concentration, but it decreased when the removal efficiency was dropped (i.e., 15,000 mg/L). Pyrosequencing of 16S rRNA gene amplicon revealed that the dominant *Archaea* was *Methanomethylovorans* that are associated to methanol utilization.

(2) Based on the 16S rRNA gene pyrosequencing, the main sulfate-reducing bacteria was *Desulfovibrionales* and *Syntrophobacterales* belong to *Proteobacteria* with the increasing of sulfate concentration in phase II.

(3) According to principal coordinate analysis, COD concentration caused more effects on microbial diversity than COD/SO_4^{2-} ratio conditions.

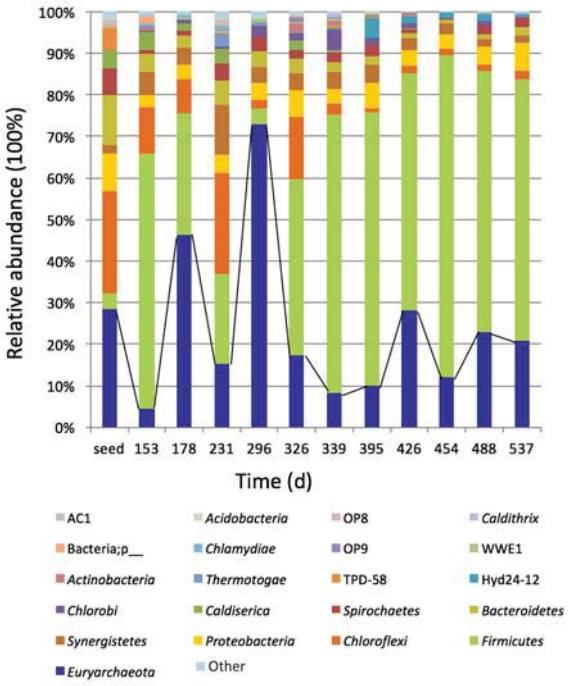

Fig. 2, Prokaryotic community compositions of a methanol-feeding UASB reactor. 'Other' indicates the sum of rare phyla with the abundance of <0.5% in samples.

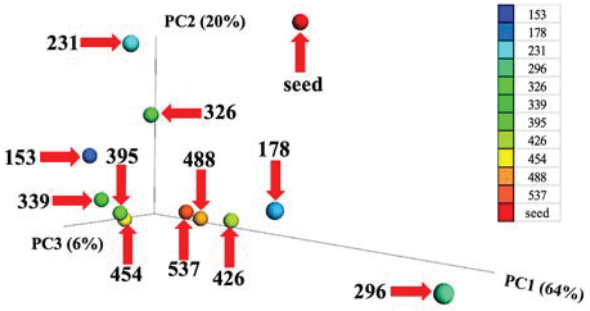

Fig. 3, Principal coordinate analysis of samples